

AD-A143 984

OPTICAL ACQUISITION IMAGE AND DATA COMPRESSION(U) CITY
COLL NEW YORK DEPT OF ELECTRICAL ENGINEERING
G EICHMANN JUN 84 447104-1 AFOSR-TR-84-0611

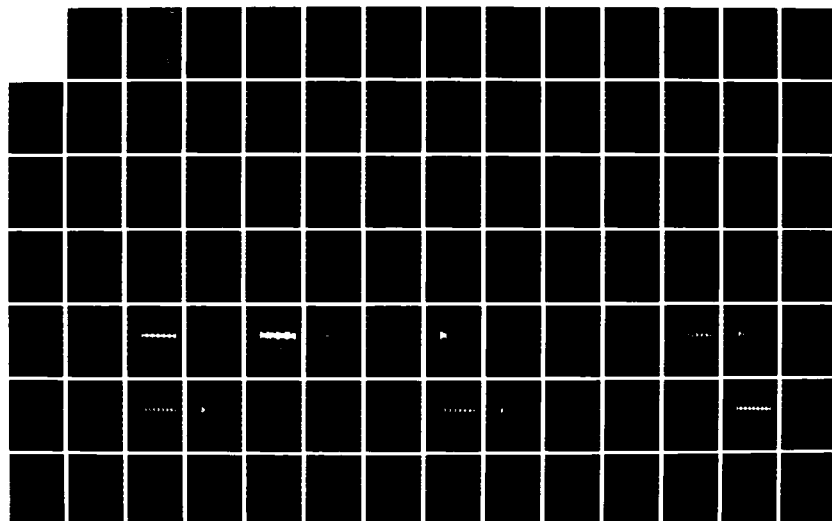
1/2

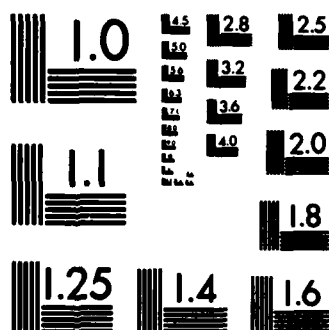
UNCLASSIFIED

AFOSR-83-0081

F/G 17/8

NL





MICROCOPY RESOLUTION TEST CHART
NATIONAL BUREAU OF STANDARDS-1963-A

AFOSR-TR. 84-0611



AD-A143 984

OPTICAL ACQUISITION, IMAGE
AND
DATA COMPRESSION

ANNUAL TECHNICAL REPORT - 447104-1

MARCH 1, 1983 - MAY 30, 1984

GRANT AFOSR-83-0081
AIR FORCE OFFICE OF SCIENTIFIC RESEARCH
BOLLING AIR FORCE BASE
WASHINGTON, D.C. 20332

DEPARTMENT OF ELECTRICAL ENGINEERING
THE CITY COLLEGE OF
THE CITY UNIVERSITY OF NEW YORK

JUNE 1984

Approved for public release;
distribution unlimited.

DTIC
ELECTE
S AUG 9 1984 D

DTIC FILE COPY

The United States Government is authorized to reproduce and distribute reprints for Governmental purposes notwithstanding any copyright notation hereon.

84 08 07 125

REPORT DOCUMENTATION PAGE		READ INSTRUCTIONS BEFORE COMPLETING FORM
1. REPORT NUMBER AFOSR-TR-84-0011 447104-T	2. GOVT ACCESSION NO. AD-A143984	3. RECIPIENT'S CATALOG NUMBER
4. TITLE (and Subtitle) Optical Acquisition, Image and Data Compression		5. TYPE OF REPORT & PERIOD COVERED Annual March 1, 1983 - May 30, 1984
		6. PERFORMING ORG. REPORT NUMBER
7. AUTHOR(s) G. Eichmann		8. CONTRACT OR GRANT NUMBER(s) AFOSR - 83 - 0081
9. PERFORMING ORGANIZATION NAME AND ADDRESS Department of Electrical Engineering City College of New York New York, N.Y. 10031		10. PROGRAM ELEMENT, PROJECT, TASK AREA & WORK UNIT NUMBERS 6/102F 2305/B1
11. CONTROLLING OFFICE NAME AND ADDRESS Air Force Office of Scientific Research Bolling Field, Washington, D.C. 20332		12. REPORT DATE June 1984
		13. NUMBER OF PAGES 153
14. MONITORING AGENCY NAME & ADDRESS (if different from Controlling Office)		15. SECURITY CLASS. (of this report) UNCLASSIFIED
		15a. DECLASSIFICATION/DOWNGRADING SCHEDULE
16. DISTRIBUTION STATEMENT (of this Report) Approved for public release; distribution unlimited.		
17. DISTRIBUTION STATEMENT (of the abstract entered in Block 20, if different from Report)		
18. SUPPLEMENTARY NOTES		
19. KEY WORDS (Continue on reverse side if necessary and identify by block number) Optical Information Processing, superresolution, spectral estimation, phase reconstruction, amplitude reconstruction.		
20. ABSTRACT (Continue on reverse side if necessary and identify by block number) This report deals with the phase estimation of low time-bandwidth product (TBP) signals. Phase and frequency of a signal is estimated for short observation time. The observation time or the spectral bandwidth is limited to the superresolving regime where the TBP is near unity. Two classes of signal estimation are presented. Superresolving frequency estimation is performed where the sinusoidal signals are buried in deep white Gaussian noise. Constrained optimization techniques,		

UNCLASSIFIED

SECURITY CLASSIFICATION OF THIS PAGE(When Data Entered)

20.

using linear programming, are used to estimate the location of the spectral peaks of the sinusoidal signals.

Time and frequency limited Hilbert transform analysis is used to reconstruct the phase from the amplitude, and the amplitude from the phase of a complex signal. In addition, three smoothing methods; a mathematical filtering method, a correction factor method, and a method of spectral partitioning, are used to improve the phase/amplitude estimate of the complex signal.

Accession For	
NTIS GRA&I	<input checked="checked" type="checkbox"/>
DTIC TAB	<input type="checkbox"/>
Unannounced	<input type="checkbox"/>
Justification	
By	
Distribution/	
Availability Codes	
Dist	Avail and/or Special
ALL	



UNCLASSIFIED

SECURITY CLASSIFICATION OF THIS PAGE(When Data Entered)

LOW TIME-BANDWIDTH PRODUCT
SIGNAL PHASE ESTIMATION

by

JAROSLAV EDVARD KEYBL

A dissertation
submitted to the Graduate Faculty in Engineering
in partial fulfillment of the requirements
for the degree of
Doctor of Philosophy
The City University of New York

1983

AIR FORCE OFFICE OF SCIENTIFIC RESEARCH (AFOSR)
NOTICE OF REPRODUCTION
This document is the property of the Air Force Office of Scientific Research (AFOSR) and is loaned to you for your use only. It is not to be distributed outside your organization without the prior written consent of AFOSR.
MATTHEW J. KENNEDY
Chief, Technical Information Division

COPYRIGHT BY
JAROSLAV EDVARD KEYBL
1984

This manuscript has been read and accepted for the Graduate Faculty in Engineering in satisfaction of the dissertation requirement for the degree of Doctor of Philosophy.

April 11, 1984
date

Gerge Zichem
Chairman of Examining Committee

April 11, 1984
date

Paul R. Karmel
Executive Officer

Prof. G. Eichmann

Prof. J. Barba

Prof. F. Thau

Dr. I. Kadar

Dr. R. Mammone

Supervisory Committee

The City University of New York

ACKNOWLEDGEMENT

I would like to take this opportunity to thank Professor George Eichmann for his valuable help during the research and writing of this manuscript.

I would also like to especially thank my wife Alina for her support, encouragement and assistance during the years of this endeavor.

J.E.K.

TABLE OF CONTENTS

Chapter 1	INTRODUCTION.....	1
	1.0 Introduction.....	1
	1.1 Spectral Estimation of Two Pulses.....	3
	1.2 Modified Hilbert Transform.....	4
Chapter 2	ESTIMATION OF CLOSELY SPACED FREQUENCIES BURIED IN NOISE USING LINEAR PROGRAMMING....	6
	2.0 Introduction.....	6
	2.1 Parameter Estimation.....	17
	2.2 1, Norm Formulation and Linear Programming.....	29
	2.3 Computer Simulation and Results.....	33
	2.4 Conclusion.....	42
Chapter 3	FINITE TIME-BANDWIDTH PRODUCT HILBERT TRANSFORM.....	69
	3.0 Introduction.....	69
	3.1 Modified Hilbert Transform.....	83
	3.2 Phase Retrieval Problem.....	97
	3.3 Conclusion.....	113
Chapter 4	SUMMARY AND EXTENSIONS.....	138
	4.0 Introduction.....	138
	4.1 Extensions of Methods.....	139
	APPENDIX.....	141
Figures	Figures for Chapter 2.....	44
	Figures for Chapter 3.....	114
	Figures for Appendix.....	146
References	148

LIST OF FIGURES

Figure	Title	Page
2.4.1	Test signal $s(n)$ with no noise and all 512 points are used.	44
2.4.2	Log magnitude of spectrum of $s(n)$ having no noise and all 512 points are used in evaluating the Fourier transform.	45
2.4.3	Signal $s(n)$ when white Gaussian noise of variance $\sigma^2=1.0$ is added.	46
2.4.4	Log magnitude of the spectrum of $s(n)$ with noise variance $\sigma^2=1.0$.	47
2.4.5	First quadrant of the z -plane showing the locations of the poles and zeros of the Z -transform of $s(n)$.	48
2.4.6	Signal $s(n)$ with $TBW=0.719$ and noise variance $\sigma^2=1.0$.	49
2.4.7	Log magnitude of spectrum when the $TBW=0.719$ and noise has variance $\sigma^2=1.0$.	50
2.4.8	Log magnitude of the estimated spectrum obtained using the new method where the normalized frequencies of the positive pulses are given by $f_1=0.2148$ and $f_2=0.2285$.	51
2.4.9	Location of poles and zeros in the first quadrant of the z -plane obtained using the new method when $TBW=0.719$ and variance $\sigma^2=1.0$.	52
2.4.10	Estimated signal $s(n)$ obtained by taking the inverse Z -transform of the transfer function made up of the estimated poles and zeros.	53
2.4.11	Signal $s(n)$ where the $TBW=0.719$ and the variance of the noise has been in-	

	creased to $\sigma^2=5.0$.	54
2.4.12	Log magnitude of the spectrum of the signal with TBW=0.719 and $\sigma^2=5.0$.	55
2.4.13	Log magnitude of the estimated spectrum using new method with positive peaks occurring at the normalized frequencies $\tilde{f}_1=0.2148$ and $\tilde{f}_2=0.2304$.	56
2.4.14	Locations of estimated poles and zeros in the first quadrant of the z-plane with TBW=0.719 and $\sigma^2=5.0$.	57
2.4.15	Estimated signal $s(n)$ formed by inverse Z-transforming the transfer function made up of the estimated poles and zeros.	58
2.4.16	Signal $s(n)$ when TBW=0.5 and the noise has variance $\sigma^2=1.0$.	59
2.4.17	Log magnitude of the spectrum of the signal $s(n)$ with TBW=0.5 and $\sigma^2=1.0$.	60
2.4.18	Log magnitude of the estimated spectrum using the new method with positive peaks occurring at normalized frequencies $\tilde{f}_1=0.2148$ and $\tilde{f}_2=0.2285$.	61
2.4.19	Locations of estimated poles and zeros in the first quadrant of the z-plane of signal $s(n)$ having TBW=0.5 and $\sigma^2=1.0$.	62
2.4.20	Estimated signal $s(n)$ obtained by taking the inverse Z-transform of the transfer function made up of the estimated poles and zeros.	63
2.4.21	Short time duration signal $s(n)$ where TBW=0.359 and the noise variance is 1.0.	64
2.4.22	Log magnitude of spectrum of $s(n)$ for the short time duration signal $s(n)$.	65
2.4.23	Estimated spectrum using new method where positive peaks occur at normalized frequencies $\tilde{f}_1=0.2148$ and $\tilde{f}_2=0.2305$.	66

2.4.24	Locations of the estimated poles and zeros in the first quadrant of the z-plane.	67
2.4.25	Estimated signal $s(n)$ obtained by inverse Z-transforming the transfer function with the estimated poles and zeros.	68
3.1.1	Modified Hilbert transform kernel with TBP=12.	114
3.1.2	Modified Hilbert transform kernel with TBP=3.	115
3.1.3	Estimated imaginary part using the modified Hilbert transform with normalizing constants $KR=0.5$, $KI=0.362$ and $KE=0.360$.	116
3.1.4	Estimated real part using the modified Hilbert transform with normalizing constants $KR=0.5$, $KI=0.362$ and $KE=0.494$.	117
3.1.5	Estimated imaginary part using the modified Hilbert transform where TBP is reduced to 3 with normalizing constants $KR=0.5$, $KI=0.362$ and $KE=0.356$.	118
3.1.6	Estimate of the imaginary part of the spectrum of an exponential function using the modified Hilbert transform, with normalizing constants $KR=2.0$, $KI=1.0$ and $KE=1.0$.	119
3.2.1	Estimate of phase from magnitude measurement of the Fourier transform of the exponential signal with normalizing constants $KR=1.841$, $KI=1.491$ and $KE=2.561$.	120
3.2.2	Estimated phase of spectrum of an exponential signal for TBP=0.1 with $KR=0.693$, $KI=0.104$ and $KE=0.082$.	121
3.2.3	Estimated phase of the spectrum of an exponential signal for TBP=0.5 with $KR=0.693$, $KI=0.482$ and $KE=0.520$.	122

3.2.4	Estimated phase of the spectrum of an exponential signal for TBP=2.0 with KR=0.693, KI=1.125 and KE=0.473.	123
3.2.5	Estimated phase of the spectrum of an exponential signal after Gaussian filtering with $\sigma^2=4.0$ where KR=2.461, KI=1.125 and KE=2.390.	124
3.2.6	Estimated phase of the spectrum of an exponential signal after Gaussian filtering with $\sigma^2=0.5$ where KR=2.133, KI=1.125 and KE=1.981.	125
3.2.7	Estimated phase of the spectrum of an exponential signal after Gaussian filtering with $\sigma^2=0.01$ where KR=1.161, KI=1.125 and KE=0.821.	126
3.2.8	Estimated real part of spectrum of exponential signal with KR=7.389 and KE=7.389.	127
3.2.9	Estimated imaginary part of spectrum of exponential signal with KI=2.97 and KE=2.46.	128
3.2.10	Fourier transform of signal obtained from estimated real and imaginary parts.	129
3.2.11	Correction factor for phase estimation.	130
3.2.12	Corrected phase estimate using the correction factor for the phase of the spectrum of an exponential signal.	131
3.2.13	Phase estimate of the shifted interval from f=0.1 to 0.2 of the spectrum of an exponential signal where KI=0.102 and KE=0.081.	132
3.2.14	Phase estimate of the shifted interval from f=2.0 to 2.1 of the spectrum of an exponential signal where KI=0.019 and KE=0.073.	133
3.2.15	Phase estimate of the shifted interval from f=6.5 to 6.6 of the spectrum of an exponential signal where KI=0.002 and	

	KE=0.032.	134
3.2.16	Estimate of the phase of the spectrum of the exponential signal after having partitioned the interval into ten segments with KI=0.808 and KE=0.804.	135
3.2.17	Phase estimate of an analytic signal with KR=0.233, KI=0.201 and KE=0.201.	136
3.2.18	Phase estimate of a periodic analytic signal whose bandwidth is larger, with KI=0.403 and KE=0.416.	137
A.1	Observations of a 45° line over a unit square showing the l_1 , l_2 and l_∞ curve fits of the line.	146
A.2	The l_1 , l_2 and l_∞ fits when one of the observations is wild.	147

Chapter 1

INTRODUCTION

1.0 Introduction

In the spectral estimation of signals one comes across a problem when components of the spectral response are spaced closely together, and the problem is further complicated when the signal is noisy. There is a point up to which it is possible to resolve two pulses that are placed closely together. Beyond this point it can only be done if some a priori information is given about the signal. The point at which it becomes difficult without a priori knowledge can be obtained from the sampling theorem, and is given by

$$T \cdot B = 0.5 \qquad (1.0-1)$$

where the T represents the duration of time that the signal is observed, and B is the bandwidth of the signal. Equation (1.0-1) states that the limiting time-bandwidth product is equal to 0.5. If the product is greater than 0.5 it is possible to obtain a good estimate of the spectrum even when noise is present. On the other hand, if the product is less than 0.5 it is extremely difficult to

resolve two peaks that are spaced closely together. The only way to be able to resolve the two peaks is to have knowledge about the signal. This knowledge can then be formulated to give one a set of linear equations with equality and inequality constraints. These equations along with a minimizing procedure can be used to obtain or improve the estimate. In this thesis we show a method to obtain an estimate of two closely spaced pulses in the spectral domain when the time-bandwidth product is less than 0.5. The knowledge that we assume is that there are only two pulses in the frequency domain.

In signal processing there is a class of signals that one comes across having the property that they only exist for positive time. This class of signals are termed causal. If the signal is also real, then there is a special relationship between the real and imaginary parts of its Fourier transform. The relationship that exists is that the real and imaginary parts of the Fourier transform are related by the Hilbert transform. From this one need only know the real or imaginary part of the spectrum and the other part can be easily calculated. The dual to this is that the spectrum contains only real components for positive frequencies. Then the real and imaginary parts of the time signal are related through the Hilbert transform. This type of time signal is given the name analytic. One

of the uses of the Hilbert transform is in the area of phase retrieval. The problem can be stated that given only the modulus of a signal, whether it be in the time or frequency domains, determine the phase. Under the conditions that the signals are analytic or causal, the Hilbert transform holds between the modulus and phase. It is a well known fact that when determining the phase, if the signal has zeros that occur in the upper half of the complex z -plane, then the phase cannot be found. For this reason processing of the modulus has to be performed before or after the estimate of the phase has been obtained.

1.1 Spectral Estimation of Two Pulses

When it is desired to resolve two pulses spaced closely together with a time-bandwidth product of less than 0.5, more information has to be known a priori. The information that we are given is that there are two pulses, and this is all that is needed to resolve the two pulses. The method of solution is based on knowing that two pulses in the frequency domain corresponds to the sum of two cosines in the time domain. Since we are using digital signal processing methods where we are sampling the time function, we can represent the two cosines in terms of their Z -transform. From the Z -transform we can obtain a set of linear equations plus a set of inequalities based on the

coefficients of the Z-transform. These equations are then used with mathematical programming techniques to provide an optimal transfer function to describe the two pulses that originally smeared into one when the time-bandwidth product is less than 0.5.

1.2 Modified Hilbert Transform

Let us consider the evaluation of the Hilbert transform. It involves the convolution of a signal with a kernel given by

$$K=1/t. \qquad (1.2-1)$$

If numerical methods are used to evaluate the convolution, then difficulties arise because the kernel has a singularity which makes certain values go to infinity during its evaluation. To overcome this difficulty, the fast Fourier transform algorithm has been used to evaluate the convolution. In certain applications this leads to another problem. One may find that the frequency spread of the function times the kernel exceeds the frequency domain defined by the inverse of the sampling distance, and consequently the Fourier transform is distorted. In this way, the computer evaluation of the convolution integral yields large errors.

A new form of the Hilbert transform is given whose kernel does not have the problems that exist for the other form of the Hilbert transform. This new Hilbert transform will be applied to the phase retrieval problem to show that similar results can be obtained.

Chapter 2

ESTIMATION OF CLOSELY SPACED FREQUENCIES BURIED IN NOISE USING LINEAR PROGRAMMING

2.0 Introduction

In signal estimation one finds that there exists a time-frequency duality in that the signal may be estimated either in the time or frequency domain. If a portion of the signal is known for a specific length of time, the method where the signal is estimated outside the time interval is referred to as signal extrapolation. If on the other hand the signal is observed over the same length of time and from these observations the power spectral density of the signal or simply the spectrum is to be determined, the process is called spectral estimation. If the signal is known over an infinite interval, the Fourier transform of its autocorrelation yields the power spectral density. In either case, if the signal is estimated in one domain the estimate of the signal in the other domain can be obtained by using the Fourier or Z transforms.

There are numerous methods that have been developed for signal extrapolation and spectral estimation. In extra-

polating a signal outside its observation interval, it is a well known fact that if the signal is continuous, deterministic and bandlimited it is possible to perform the extrapolation without error. This is because such a signal is analytic and the Taylor series expansion can be used since in principle, all the derivatives within the observed interval of the signal can be evaluated. This is called analytic continuation. However, in practice the above procedure is not feasible because if the observed data contains noise, the evaluation of the derivatives would be inaccurate since the derivative is a noise-sensitive process. Slepian et al. [1] proposed an algorithm based on a series expansion in terms of basis functions called prolate spheroidal wave functions. These functions are orthogonal over the observation interval as well as over the infinite interval. The series coefficients can be evaluated from the observations given but the series is valid for all time. This method is limited by noise and truncation errors. In general the numerical generation of these functions is very difficult. A method proposed by Papoulis [2] reduces the mean-square error between the estimate and the original (time-unlimited) signal at successive iterations. Using this error energy reduction procedure and the properties of the prolate spheroidal wave functions, Papoulis has shown that this algorithm converges to the original time unlimited signal. The error energy

reduction procedure which Papoulis uses was first used by Gerchberg [3] in order to extend a known segment of an analytic spectrum. Gerchberg viewed the limited spectrum as the sum of the true spectrum and an error spectrum. In the algorithm proposed it was not the idea to construct the spectrum perfectly out to some new limit but to reduce the energy (squared function integrated) of the error spectrum. The error spectrum is equal to and opposite to the true spectrum in the area outside where the true spectrum is known. The procedure was shown to be very effective against noisy data.

For discrete-time signals, the analyticity property vanishes due to sampling. Therefore, the extrapolated estimate need not coincide with the original signal. Other constraints besides the band-limited assumption must be imposed on the estimate to achieve a unique solution. Much of the work on extrapolation of discrete-time signals is recent. Sabri and Steenaart [4] suggested a discrete version of the iterative algorithm proposed by Papoulis [2]. The algorithm derived a solution by finding an extrapolation matrix. Cadzow [5] has proposed a different extrapolation matrix which does not have the existence problems of the extrapolation matrix suggested in [4] and has some dimensionality advantages. Much of the theory of extrapolation has been developed for continuous-time signals, and a solu-

tion for the discrete case has been obtained by sampling the continuous-time solution.

Estimation of the spectrum of discretely sampled deterministic signals has usually been based on procedures using the fast Fourier transform. These methods are computationally efficient and produce reasonable results for a large class of applications. Even with these advantages the fast Fourier transform approach has two limitations. The first and most prominent limitation is the frequency resolution, i.e., the ability to distinguish the spectral responses of two or more signals. The frequency resolution is approximately given by the reciprocal of the time interval over which the sampled data is available. The second limitation is the windowing of the data when processing with the fast Fourier transform. This windowing occurs because in order to use the fast Fourier transform the signal is truncated at some time and assumed to be periodic beyond this point [6]. If the window used is a constant amplitude window, then its Fourier transform is the sampling function. When in the spectrum there is an impulse, the convolution of this impulse with the sampling function produces a spectrum where the energy of the impulse is no longer localized at one frequency but leaks into the side-lobes of the sampling function. This leakage can have an effect on other spectral responses that are present. These

effects can cause weak signal responses to be masked by higher sidelobes from the stronger spectral responses. By selecting tapered data windows such as Hanning, Hamming or Bartlett windows [7], the sidelobe leakage can be reduced but at the expense of reduced resolution.

These two limitations of the fast Fourier transform are troublesome when short data records are analyzed. Short data records are a common occurrence because many measured processes are brief in duration. Some applications where short data records are encountered are neurophysics [8,9], geophysics [10], speech communication [11,12], radar [13], sonar [14], and direction finding [15]. Due to the inherent limitations of the fast Fourier transform, many alternative spectral estimation procedures have been proposed.

In a classical paper by Blackman and Tukey [16], a practical implementation of Wiener's [17] autocorrelation approach to power spectrum estimation when using sampled data sequences was used. The method first estimates the autocorrelation lags from the measured data, windows the autocorrelation estimates in an appropriate manner, and then Fourier transforms the windowed lag estimates to obtain the power spectral estimate. This method was very popular until the introduction of the fast Fourier transform algorithm by Cooley and Tukey [18]. This renewed

interest in the periodogram which is obtained as the squared magnitude of the output values from a fast Fourier transform performed directly on the data set. The maximum entropy spectral estimation method proposed by Burg [19] is based upon an extrapolation of a segment of a known autocorrelation function for lags which are not known. In this way the characteristic smearing of the estimated spectrum due to the truncation of the autocorrelation function can be removed. Burg argued that the extrapolation should be made so that the time series characterized by the extrapolated autocorrelation function has maximum entropy. In linear prediction [20], the signal is modeled as a linear combination of past outputs and inputs. When only the present input is used, the coefficients of the model are solved for by minimizing the total squared error with respect to each of the coefficients. A very efficient algorithm has been developed by Levinson [21] and Durbin [22] for solving the equation for the coefficients. A more extensive overview is given in papers by Jain et al. [23] on extrapolation algorithms for discrete signals and Kay et al. [24] on spectrum estimation.

A major concern of spectral and time series estimation is that of system modeling. Often if there is more knowledge about the process from which the data is taken, one is able to make a more reasonable assumption other than the

assumption that the data is zero outside the observed interval. A priori information or assumptions may permit selection of an exact model for the process, or at least a model that is a good approximation to the actual process. It is usually possible to obtain a better spectral estimate based on the model by determining the parameters of the model from the observations. By using modeling, spectral estimation becomes a three step process. The first step is to select a time series model. The second step is to estimate the parameters of the assumed model using the data samples or auto correlation lags. The third step is to use the estimated parameters and substitute them into the theoretical spectrum implied by the model. The motivation for the modeling approach to spectral estimation is the higher frequency resolution achieved over the traditional techniques such as the periodogram [24]. It is easy to see that if one is successful in developing a parametric model for the behavior of some signal, then the model can be used for different applications.

In time series analysis, the continuous-time signal $s(t)$ is sampled to obtain a discrete-time signal $s(nT)$, also termed a time series, where n is an integer variable and T is the sampling interval. The sampling frequency is given as $f=1/T$. The expression $s(nT)$ can be abbreviated as $s(n)$ by normalizing the discrete time scale by T .

The most powerful model in use today is the ARMA model where a signal $s(n)$ is considered to be the output of some system with an unknown input $u(n)$ such that the following relationship holds

$$s(n) = - \sum_{i=1}^p a(i)s(n-i) + G \sum_{l=0}^q b(l)u(n-l), b(0)=1 \quad (2.0-1)$$

where $a(i), 1 \leq i \leq p, b(l), 1 \leq l \leq q$, and the gain G are the parameters of the hypothesized system. In equation (2.0-1) the output $s(n)$ is a linear function of past outputs and present and past inputs. The signal is predictable from linear combinations of past outputs and inputs, and therefore it has been termed linear prediction.

Equation (2.0-1) can also be expressed in the frequency domain by taking the Z transform of both sides of the equation. If $H(z)$ is the transfer function of the system, then we have that

$$\begin{aligned} H(z) &= S(z)/U(z) \\ &= G \frac{1 + \sum_{l=1}^q b(l)z^{-l}}{1 + \sum_{i=1}^p a(i)z^{-i}} \end{aligned} \quad (2.0-2)$$

where

$$S(z) = \sum_{n=0}^{\infty} s(n)z^{-n} \quad (2.0-3)$$

is the Z transform of $s(n)$, and $U(z)$ is the Z transform of $u(n)$. $H(z)$ in (2.0-2) is the general pole-zero model. The roots of the numerator are the zeros and the roots of the denominator are the poles of the model.

There are two special cases of the model which are also of interest:

- 1) all-zero model: $a(i)=0, 1 \leq i \leq p$
- 2) all-pole model: $b(l)=0, 1 \leq l \leq q$.

In statistical literature the all-zero model is known as the moving average (MA) model, and the all-pole model is known as the autoregressive (AR) model. The pole-zero model is then known as the autoregressive moving average (ARMA) model. In this chapter only the pole-zero model and the all-pole model will be considered.

In many applications one finds that the spectrum of the signal is composed of two closely spaced impulses. This situation can appear in radar where one of the impulses is due to a jamming signal and the other is produced by a desired signal. If the energy of the desired signal is small compared to the energy of the jamming signal, when the time over which the total signal is observed is small the resultant spectrum has the two impulses smeared togeth-

er. From this smeared spectrum it is desirable to locate the signal with the smaller energy. Kaveh [25] and Cadzow [26] have proposed methods for estimating the parameters of an ARMA model from the observed data samples. In both methods it is found that the order of the ARMA models has to be higher than for the theoretical case when high resolution of noisy signals is desired. The phenomenon of the smearing of the pulses into one broader pulse is due to the multiplication of the actual time signal with a rectangular window to produce the short time observations. In the frequency domain the transform of the short time signal is a convolution of the desired transform with the transform of the rectangular window. If the signal is concentrated in a narrow bandwidth, this convolution operation will spread the energy of the process into adjacent frequency regions. The convolution of the window transform with that of the actual signal transform means that the most narrow spectral response of the resultant transform is limited to that of the main-lobe width of the window transform, independent of the data. For the rectangular window, the main-lobe width is approximately the inverse of the observation time. When additive noise is also present, the spectral response whose energy level is smaller than the noise energy level can be hidden by the noise making it difficult to determine that particular spectral response. Gerchberg [3], and Mammone and Eichmann [27,28]

have devised methods for estimating the spectrum when there is a lack of spectral resolution due to windowing.

In this chapter a new method for estimating the coefficients of an ARMA process is introduced. The ARMA process considered is one whose spectrum contains two impulses closely spaced together in frequency and the power of one impulse is larger than the other impulse. This is the case that would be found in radar. The data is observed for a very short time, which along with additive noise makes it difficult to distinguish the two impulses from one another. The method of solution assumes two things. First, it is assumed that the approximate region in the frequency domain where the two impulses occur is known. The second assumption is that the signal is known to be the sum of two sinusoids whose spectrum is given by two impulses. This assumption can be made by looking at the resultant spectrum of the time windowed signal. From the first assumption it is known where approximately the pulses are to be. In that region the spectrum is very broad which could be only possible if the sampling function is convolved with two impulses and not with one impulse. The method of solution uses linear programming to solve for the coefficients of the ARMA model. Linear programming has been used for spectrum estimation by Mammone and Eichmann [27,28] as well as Levy et al. [29]. In this method, linear programming is

used to minimize the l_1 norm of the absolute values of the error. The error is the difference between the actual spectrum and the one obtained from the ARMA model used in the region where the response is known to be. This error is sometimes termed the residual error. The new method which estimates the spectrum and from which the time signal estimate can be obtained is demonstrated by computer simulations.

2.1 Parameter Estimation

The method by which the parameters of the pole-zero model will be estimated is a two step process, first, to estimate the denominator coefficients and second, to estimate the coefficients of the numerator independently. What this method is doing is to estimate the coefficients of the transfer function $H(z)$. The Z transform of the signal $S(z)$ can be thought of as the output of the filter $H(z)$, with an input function $U(z)$. If the input $u(n)$ is taken as a unit impulse, then one has that the transfer function $H(z)$, and the signal $S(z)$ are identical, or

$$H(z)=S(z). \quad (2.1-1)$$

Therefore, by estimating the parameters of $H(z)$ one is also estimating the parameters of $S(z)$.

The first step in the estimation of the parameters will be to estimate the coefficients of the denominator, $a(i)$. Equation (2.0-1) can be rewritten in the form

$$s(n) = - \sum_{i=1}^p a(i)s(n-i) + B(n) \quad (2.1-2)$$

where

$$B(n) = G \sum_{l=0}^q b(l)u(n-l), \quad b(0)=1.$$

If in (2.1-2) one takes the summation to be an approximation of the signal $s(n)$, one has that the approximation $s'(n)$ is

$$s'(n) = - \sum_{i=1}^p a(i)s(n-i). \quad (2.1-3)$$

Then the error between the actual value $s(n)$ and the estimated value $s'(n)$ is given by

$$B(n) = s(n) - s'(n) = s(n) + \sum_{i=1}^p a(i)s(n-i). \quad (2.1-4)$$

The value $B(n)$ is then taken to be a form of the residual.

This method estimates the parameters from data in the frequency domain, so that (2.1-2) is converted into the frequency domain by taking the discrete Fourier transform

(DFT) of both sides of the equation. Since the fast Fourier transform (FFT) will be used in all the simulations, the DFT is used instead of the Z transform. This is possible because a periodic sequence has a DFT which can be interpreted as samples on the unit circle, equally spaced in angle, of the Z transform of one period. If a signal is periodic with period N, it is possible to represent this signal in terms of a Fourier series consisting of a sum of sines and cosines or equivalently complex exponential sequences with frequencies that are integer multiples of the fundamental frequency $2\pi/N$ associated with the periodic sequence [6]. The DFT analysis and synthesis pair are expressed as

$$X(k) = \sum_{n=0}^{N-1} x(n) \exp(-j2\pi kn/N)$$

$$x(n) = \frac{1}{N} \sum_{k=0}^{N-1} X(k) \exp(j2\pi kn/N)$$

where both $x(n)$ and $X(k)$ are periodic. This gives us

$$\begin{aligned} & \sum_{n=0}^{N-1} s(n) \exp(-j2\pi nk/N) = \\ & - \sum_{i=0}^{N-1} \exp(-j2\pi ik/N) a(i) \sum_{n=0}^{N-1} s(n) \exp(-j2\pi nk/N) \\ & + B \exp(j2\pi nk/N) \end{aligned} \quad (2.1-5)$$

Equation (2.1-5) represents the relationship between the

DFT of the signal $s(n)$, the DFT of the convolution sum (where $p < N$, so that the rest of the $a(i)$'s are set to zero), and the DFT of the residual. This equation can be written in a simpler form as

$$S(k) = - \left[\sum_{i=1}^p a(i) \exp(-j2\pi i k / N) \right] S(k) + B(k) \quad (2.1-6)$$

where k ranges between the values of 0 and $N-1$. The variables $S(k)$ and $B(k)$ are complex numbers so that they may be written in the form

$$\begin{aligned} S(k) &= S'(k) + jS''(k) \\ B(k) &= B'(k) + jB''(k). \end{aligned} \quad (2.1-7)$$

By making use of Euler's formula for the exponent, (2.1-6) is written as

$$\begin{aligned} S'(k) + jS''(k) &= \\ &- \sum_{i=1}^p a(i) (\cos(2\pi i k / N) - j \sin(2\pi i k / N)) (S'(k) + jS''(k)) \\ &+ (B'(k) + jB''(k)) \\ &= - \sum_{i=1}^p a(i) (S'(k) \cos(2\pi i k / N) + S''(k) \sin(2\pi i k / N)) + B'(k) \\ &- j \left(\sum_{i=1}^p a(i) (S''(k) \cos(2\pi i k / N) - S'(k) \sin(2\pi i k / N)) - B''(k) \right) \end{aligned} \quad (2.1-8)$$

From (2.1-8) there are two sets of equations, one for the real part and the other for the imaginary part given by

$$S'(k) = - \sum_{i=1}^P a(i) (S'(k) \cos(2\pi i k / N) + S''(k) \sin(2\pi i k / N)) + B'(k) \quad (2.1-9)$$

$$S''(k) = - \sum_{i=1}^P a(i) (S''(k) \cos(2\pi i k / N) - S'(k) \sin(2\pi i k / N)) + B''(k) \quad (2.1-10)$$

Because linear programming will be used to solve for the coefficients $a(i)$, we can also specify the range of the $a(i)$'s to help in the solution. The range of the coefficients $a(i)$ can be specified because it is known that the signal $s(n)$ is made up of the sum of two cosines of different but closely spaced frequencies. The denominator of the Z transform of a cosine wave can be derived as follows. From the definition of the Z transform and the exponential representation of the cosine one has

$$\cos(wkT) \longrightarrow \sum_{k=0}^{\infty} 0.5 \exp(jwkT) z^{-k} + \sum_{k=0}^{\infty} 0.5 \exp(-jwkT) z^{-k} \quad (2.1-11)$$

In each of the summations the exponential can be multiplied by z and can be written as

$$\begin{aligned} \exp(jwkT) z^{-k} &= (z^{-1} \exp(jwkT))^k \\ \exp(-jwkT) z^{-k} &= (z^{-1} \exp(-jwkT))^k \end{aligned} \quad (2.1.12)$$

By substituting each term into the appropriate summation and using the infinite summation identity that

$$\sum_{k=0}^{\infty} a^{-k} = \frac{1}{1-a^{-k}} \quad (2.1-13)$$

Equation (2.1-11) is written as

$$\begin{aligned} \cos(wkT) &\leftrightarrow 0.5 \left[\frac{1}{1-z^{-1} \exp(jwT)} + \frac{1}{1-z^{-1} \exp(-jwT)} \right] \\ &= 0.5 \frac{1-z^{-1} \exp(-jwT) + 1-z^{-1} \exp(jwT)}{(1-z^{-1} \exp(jwT))(1-z^{-1} \exp(-jwT))} = \frac{N(z)}{D(z)} \end{aligned} \quad (2.1-14)$$

By multiplying the denominator one obtains

$$D(z) = 1 - (\exp(jwT) + \exp(-jwT))z^{-1} + z^{-2} \quad (2.1-15)$$

Equation (2.1-15) can also be reduced to the form

$$D(z) = 1 - 2\cos wT z^{-1} + z^{-2} \quad (2.1-11)$$

where wT is the normalized radian frequency of the cosine wave, and T is the sampling interval. Knowing that $s(n)$ has two cosine waves, the Z transform $S(z)$ has to have the product of the denominator of each of the cosine waves to give

$$D'(z) = 1 - 2(\cos w_1 T + \cos w_2 T)z^{-1} + 2(1 + 2\cos w_1 T \cos w_2 T)z^{-2}$$

$$-2(\cos w_1 T + \cos w_2 T) z^{-3} + z^{-4} \quad (2.1-17)$$

where w_1 and w_2 are the two radian frequencies of the cosines. Equation (2.1-17) can be written as

$$D'(z) = 1 + a(1)z^{-1} + a(2)z^{-2} + a(3)z^{-3} + a(4)z^{-4}. \quad (2.1-18)$$

where

$$\begin{aligned} a(1) &= -2(\cos w_1 T + \cos w_2 T) \\ a(2) &= 2(1 + 2\cos w_1 T \cos w_2 T) \\ a(3) &= -2(\cos w_1 T + \cos w_2 T) \\ a(4) &= 1. \end{aligned}$$

Each of the coefficients in (2.1-18) contains cosines. The limit of a cosine is -1 and +1. These upper and lower limits of the cosine can be used in the expressions for the coefficients to give the limits on these coefficients. This gives the limits as

$$\begin{aligned} -4 &\leq a(1) \leq 4 \\ -2 &\leq a(2) \leq 6 \\ a(3) &= a(1) \\ a(4) &= 1. \end{aligned} \quad (2.1-19)$$

A system is said to be stable if all the poles of its transfer function are contained inside the unit circle of the z -plane. In the special case of sinusoids one finds the poles to be located on the unit circle so that the system

can be termed marginally stable. By marginally stable it is meant that the response is oscillating but the poles are not outside the unit circle. Since the sinusoid is an oscillating function, its poles have to be located on the unit circle. Therefore, if a sinusoidal response is termed stable, it is only because it has no poles that are located outside the unit circle. If the solution gives values according to (2.1-19) then one is assured a stable filter because one obtains these limits through the Z transform of the cosine wave which can be called a stable function.

Equation (2.1-6) can be written as

$$(1 + \sum_{i=1}^p a(i) \exp(-j2\pi i k/N)) S(k) = B(k) \quad (2.1-20)$$

By evaluating the z in (2.1-18) on the unit circle one has

$$D'(\exp(j2\pi i k/N)) = 1 + \sum_{i=1}^4 a(i) \exp(-j2\pi i k/N) \quad (2.1-21)$$

which is seen to be identical to the term in the brackets of (2.1-20) with $p=4$. Therefore, we know that there are only four unknown coefficients in the denominator of the filter $H(z)$. Based on the assumption that the signal contains two sinusoids, it is possible to determine the exact number of coefficients for the denominator of the filter $H(z)$. This is possible because the method of solution

will be able to give results which are close to the actual values even when noise is added. In methods where noise plays a large role in the estimation of coefficients, the order of the models which determine the number of coefficients used has to be larger than the theoretical number. In many such cases the choice of the model order is based on trying different orders until the best results are obtained [27].

If one was only interested in obtaining the frequencies of the signal, by factoring the denominator polynomial one could obtain the radian frequencies of the signal from the argument of the complex roots. Since it is also of interest to obtain the time signal, it becomes necessary to go on to the second step of the estimation process where one has to first do some rearranging of (2.0-2) in order to estimate the coefficients of the numerator in a manner similar to the one just described. It is not possible to use $B(k)$ that comes from the solution of the first part for the coefficients of the denominator, because if the signal has noise added onto it, by minimizing this residual, the noise becomes part of this residual term. Therefore, the first thing one has to do, is to take (2.0-2) and invert it, to give

$$\frac{G}{H(z)} = \frac{1 + \sum_{i=1}^p a(i)z^{-i}}{1 + \sum_{l=1}^q b(l)z^{-l}} \quad (2.1-22)$$

where for simplicity we will replace the $H(z)$ term by $S(z)$ and the quotient $G/S(z)$ by $S^*(z)$. This is done because the same method is used to estimate the coefficients $b(l)$. The gain G cannot be found using this method so that the signal estimate will always be normalized to one. From (2.1-22) we obtain an expression similar to (2.1-2) with a residual $A(n)$ given by

$$s^*(n) = - \sum_{l=1}^q b(l)s^*(n-l) + A(n) \quad (2.1-23)$$

where $s^*(n)$ is the inverse Z transform of $S^*(z)$. Going through the same analysis as before we obtain the following two equations similar to (2.1-9) and (2.1-10),

$$S^{*'}(k) = - \sum_{l=1}^q b(l)(S^{*'}(k)\cos(2\pi lk/N) + S^{*''}(k)\sin(2\pi lk/N)) + A'(k) \quad (2.1-24)$$

$$S^{*''}(k) = - \sum_{l=1}^q b(l)(S^{*''}(k)\cos(2\pi lk/N) + S^{*'}(k)\sin(2\pi lk/N)) + A''(k) \quad (2.1-25)$$

where $S^{*'}(k), A'(k)$ are the real parts and $S^{*''}(k), A''(k)$ are the imaginary parts of $S^*(k)$ and $A(k)$.

In order to obtain the range of values of the $b(1)$'s, the numerator $N(z)$ of the Z transform of the sum of two cosines is given by

$$\begin{aligned} N(z) = & (A_1 + A_2) - (A_1 (\cos w_1 T + 2 \cos w_2 T) + A_2 (\cos w_2 T + 2 \cos w_1 T)) z^{-1} \\ & + (A_1 + A_2) (1 + 2 \cos w_1 T \cos w_2 T) z^{-2} \\ & - (A_1 \cos w_1 T + A_2 \cos w_2 T) z^{-3} \end{aligned} \quad (2.1-26)$$

where A_1 and A_2 are the amplitudes of the cosines and $w_1 T$ and $w_2 T$ are as before. Again we have that the values of the cosines in (2.1-26) are between -1 and 1 so that we can obtain the range of the $b(1)$'s. When substituting in the limiting values of the cosines into (2.1-26) it is noticed that each coefficient has the sum of $(A_1 + A_2)$. This sum is the gain factor G which cannot be found using this method so that it is factored out of the numerator. Equation (2.1-26) can then be represented as

$$N'(z) = 1 + b'(1)z^{-1} + b'(2)z^{-2} + b'(3)z^{-3} \quad (2.1-27)$$

where

$$N'(z) = N(z) / (A_1 + A_2).$$

The modified coefficients of the numerator $b'(1)$ have the following ranges

$$-3 \leq b'(1) \leq 3$$

$$-3 \leq b'(2) \leq 3$$

$$-1 \leq b'(3) \leq 1$$

(2.1-28)

Again we are assured a stable filter if the coefficients are within these ranges. It can be shown as before that (2.1-24) and (2.1-25) can be used to find the numerator coefficients of $H(z)$ with $q=3$.

Once the coefficients of both the numerator and denominator have been calculated, one can obtain the spectrum from $H(z)$ or the normalized estimate of the time series by taking the inverse z transform of $H(z)$. The inverse z transform is chosen for determining the estimated time signal because it is possible to obtain a closed form solution of the estimate. From this closed form the ratio of the amplitudes and the phases can be obtained to compare with the exact solution. So far there has been no mention of exactly how the coefficients are to be solved for. In the next section a discussion of how the problem is formulated to linear programming which is the method of solution used to obtain the unknown values of the coefficients is discussed.

2.2 1, Norm Formulation and Linear Programming

A linear optimization problem can be stated in the form

$$\begin{aligned} &\text{minimize } \sum_i (c(i) - Dx) \\ &\text{subject to } Px \leq q \\ &\qquad\qquad Gx = h \end{aligned} \qquad (2.2-1)$$

where the term in the summation is called the objective, and the two sets of linear equations are the conditions of the problem. An optimum solution is obtained when the conditions of the problem and the given objective are satisfied simultaneously. A minimum feasible solution satisfies (2.2-1) and the condition that all the x 's of the solution are nonnegative. The minimum feasible solution is obtained using linear programming methods which were first introduced by Dantzig [30].

In many applications of the linear optimization problem, the solution vector must have both positive and negative values. To overcome this problem the solution vector is replaced by the difference of two positive valued vectors given by $x-y$. Looking at (2.2-1) a special form of the optimization is obtained if the variables $c(i)$ and D of the objective are replaced by the variables h and G respectively. It is seen that by doing this substitution

the objective is the summation of the difference between a value obtained by multiplying the solution vector x with the matrix G , and the known quantity h . This summation which can be termed the residual is zero only when the conditions are satisfied exactly. In the cases where they are not, the residual will be a positive or negative number. Therefore, one can write the objective as

$$\text{minimize } \sum (h - Gx + Gy) \quad (2.2-2)$$

or

$$\text{minimize } \sum (u - v) \quad (2.2-3)$$

where u and v are positive valued vectors to be consistent with the linear programming formulation. From (2.2-2) and (2.2-3) one has

$$Gx - Gy + u - v = h \quad (2.2-4)$$

where $x \geq 0$

$y \geq 0$

$u \geq 0$

$v \geq 0$.

Using (2.2-3) and (2.2-4), equation (2.2-1) is rewritten as

$$\begin{aligned}
 &\text{minimize} && \sum u-v \\
 &\text{subject to} && Px-Py \leq q \\
 &&& Gx-Gy+u-v=h
 \end{aligned}
 \tag{2.2-5}$$

In this form the linear optimization problem is minimizing the l_1 norm of the residual $(u-v)$.

The variables x, y, u, v of the linear optimization problem can be solved for using the simplex method [31]. In the simplex method once a feasible solution has been determined, a minimum feasible solution is obtained in a finite number of steps. These steps, consist of finding a new feasible solution whose corresponding value of the objective function is less than the value of the objective function in the preceding case. This process continues until a minimum solution has been reached. One is never guaranteed that a solution exists. If no solution exists it is either because no solution exists in terms of nonnegative values of the variables can be found or a nonnegative solution yields an infinite value to the objective function.

It is found that for the problem of section 2.1, it is possible to obtain a minimum feasible solution in determining the coefficients of the ARMA model. The next step is to show how one goes about relating the problem of section 2.1 to the linear optimization problem.

In (2.2-5) it is seen that the variable q is part of the inequality condition. When the equation for the determination of the denominator coefficients was being derived, it was seen from (2.1-9) that the coefficients have limiting values. Two of these conditions can be placed into the inequality condition of (2.2-5). As an example the inequality

$$-4 \leq a(1) \leq 4 \quad (2.2-6)$$

can be written as

$$\begin{aligned} a(1) &\leq 4 \\ -a(1) &\leq 4 \end{aligned} \quad (2.2-7)$$

The first inequality of (2.2-7) represents the upper limit and the second inequality represents the lower limit of (2.2-6). The last two conditions of (2.1-19) can be placed into the equality condition of (2.2-5). Equations (2.1-9) and (2.1-10) can also be placed into the equality conditions of (2.2-5). The $a(i)$'s of the equations are the unknowns being solved for, the $S'(k)$ and $S''(k)$ on the left side of the equals sign make up the vector h , the $B'(k)$ and $B''(k)$ are the residuals which are to be minimized, and the matrix G is made up of the terms involving the sines and cosines. By making these substitutions into the lin-

ear programming format, one is able to solve for the unknown coefficients. An identical analysis can be made for determining the coefficients of the numerator from (2.1-24), (2.1-25) and (2.1-28).

2.3 Computer Simulation and Results

The method of solution was simulated using the Simplex Linear Programming subroutines contained in the International Mathematical and Statistical Library (IMSL) Fortran callable subroutine package. CUNY's IBM computer system was used. To show how effective this new method is, we chose a signal whose FT contains two frequency pulses in the frequency domain which could be placed closely together. To satisfy this condition we chose

$$s(n) = \sqrt{2} \cos(2\pi(110)n/N) + \sqrt{20} \cos(2\pi(114)n/N) + w(n) \quad (2.3-1)$$

where $0 \leq n \leq 511$, $N=512$ and $w(n)$ is Gaussian noise with variance σ^2 . The signal-to-noise ratio (SNR) of the first cosine is given by $10\log(1/\sigma^2)$ and of the second $10\log(10/\sigma^2)$. The bandwidth is given by

$$\Delta f = (114-110)/N = 0.0078125$$

which will be used in the determination of the time-bandwidth product.

Fig. 2.3.1 shows the signal $s(n)$ when there is no noise and all 512 points are used. We can see that $s(n)$ contains an envelope of a sinusoid with six periods in the 512 points shown. Fig. 2.3.2 shows the log of the magnitude of the Fourier transform of $s(n)$, where we see two pulses located at the frequencies of the signal. The rest of the magnitudes are so close to zero that their logs are very negative and cannot be shown in the figure. In Fig. 2.3.3 we have added noise with a variance $\sigma^2 = 1.0$ and we see that it is impossible to distinguish how many periods the envelope of the signal contains. The spectrum of this noisy signal is shown in Fig. 2.3.4 where one of the things that one notices right away is that the spectrum is now centered about the 0.0 db level. This corresponds to the spectrum of the noise being added to the spectrum of the signal. The reason why the noise did not affect the pulses is because the noise is not large enough to bury any of the pulses when all of the points are used in determining the spectrum. Noise plays a large role in the determination of the location of these pulses when not all the points are used and the two pulses begin to smear together.

In order to be able to compare the location of the poles

and zeros of $s(n)$, Fig. 2.3.5 shows the first quadrant of the z -plane. We chose to show only the first quadrant because all the poles and zeros of our $s(n)$ can be shown here with the understanding that for complex poles and zeros, there are mirror images of these poles and zeros in the fourth quadrant. Fig. 2.3.5 shows two poles located on the unit circle which represent the locations of the two pulses in the spectrum. The zero in between the poles on the unit circle is the dip that occurs between the two pulses in the spectrum of Fig. 2.3.2. The zeros on the real axis along with the complex poles and zeros are used to calculate the amplitudes and phases of the signal $s(n)$.

In order to have a uniform method of measure when truncating the signal $s(n)$, we define the time bandwidth product (TBW) as the number of samples used multiplied by the normalized bandwidth of the signal which was defined earlier for our case. This definition can be explained by looking at the spectrum of a DFT having length N . The DFT is a two-sided transform so that the spectrum has both positive and negative frequencies. The maximum frequency of the spectrum is $N/2$ which in terms of a normalized frequency can be divided by N to give $1/2$. This frequency is known as the Nyquist frequency because it gives the separation between time samples as $1/N$. The Nyquist frequency is also the bandwidth of the signal since it is assumed that the

spectrum has a periodic extension beyond this frequency. Therefore, if all N time samples are used, the time-bandwidth product is given by

$$TBW = N \cdot (1/N) \cdot (N/2) = N/2$$

from which the normalized TBW is given by $1/2$. For the DFT, the separation of time samples is given by $1/N$. If the bandwidth of the signal is taken to be less than $N/2$, it is seen that the normalized bandwidth will be less even when all of the N samples are used. A normalized TBW of less than 0.5 corresponds to choosing the separation between time samples too far apart so that the signal is undersampled. It can be seen that a $TBW=0.5$ is the limiting value for spectral resolution. If TBW becomes smaller, then any two peaks spaced closely together will become undistinguishable because they smear into one broader peak. Even when TBW is greater than 0.5, there may be difficulty in distinguishing the two peaks if the noise power is high enough to hide the weaker pulse.

For the first case to test our method, we chose to use only 92 out of the 512 samples. This gives a TBW of 0.719. In Fig. 2.3.6 we show the truncated time signal $s(n)$ with noise variance $\sigma^2=1.0$. The spectrum obtained using the FT of this signal is shown in Fig. 2.3.7. In the spectrum of Fig. 2.3.7 we see that the two pulses are smearing into one with a very shallow dip between the two peaks very close

in height to the weaker pulse. This shallow dip is due to both the TBW and the noise. The combination of the two makes for the difficulty in judging that there should be two peaks. After using our method, in calculating the coefficients of the numerator and denominator of the parametric model, we found the pulses of the spectrum to be at normalized frequencies $\tilde{f}_1=0.2148$ and $\tilde{f}_2=0.2285$ as compared to the actual values $f_1=0.2149$ and $f_2=0.2227$ which shows that we are very close to the original values with our estimates. The pulses at these frequencies are shown in Fig. 2.3.8 where the dip that is located between the two pulses is at $f=0.2231$ as compared to where it should be at $f=0.2167$. The location of the dip represents the complex zero located on the unit circle of the z-plane.

We observe that the first pulse in Fig. 2.3.8 is larger than the second one, and if we look at Fig. 2.3.2 we see the opposite. If we take a look at the location of the poles and zeros from the coefficients calculated we see that they are located as follows

poles: 0.219+j0.975	zeros: 0.166+j0.977
0.134+j0.991	0.203
	0.0

which are plotted in the z-plane in Fig. 2.3.9. The actual locations are shown in Fig. 2.3.5 and are given by

poles: 0.219+j0.975	zeros: 0.207+j0.978
---------------------	---------------------

$$0.170+j0.985$$

$$0.183$$

$$0.0$$

By comparing the location of the poles and zeros we see that there is an error in the location of the estimated ones. These errors are not that great but they have caused the first peak to be higher than the second peak. By taking the inverse Z transform of the parametric model using the coefficients calculated, we obtained the normalized signal estimate $s(n)$ given by

$$s(n)=0.612\cos(1.349n+0.1479)+0.402\cos(1.435n-0.1741) \quad (2.3-2)$$

which if we compare to (2.3-1) we see that the first cosine has a larger amplitude and both cosines have a phase which is not in (2.3-1). The estimated signal is shown in Fig. 2.3.10 where the envelope of the signal is a sinusoid having seven periods in the 512 samples compared to six for the original signal. Again this is a consequence of the error of the location of poles and zeros.

For the next case investigated we chose the same TBW product as before but increased the noise power to $\sigma^2=5.0$. The individual SNR'S are given by -7 db for the smaller amplitude cosine and 3 db for the larger amplitude cosine. Fig. 2.3.11 shows the time truncated version of the signal

which when compared to Fig. 2.3.6 shows how much higher the amplitudes are and it is impossible to see that the signal is periodic. The FT of the signal is shown in Fig. 2.3.12 where it is noticed that the spectrum is higher above the zero db line than in the previous case because the noise power is large. We see that the two peaks are separated by a very shallow dip and that there is a peak on the right side so that it looks like there are three peaks in the range of frequencies the signal is known to be in. The solution to our method gave coefficients from which the spectrum of Fig. 2.3.13 is obtained. The normalized frequencies of the peaks are $\tilde{f}_1=0.2148$ and $\tilde{f}_2=0.2304$. Comparing these values with the actual ones we see that the first peak occurs at the exact frequency and the second peak is only slightly in error. This error is due to the TBW and noise. We see that by increasing the noise five fold we are able to get as good results as when the noise was smaller. The poles and zeros from the coefficients are

poles: 0.219+j0.973	zeros: 0.177+j0.982
0.128+j0.994	0.213
	0.0

which when compared to Fig. 2.3.5 are slightly off. From the location of the poles and zeros we take the inverse Z transform of the parametric model to obtain the equation of the normalized signal $s(n)$

$$s(n)=0.435\cos(1.349n+0.0609)+0.570\cos(1.4478n+0.0961) \quad (2.3-3)$$

which when compared to (2.3-1) shows that the ratio of the amplitudes is incorrect and that the solution introduces phases which were not there originally. This signal $s(n)$ is shown in Fig. 2.3.15 where the number of periods of the envelope of the signal is eight compared to the actual number of six.

In the next case, Fig. 2.3.16 shows the time truncated version of the signal for a $TBW=0.5$ and noise with variance $\sigma^2=1.0$. The spectrum in Fig. 2.3.17 shows that the first peak is not distinguishable because the dip between the two peaks is at the same level as the first peak. With our method, the spectrum obtained is shown in Fig. 2.3.18. It shows two peaks located at $\tilde{f}_1=0.2148$ and $\tilde{f}_2=0.2285$ which are at the same locations as in the first case. By decreasing TBW our method of solution was able to get as good results as when the TBW was larger and the two peaks were more clearly defined. Again we notice that the first peak is larger which is incorrect because of the location of the poles and zeros in the z -plane. The location of the poles and zeros are

poles: 0.219+j0.976	zeros: 0.173+j0.979
0.135+j0.991	0.056

0.0

which have been plotted in Fig 2.3.19. One of the biggest errors in this case is the location of the zero on the real axis. This is causing the amplitudes to be incorrect. By taking the Z transform of the parametric model using these poles and zeros, the time signal obtained is shown in Fig. 2.3.20. The envelope of the signal has seven periods in the time shown. The normalized signal in Fig. 2.3.20 can be written as

$$s(n)=0.544\cos(1.3499n-0.0423)+0.469\cos(1.4358n+0.0924) \quad (2.3-4)$$

As a final case we chose to have a $TBW=0.359$ with a noise variance of $\sigma^2=1.0$. The short duration signal is shown in Fig. 2.3.21. The spectrum of the signal is shown in Fig. 2.3.22 where we see very broad peaks throughout with one very broad peak where the two pulses should be. This broad peak is made up of the two pulses smeared together because of the very small TBW . Looking at it, one could not tell that two pulses belong there. Therefore, to see where these two peaks occur we used our method to determine the coefficients of the parametric model. The resultant spectrum is shown in Fig. 2.3.23. The normalized frequencies of the pulses are $\tilde{f}_1=0.2148$ and $\tilde{f}_2=0.2305$. The second estimate is incorrect but is the identical location found

when the $TBW=0.718$ and the noise variance was $\sigma^2=5.0$. By decreasing the TBW , our method did no worse than for the second case investigated. The location of the poles and zeros of Fig. 2.3.24 are

poles: 0.219+j0.976	zeros: 0.159+j0.978
0.122+j0.992	0.277
	0.0

By taking the inverse Z transform of the pole-zero model, we found the normalized estimate of the signal to be

$$s(n)=0.608\cos(1.3496n+0.1452)+0.404\cos(1.4483n-0.1072)$$

(2.3-5)

which is plotted in Fig. 2.3.25.

2.4 Conclusion

We have shown a method to determine the location of two frequencies when the time bandwidth product is small and when noise is added to the signal whose variance is equal to or greater than the power of the smallest cosine. The method makes use of the representation of two impulses in the z -plane which is used to obtain constraints for the maximum and minimum values the coefficients of our parametric model can take. These constraints along with the relationship these coefficients have in the spectrum, we

used linear programming to solve the set of linear equations by minimizing the l_1 norm. Once the coefficients have been solved for we are able to obtain the normalized estimate of the time signal by inverse Z transforming the parametric model.

Four cases were used to simulate our method in showing how affective it is. It was found that by decreasing the TBW we obtained similar results to when a higher TBW was used with a larger noise power. In the last case examined the TBW was so low that the two pulses in the spectrum smeared together showing a very broad peak. Our method was able to obtain a good estimate of the frequencies. The time estimate of the signal is different because the location of the poles and zeros is not exact.

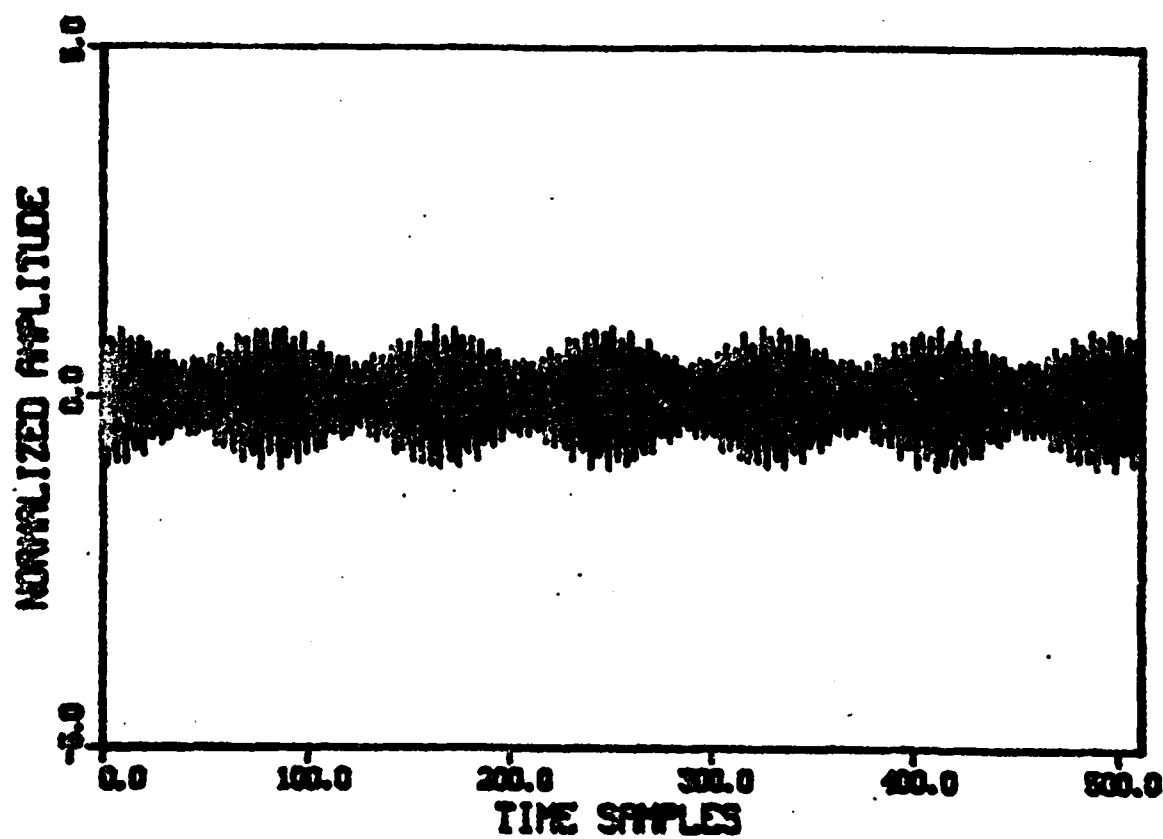


Fig. 2.4.1 Test signal $s(n)$ with no noise and all 512 points are used.

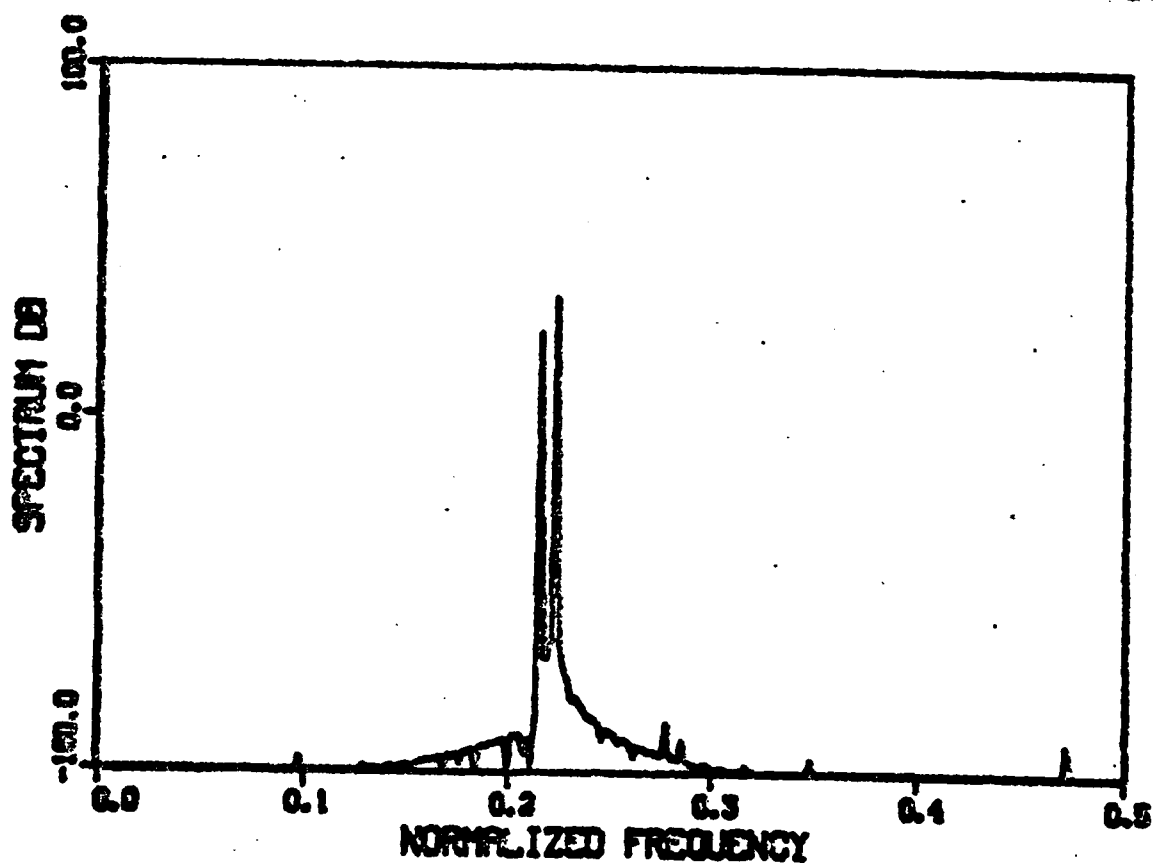


Fig. 2.4.2 Log magnitude of spectrum of $s(n)$ having no noise and all 512 points are used in evaluating the Fourier transform.

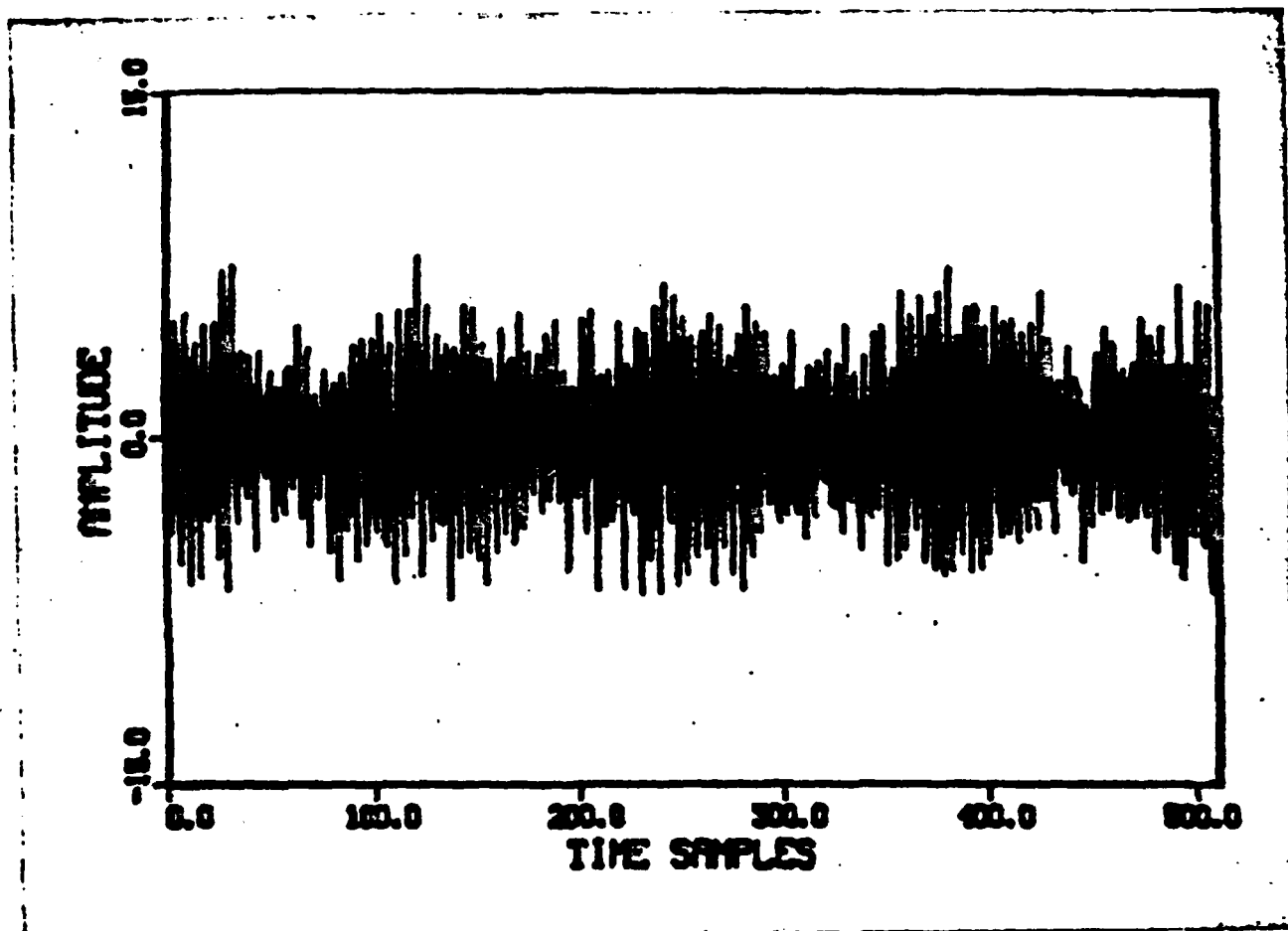


Fig. 2.4.3 Signal $s(n)$ when white Gaussian noise of variance $\sigma^2=1.0$ is added.

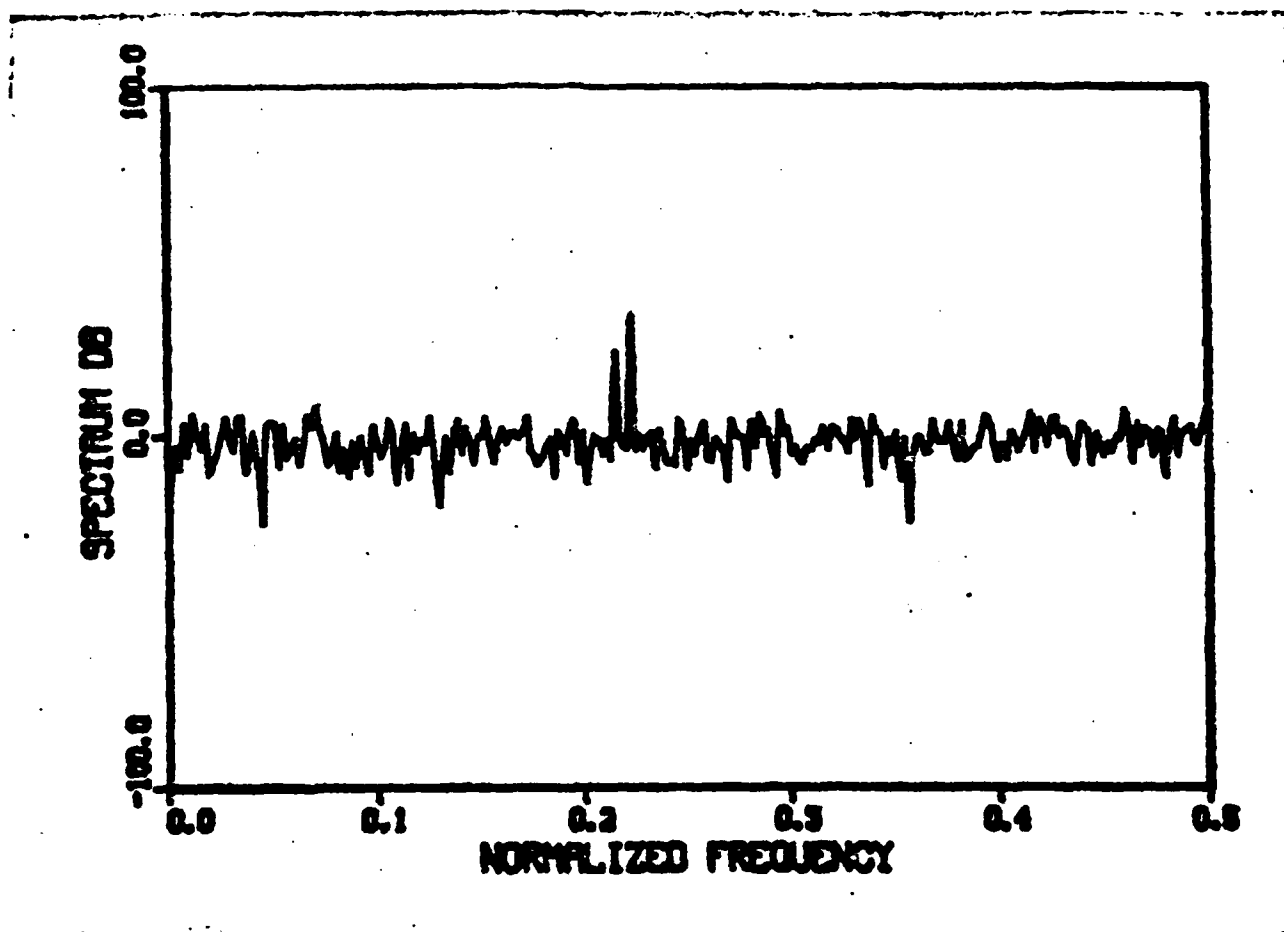


Fig. 2.4.4 Log magnitude of the spectrum of $s(n)$ with noise variance $\sigma^2=1.0$.

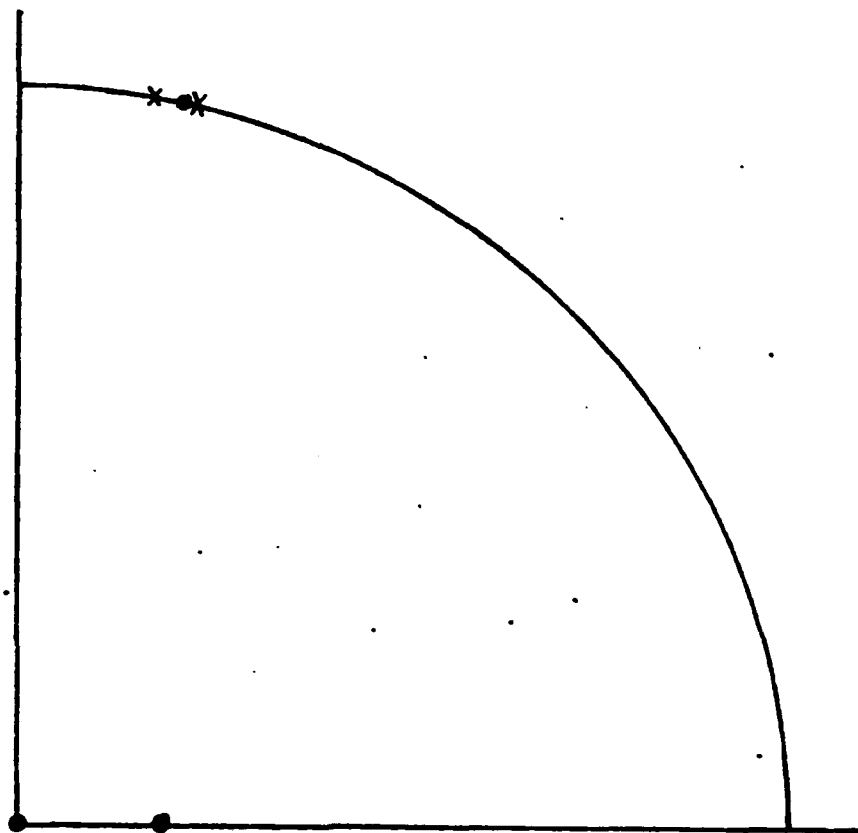


Fig. 2.4.5 First quadrant of the z -plane showing the locations of the poles and zeros of the Z -transform of $s(n)$.

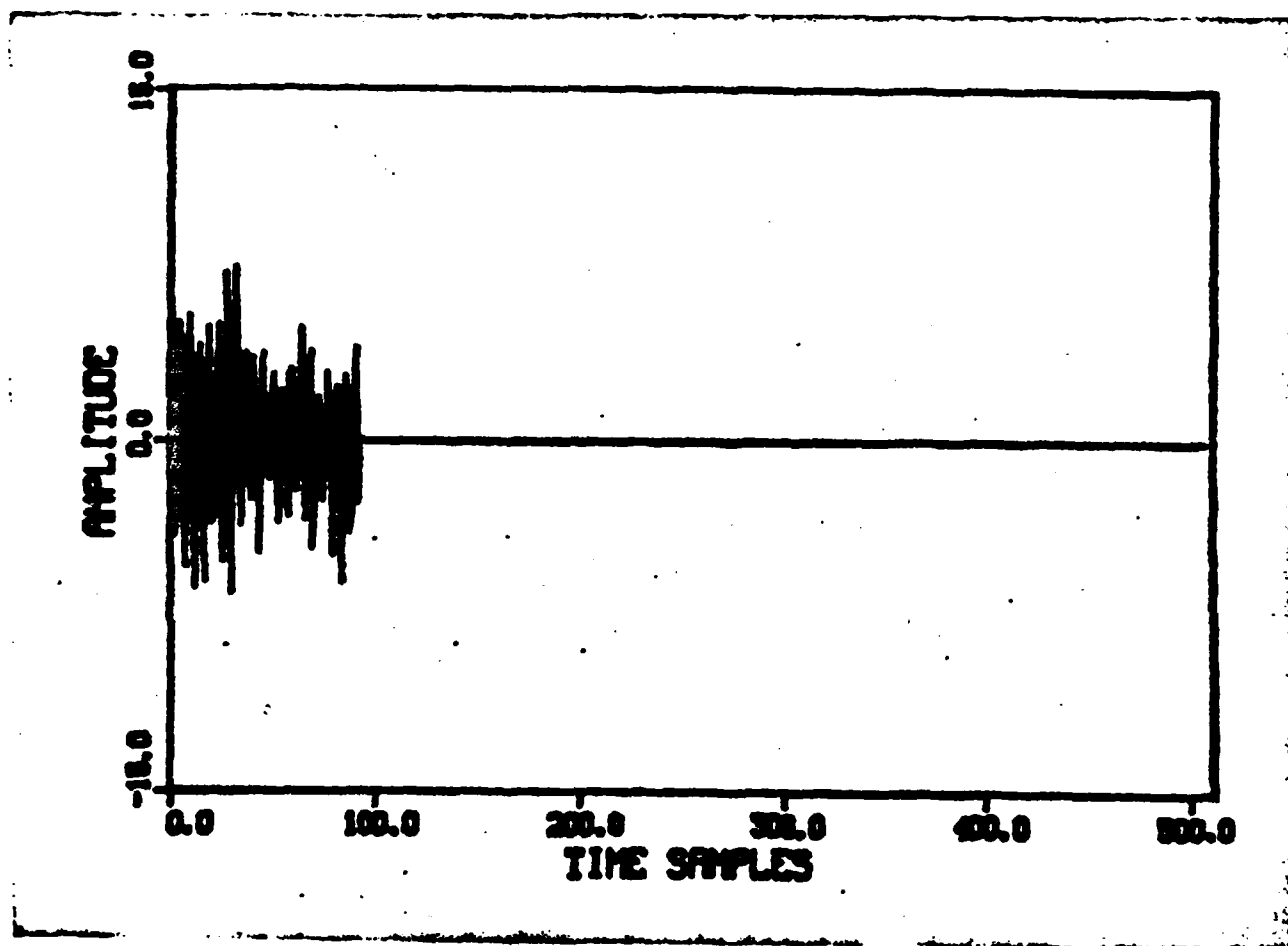


Fig. 2.4.6 Signal $s(n)$ with $TBW=0.719$ and noise variance $\sigma^2=1.0$.

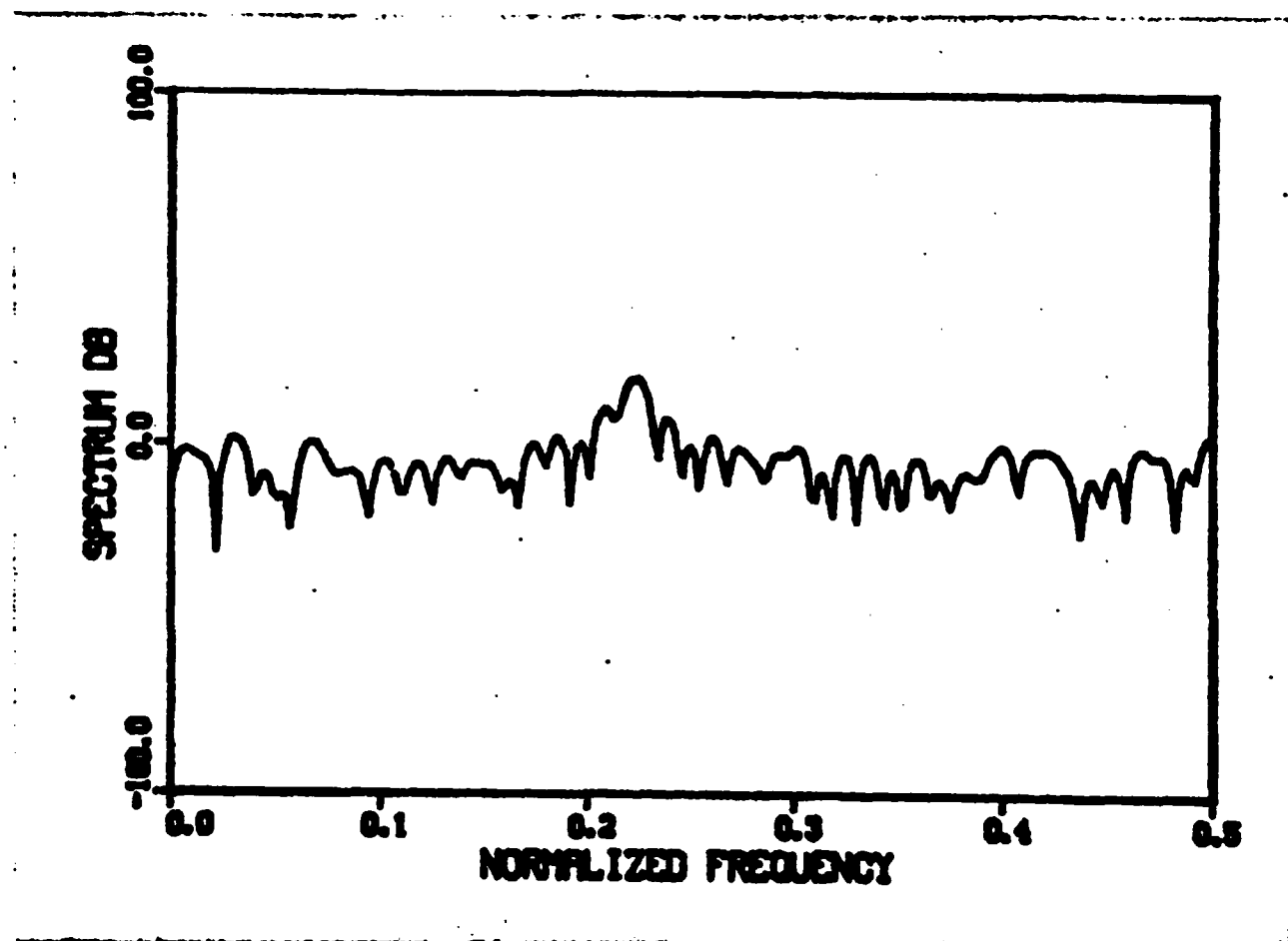


Fig. 2.4.7 Log magnitude of spectrum when the TBW=0.719 and noise has variance $\sigma^2=1.0$.

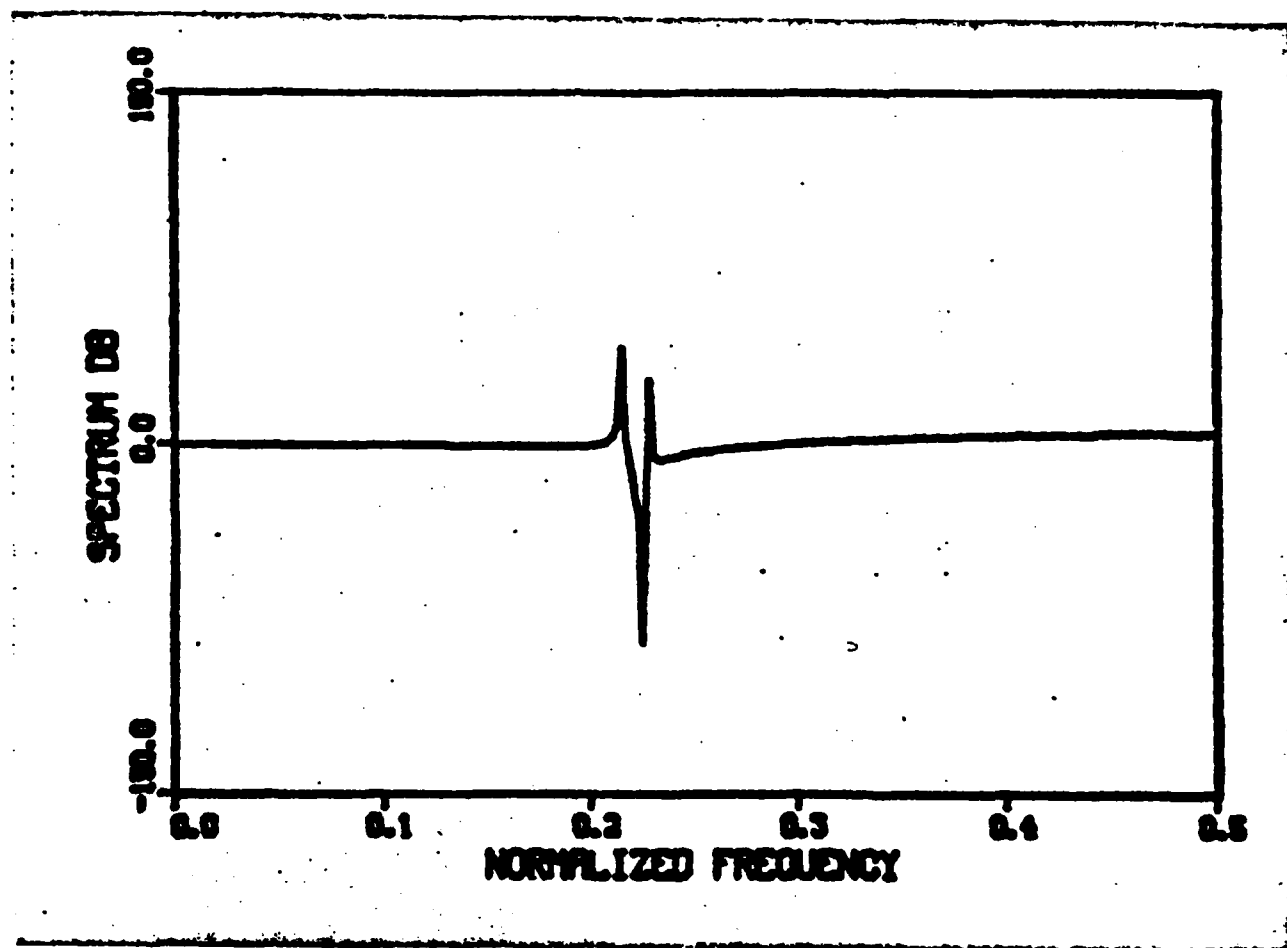


Fig. 2.4.8 Log magnitude of the estimated spectrum obtained using the new method where the normalized frequencies of the positive pulses are given by $f_1=0.2148$ and $f_2=0.2285$.

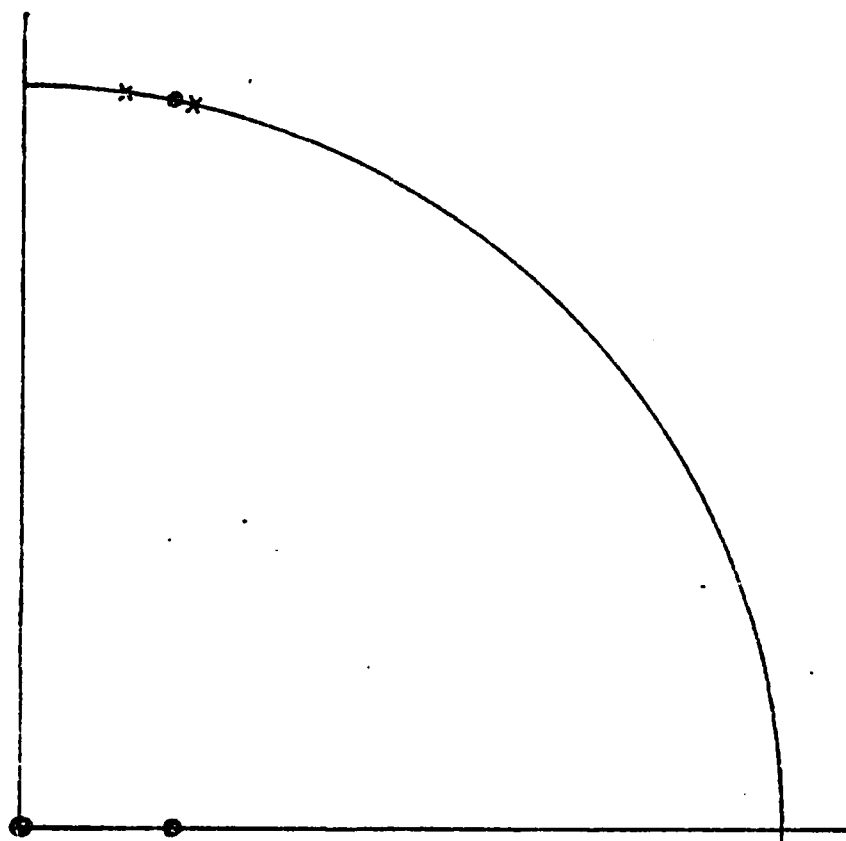


Fig. 2.4.9 Location of poles and zeros in the first quadrant of the z -plane obtained using the new method when $TBW=0.719$ and $\sigma^2=1.0$.

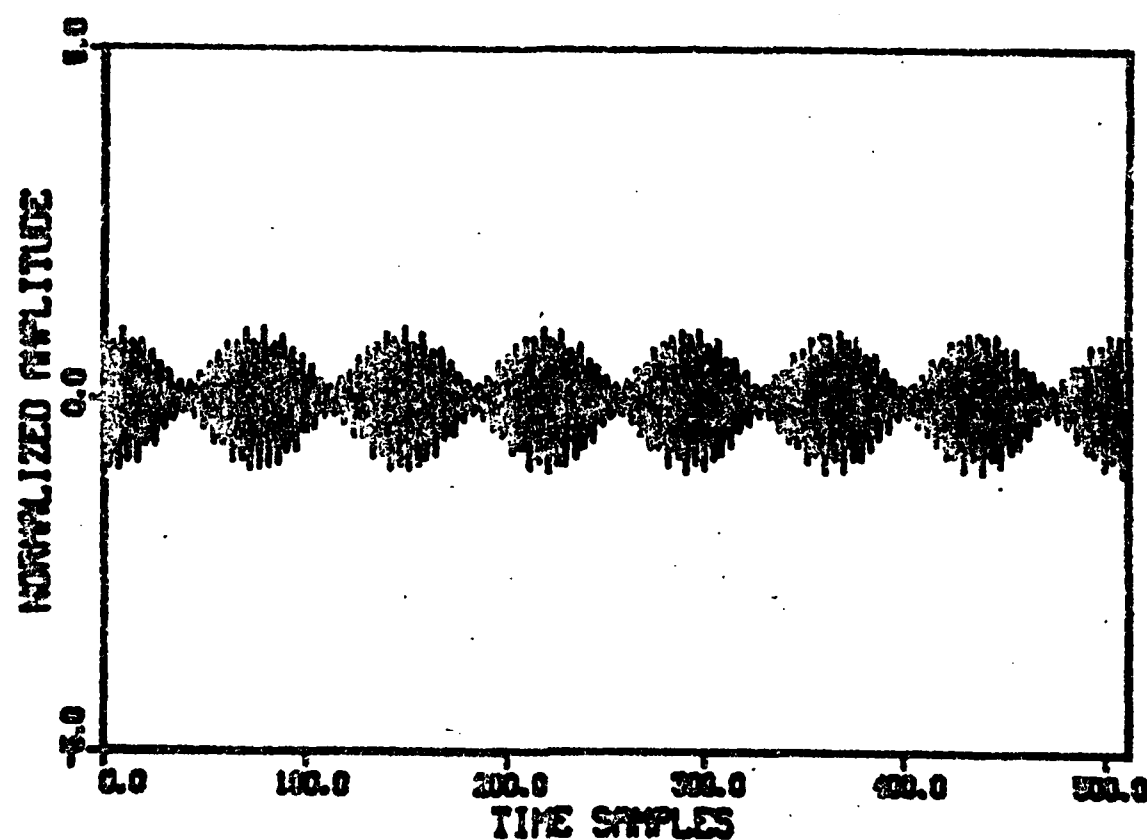


Fig. 2.4.10 Estimated signal $s(n)$ obtained by taking the inverse Z-transform of the transfer function made up of the estimated poles and zeros.

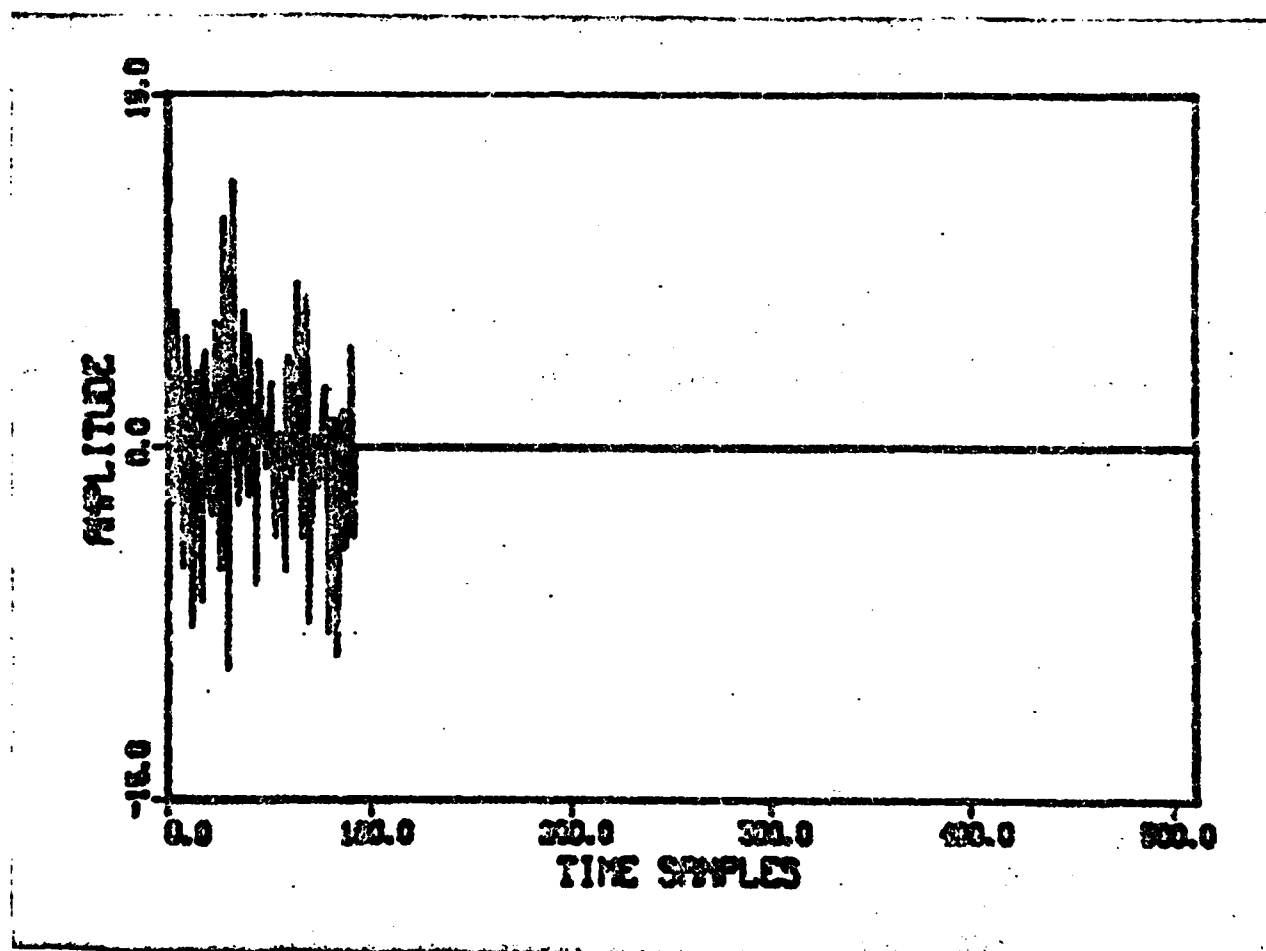


Fig. 2.4.11 Signal $s(n)$ where the $TBW=0.719$ and the variance of the noise has been increased to $\sigma^2=5.0$.

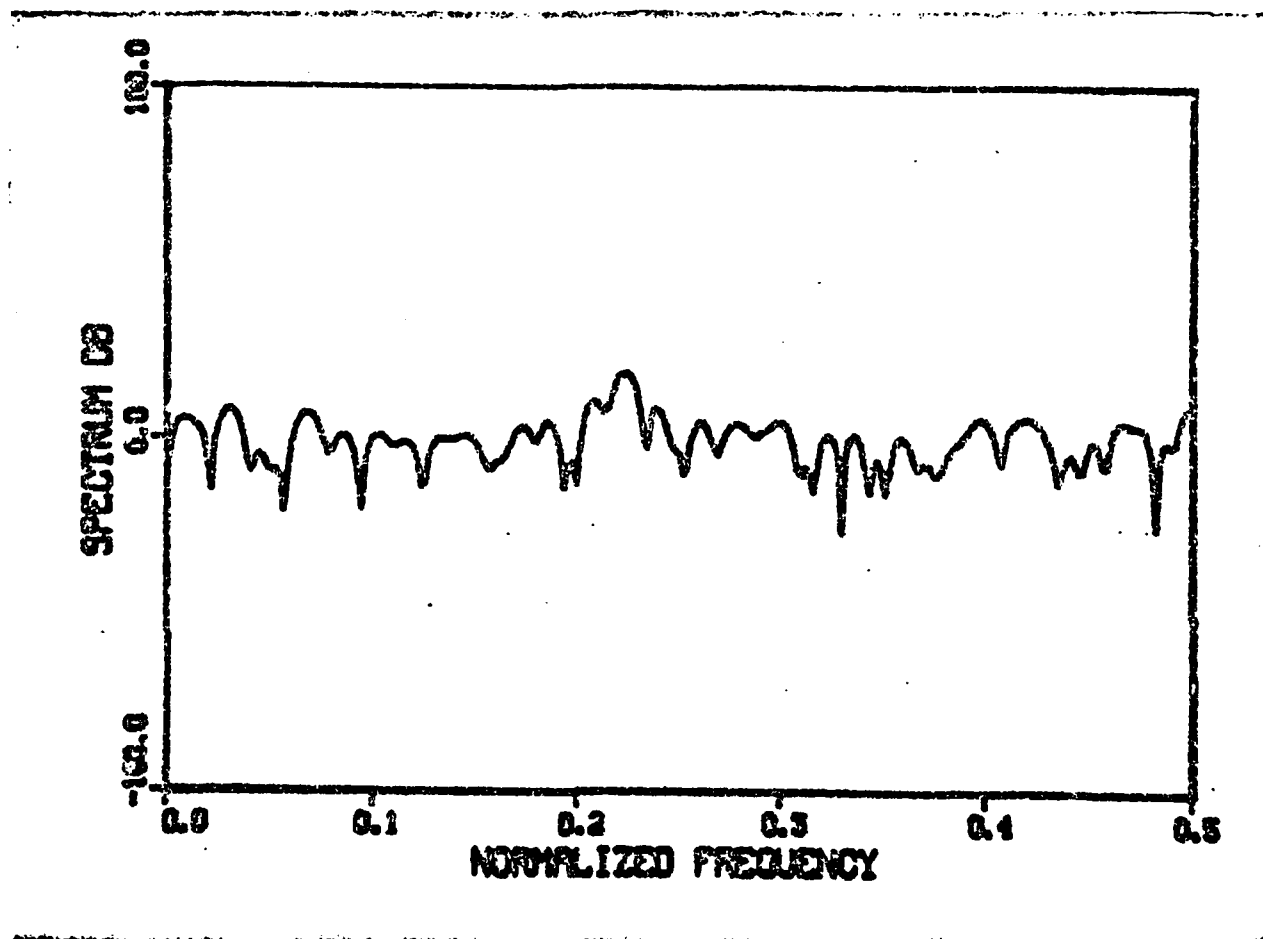


Fig. 2.4.12 Log magnitude of the spectrum of the signal with $TBW=0.719$ and $\sigma^2=5.0$.

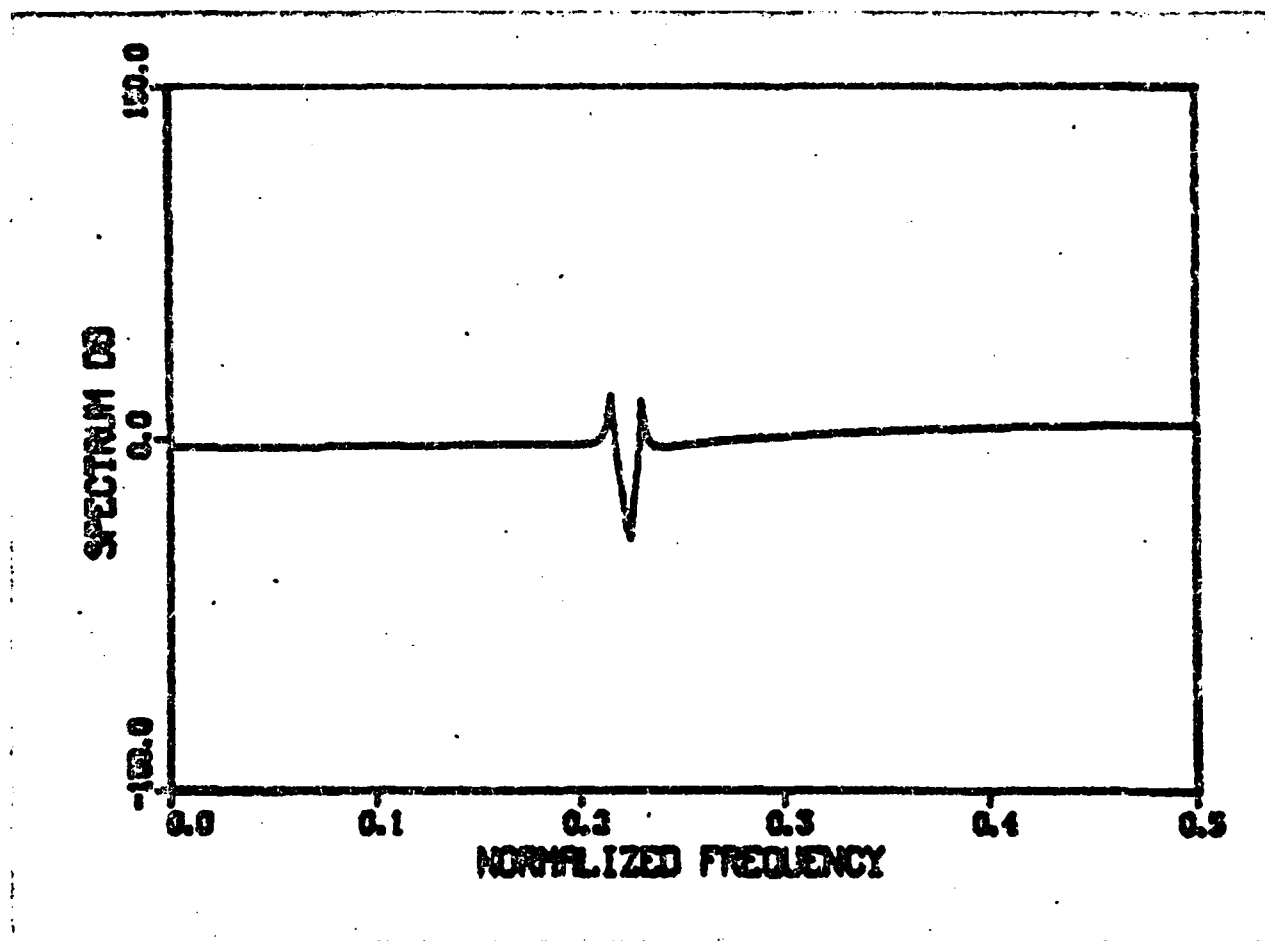


Fig. 2.4.13 Log magnitude of the estimated spectrum using new method with positive peaks occurring at the normalized frequencies $\hat{f}_1=0.2148$ and $\hat{f}_2=0.2304$.

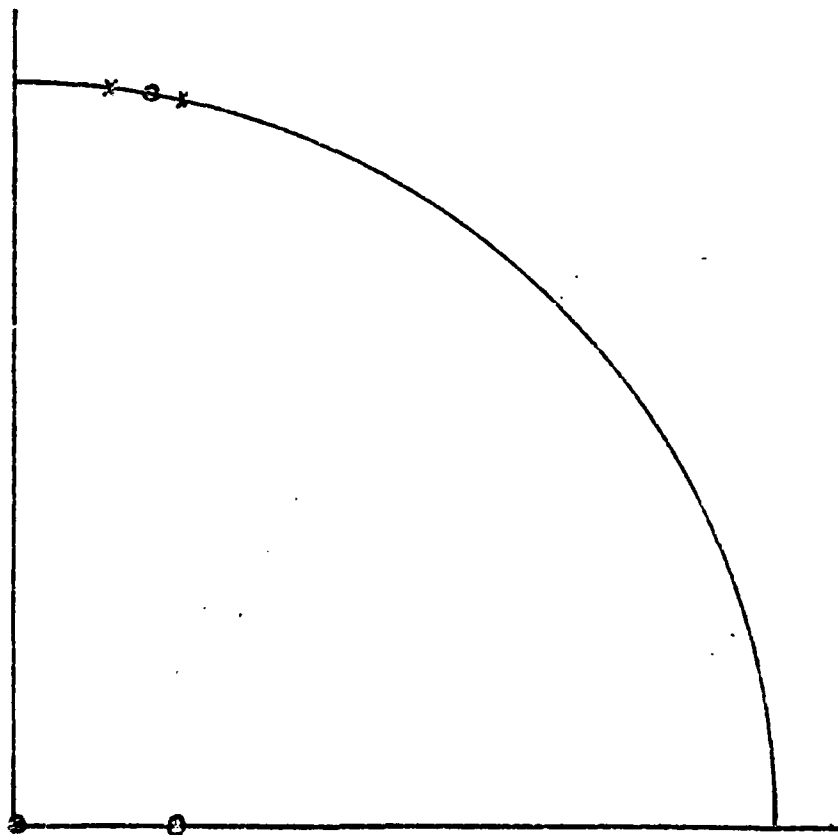


Fig. 2.4.14 Locations of estimated poles and zeros in the first quadrant of the z -plane with $TBW=0.719$ and $\sigma^2=5.0$.

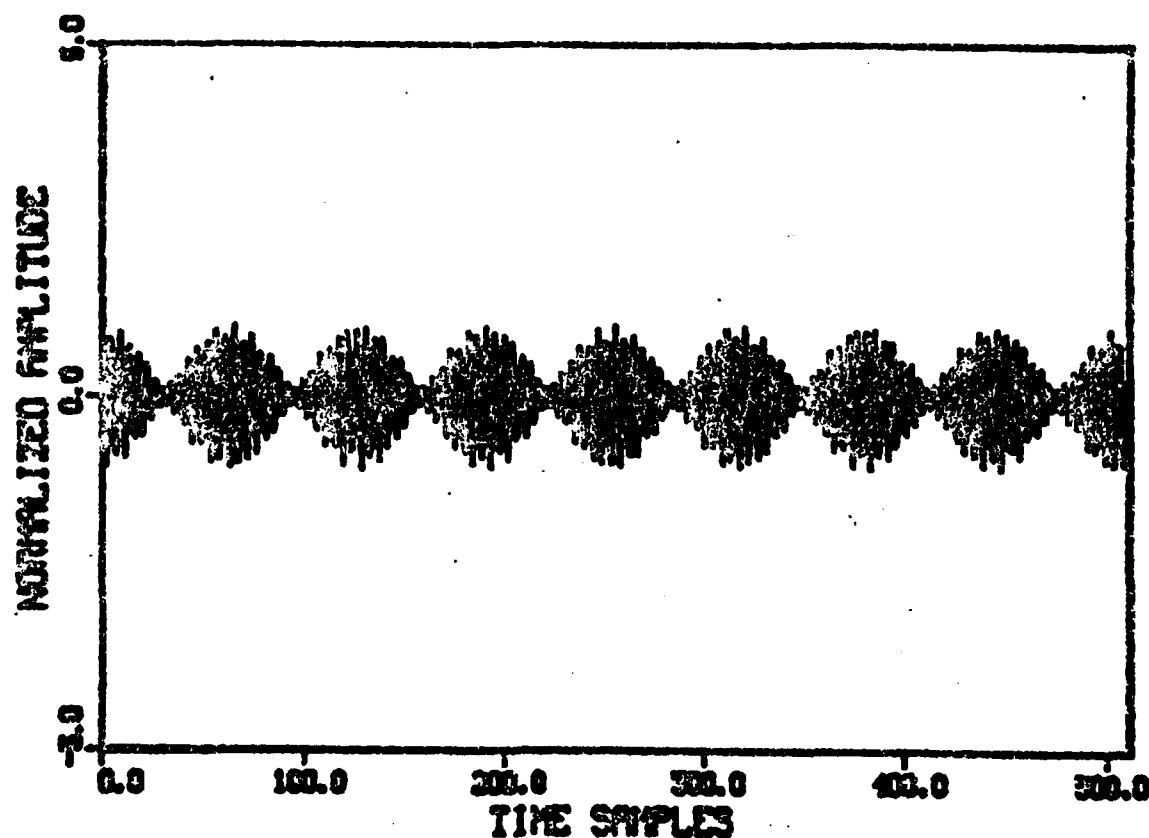


Fig. 2.4.15 Estimated signal $s(n)$ formed by inverse Z-transforming the transfer function made up of the estimated poles and zeros.

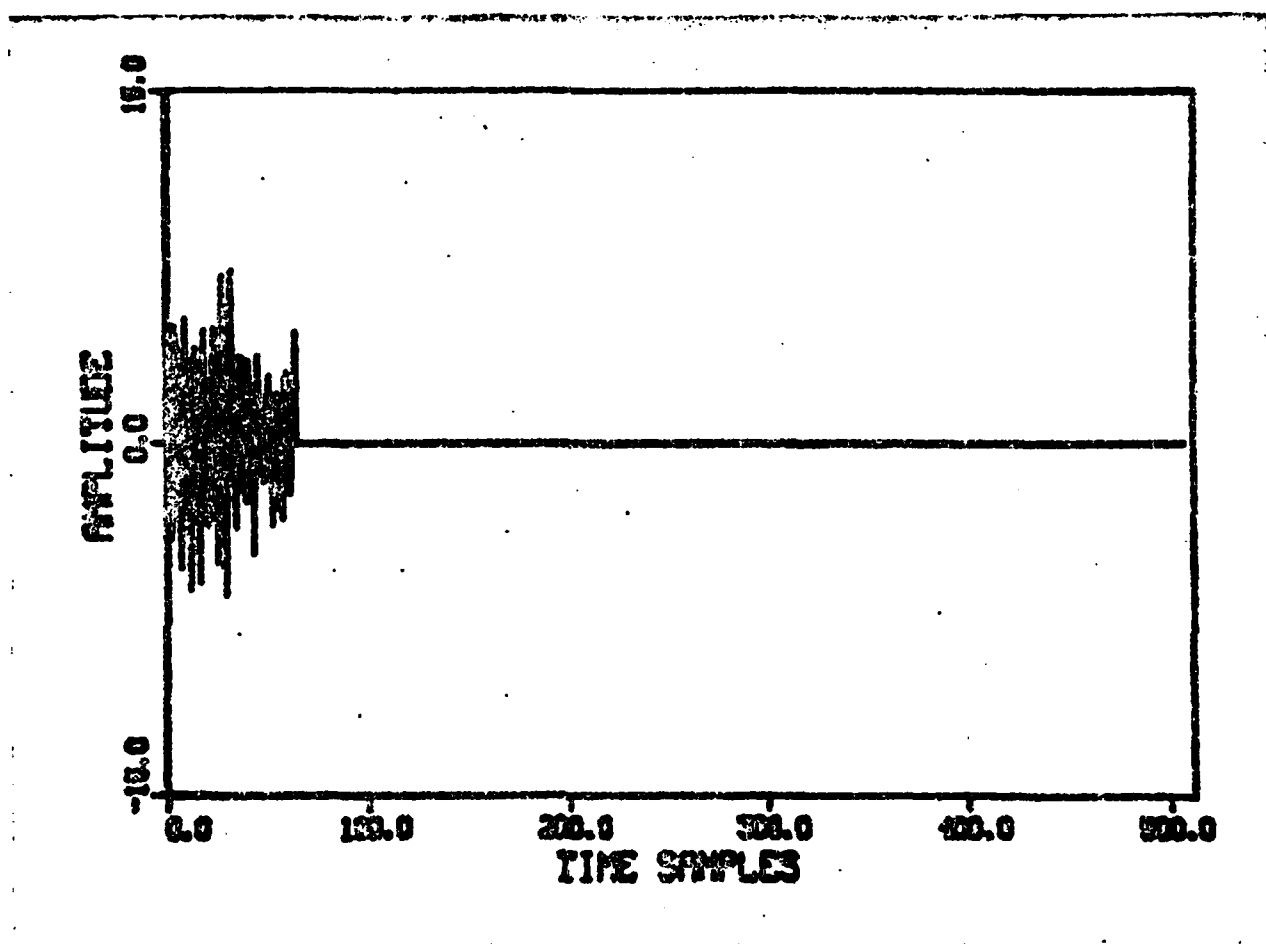


Fig. 2.4.16 Signal $s(n)$ when $TBW=0.5$ and the noise has variance $\sigma^2=1.0$.

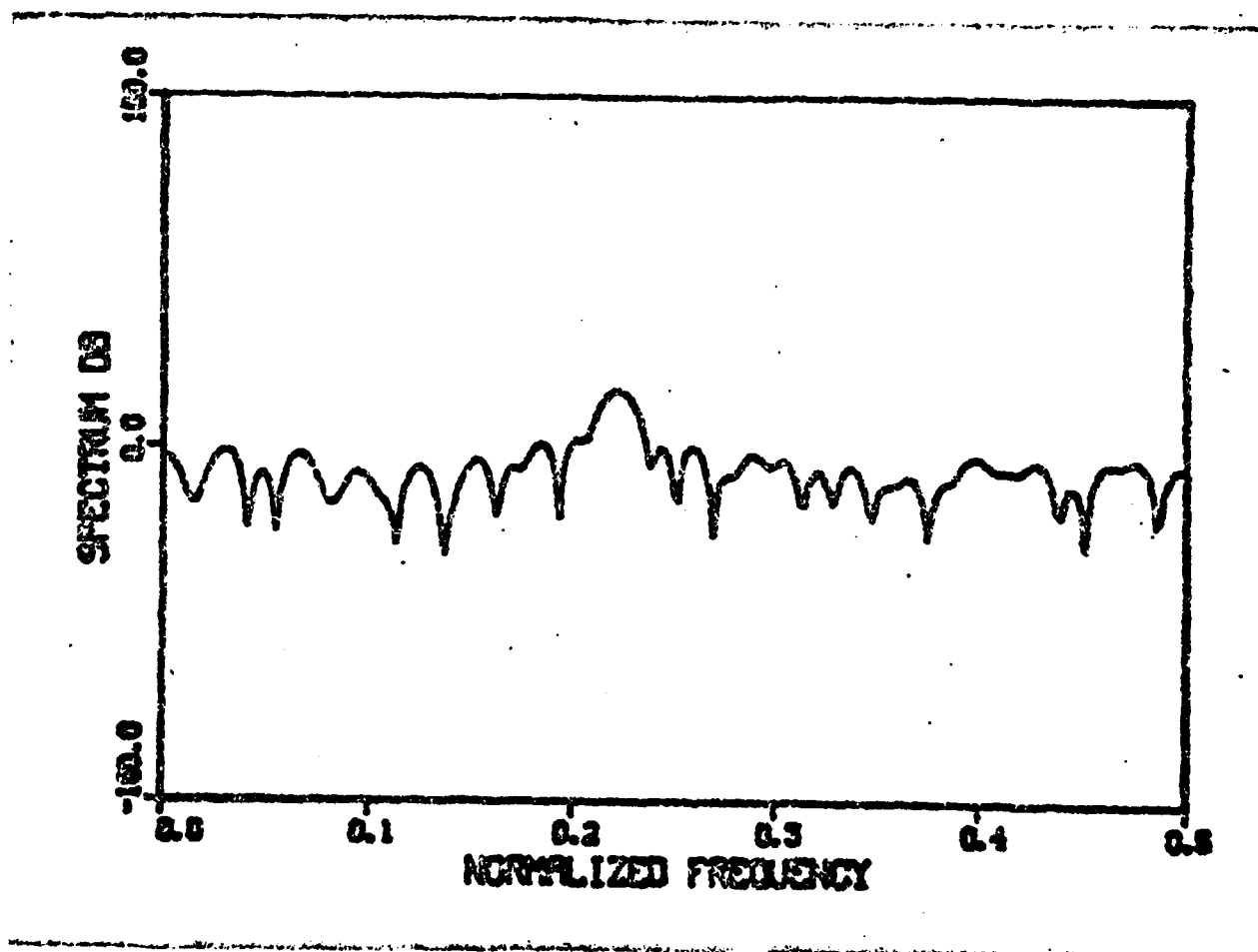


Fig. 2.4.17 Log magnitude of the spectrum of the signal $s(n)$ with $TEW=0.5$ and $\sigma^2=1.0$.

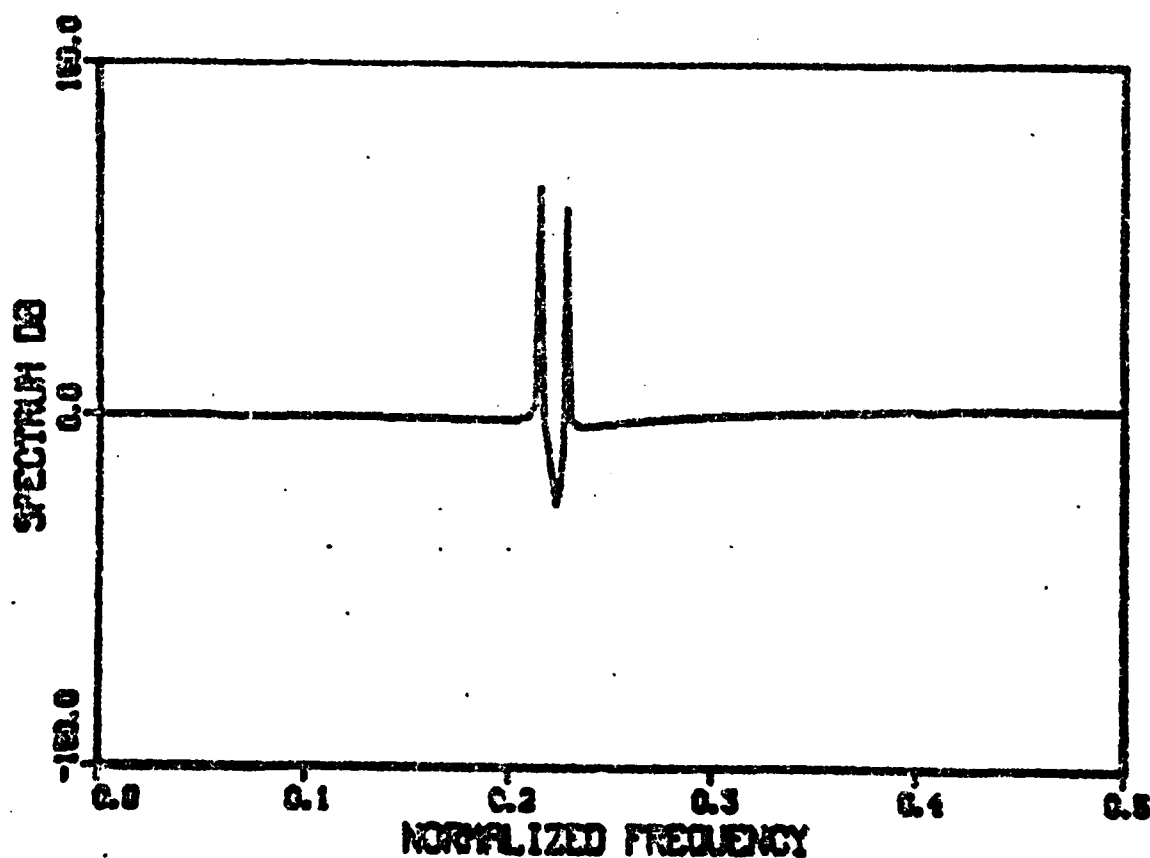


Fig. 2.4.18 Log magnitude of the estimated spectrum using the new method with positive peaks occurring at normalized frequencies $f_1=0.2148$ and $f_2=0.2285$.

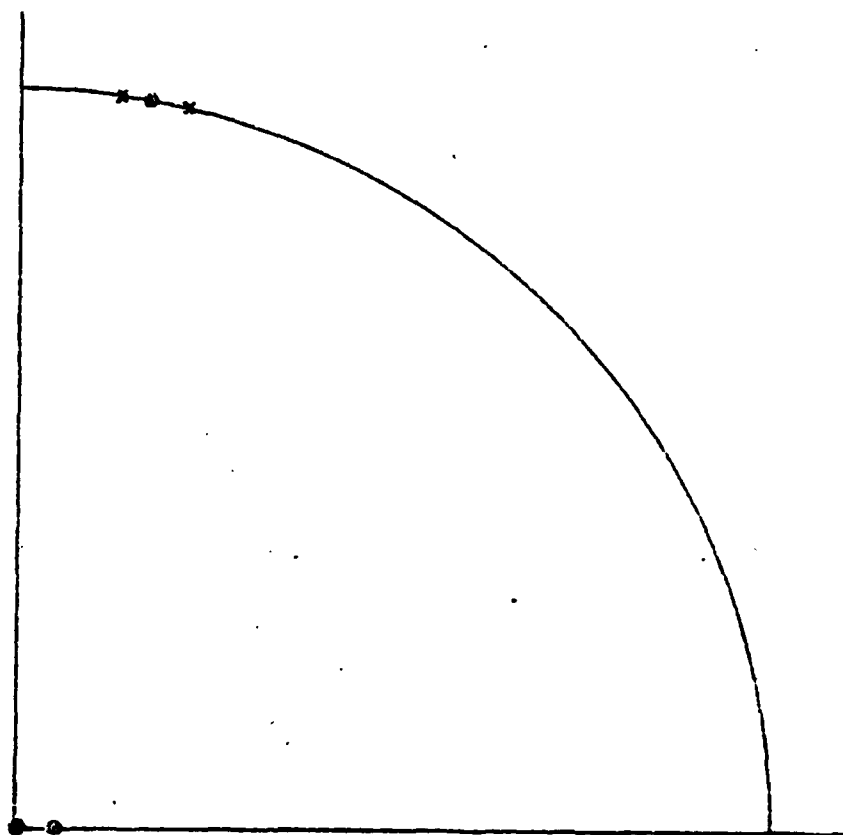


Fig. 2.4.19 Locations of estimated poles and zeros in the first quadrant of the z -plane of signal $s(n)$ having $TBW=0.5$ and $\sigma^2=1.0$.

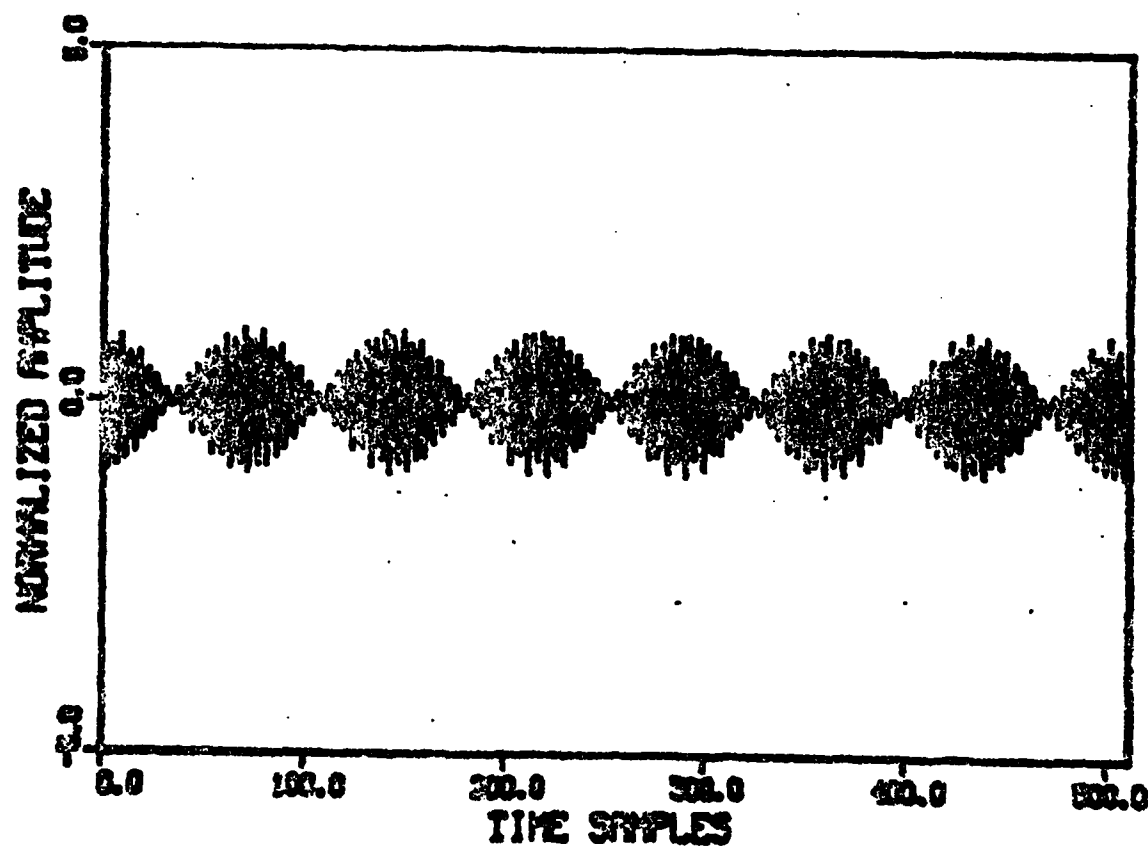


Fig. 2.4.20 Estimated signal $s(n)$ obtained by taking the inverse Z-transform of the transfer function made up of the estimated poles and zeros.

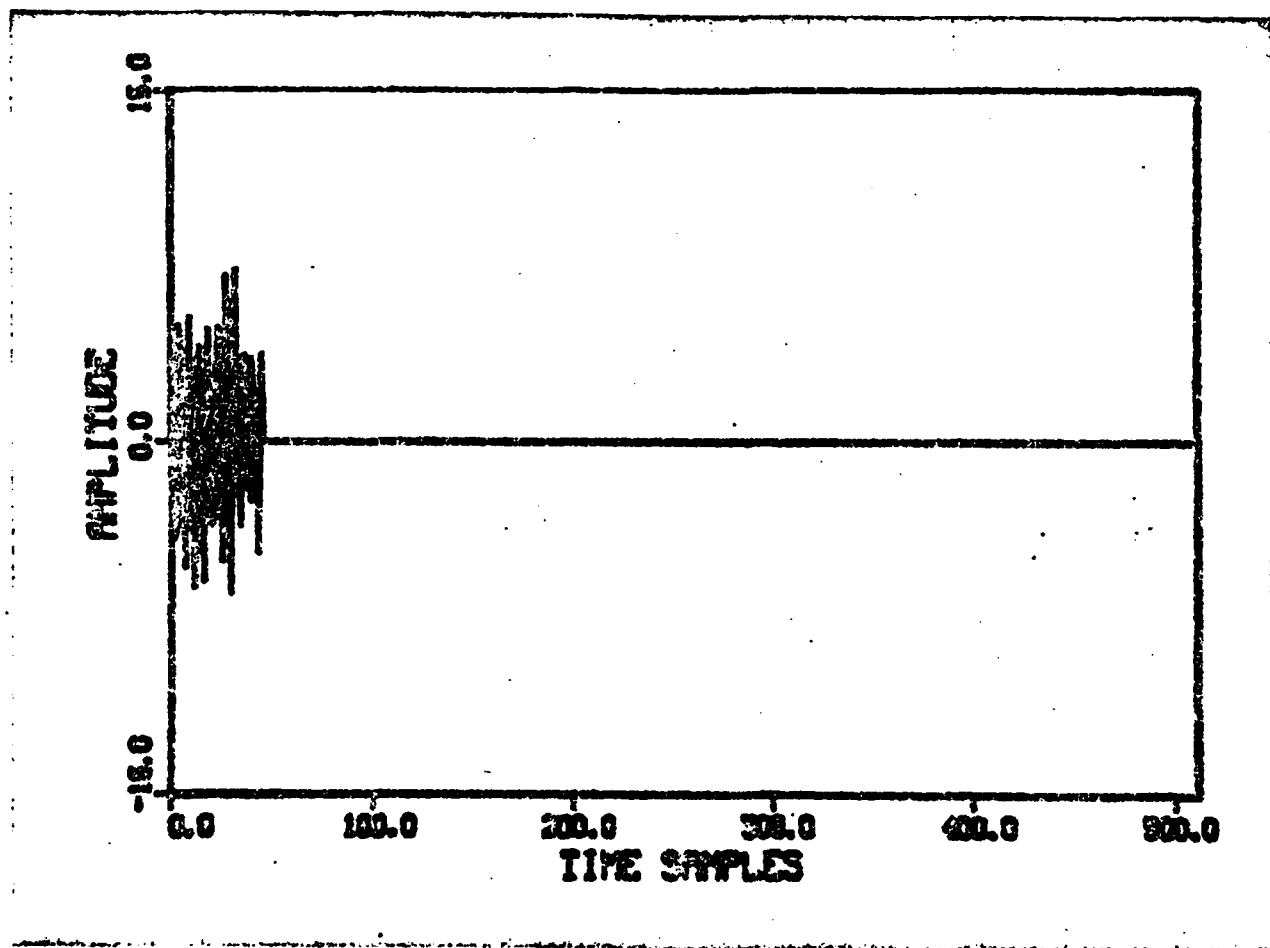


Fig. 2.4.21 Short time duration signal $s(n)$ where $TBW=0.359$ and the noise variance is $\sigma^2=1.0$.

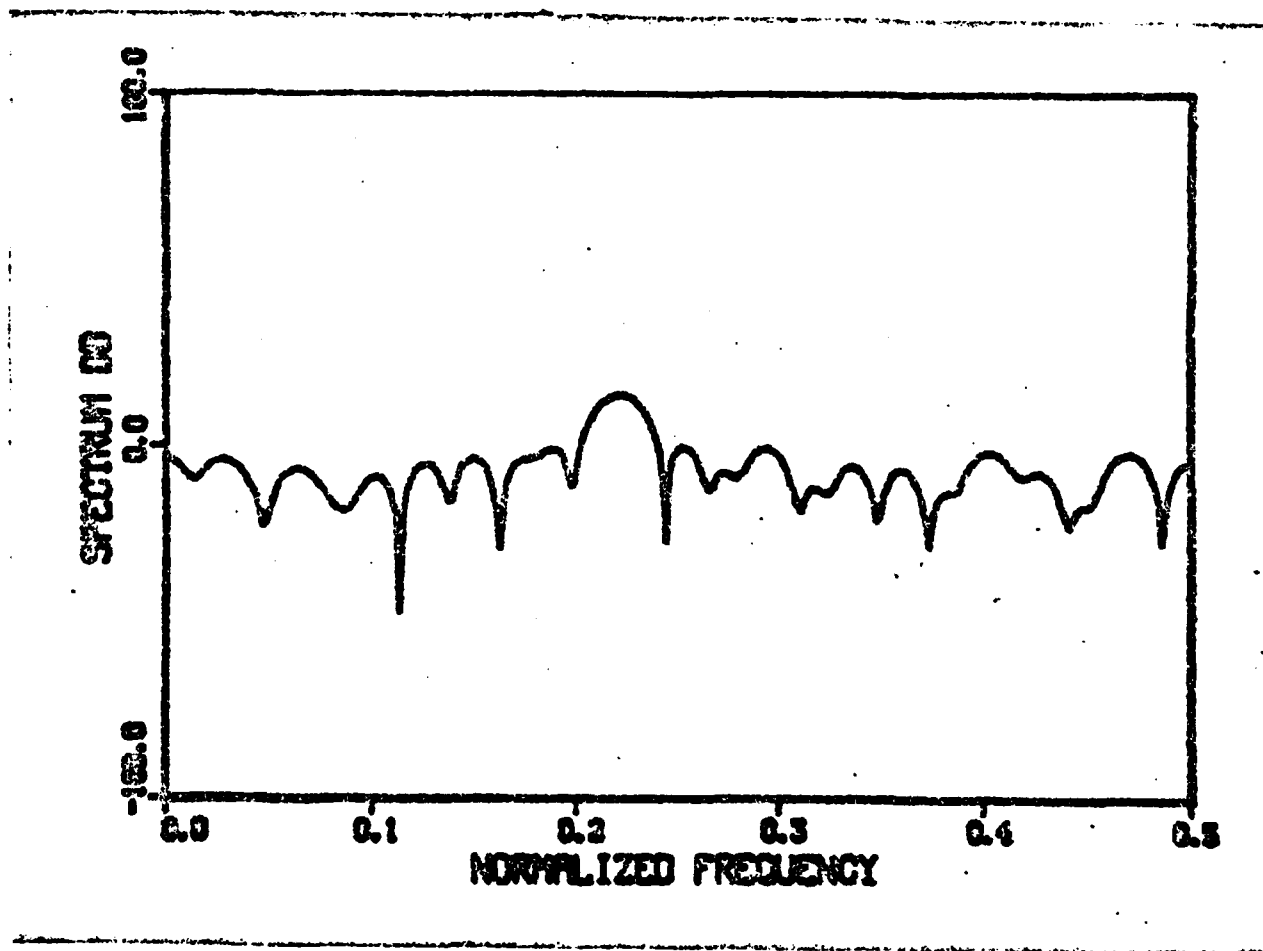


Fig. 2.4.22 Log magnitude of spectrum of $s(n)$ for the short time duration signal $s(n)$.

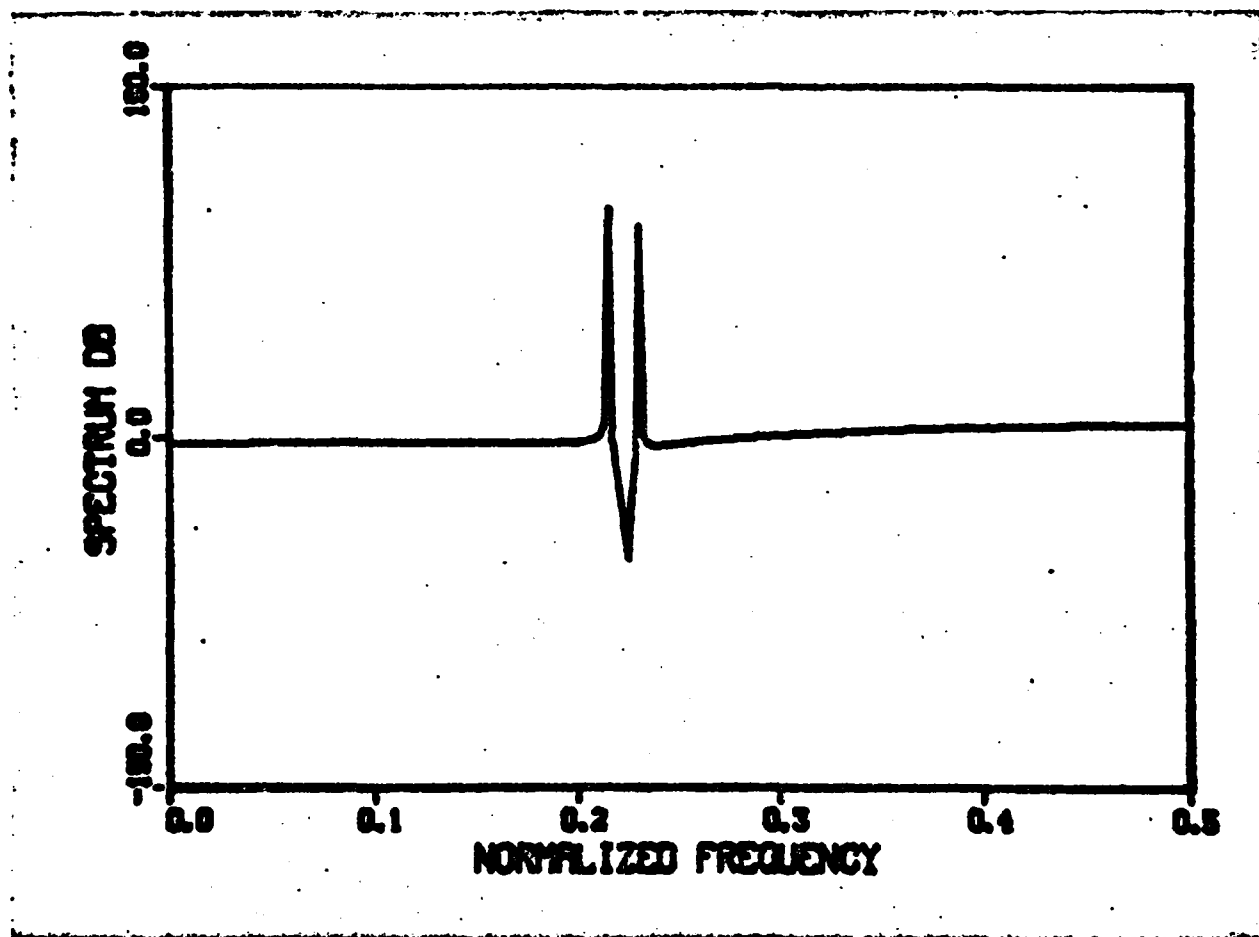


Fig. 2.4.23 Estimated spectrum using new method where positive peaks occur at normalized frequencies $f_1=0.2148$ and $f_2=0.2305$.

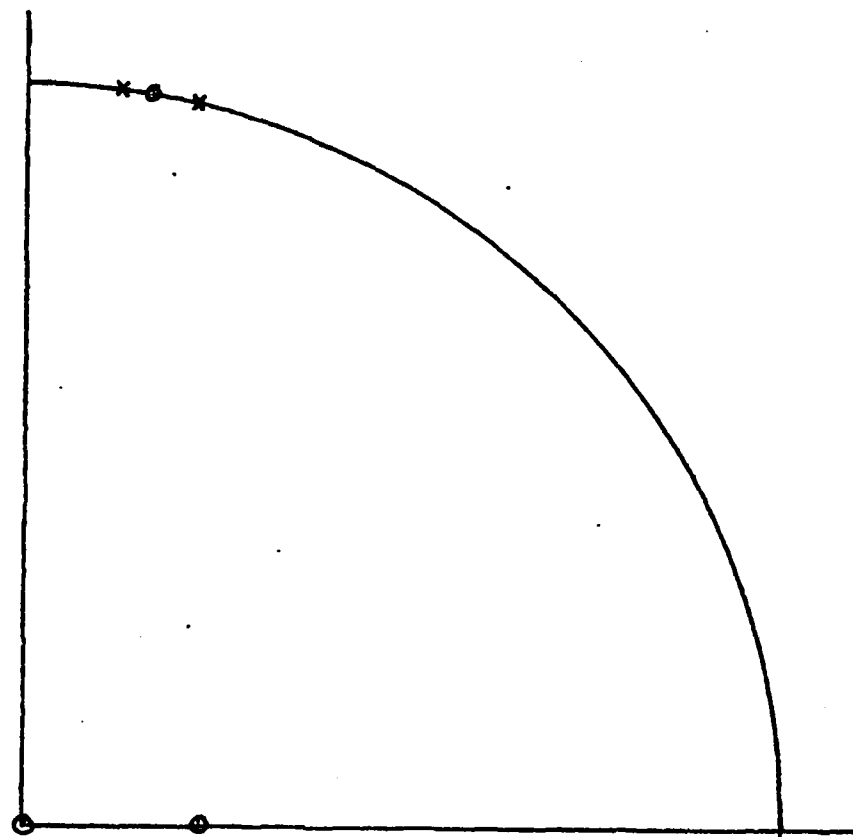


Fig. 2.4.24 Locations of the estimated poles and zeros in the first quadrant of the z -plane.

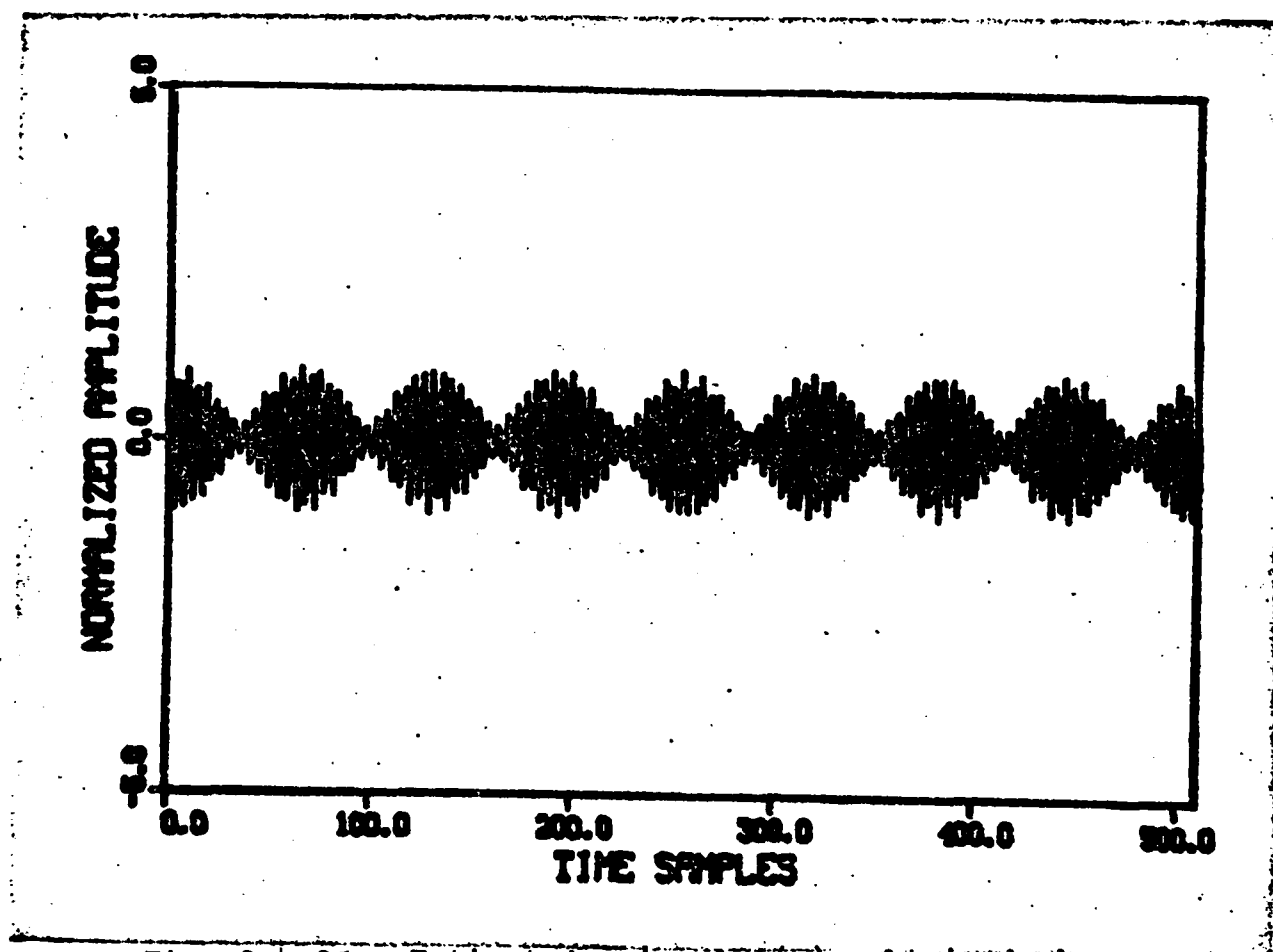


Fig. 2.4.25 Estimated signal $s(n)$ obtained by inverse Z-transforming the transfer function with the estimated poles and zeros.

Chapter 3

FINITE TIME-BANDWIDTH PRODUCT

HILBERT TRANSFORM

3.0 Introduction

When analyzing a process, one finds that under certain circumstances, the real and imaginary parts of a signal are related through a specific relationship, or the amplitude and phase are related by that same relationship. In different disciplines, the relationships are known under different names. In mathematics literature these relations are referred to as Poisson's formulas [32], in optics they are known as the dispersion relations [33], and in signal processing theory the relations are called Hilbert transform relations.

The Hilbert transform is used in the phase retrieval problem which arises when the wave phase is apparently lost or impractical to measure and only intensity data is available. This situation occurs, for example, in electron microscopy where the index of refraction structure of thin films or the height distribution of a surface is to be determined from the intensity distribution in the far

This page is intentionally left blank

field. The phase problem also occurs in coherence theory [34], signal processing [35,36,37], antenna array design [38], Fourier transform spectroscopy [39], and design of radar signals [40].

If we are given a real signal $f(t)$ that is square integrable, and bandlimited to a frequency Ω , then the signal $f(t)$ can be represented as

$$f(t) = \operatorname{Re} \tilde{f}(t) \exp j \Omega t,$$

where

$$\tilde{f}(t) = 2f_+(t) \exp -j \Omega t$$

and

$$f_+(t) = \frac{1}{2\pi} \int_0^{\infty} F(w) \exp j w t \, dw$$

By definition, the Fourier transform of $f(t)$ is truncated at $w = -\Omega$. That is, $F(w)$ is identically zero for $w < -\Omega$. Multiplying $f(t)$ by $\exp j \Omega t$ shifts the spectrum to the right by an amount Ω . The resulting complex signal has no negative frequency components.

The preenvelope of a real signal $f(t)$, is the complex-valued function

$$m(t) = f(t) + j\tilde{f}(t) \quad (3.0-1)$$

The real signal is the real part of the preenvelope $m(t)$. The preenvelope is also called the analytic signal. An analytic signal has the property that the envelope of $f(t)$ is the absolute value $|m(t)|$ of its preenvelope which is of use in modulation theory [35].

In (3.0-1) we have that the real and imaginary parts of the signal $m(t)$ are related by the Hilbert transform given by

$$\tilde{f}(t) = \frac{1}{\pi} P \int_{-\infty}^{\infty} \frac{f(\tau)}{t - \tau} d\tau = H[f(t)] \quad (3.0-2)$$

where P denotes the Cauchy principle value given by

$$\tilde{f}(t) = \frac{1}{\pi} \lim_{\epsilon \rightarrow 0} \left\{ \int_{t-\epsilon}^{\infty} \frac{f(\tau)}{t - \tau} d\tau + \int_{-\infty}^{t-\epsilon} \frac{f(\tau)}{t - \tau} d\tau \right\} \quad (3.0-3)$$

The frequency spectrum of $f(t)$ is given by its Fourier transform

$$F(w) = F[f(t)] = \int_{-\infty}^{\infty} f(t) \exp(-j2\pi ft) dt \quad (3.0-4)$$

and $F(w)$ exhibits real-even, imaginary-odd symmetry because $f(t)$ is real. The spectra of $f(t)$ and $\tilde{f}(t)$ are related through the relationship

$$F[\tilde{f}(t)] = -j \operatorname{sgn}(w) F(w) \quad (3.0-5)$$

where

$$\operatorname{sgn}(w) = \begin{cases} +1 & , w \geq 0 \\ 0 & , w = 0 \\ -1 & , w \leq 0 \end{cases} \quad (3.0-6)$$

From this the Hilbert transformation of $f(t)$ can be viewed as $f(t)$ passed through a -90° phase-shift network whose frequency and impulse responses are

$$G(w) = -j \operatorname{sgn}(w) \quad (3.06-7a)$$

$$g(t) = 1/\pi t \quad (3.0-7b)$$

Because $G(w) = -1$, we must have

$$f(t) = -H[\tilde{f}(t)] \quad (3.0-8)$$

and $f(t)$, $\tilde{f}(t)$ are termed a Hilbert pair.

The spectrum of $m(t)$ is shown to have zero negative frequency components by substituting (3.0-5) into the Fourier transform of (3.0-1). This gives us

$$M(w) = F(w) + jF[f(t)] \quad (3.0-9)$$

or

$$\begin{aligned} M(w) &= F(w) + j(-j \operatorname{sgn}(w) F(w)) \\ &= F(w) [1 + \operatorname{sgn}(w)] \end{aligned} \quad (3.0-10)$$

For w less than 0, from (3.0-6) we see that the sign function is -1 and the function $M(w)$ disappears. For w greater than 0, $M(w) = 2F(w)$, and for $w=0$ $M(w) = F(0)$. This can be rewritten as

$$M(w) = \begin{cases} 2F(w) & , w > 0 \\ F(0) & , w = 0 \\ 0 & , w < 0 \end{cases} \quad (3.0-11)$$

When the spectrum of $M(w)$ is bandlimited to $+\Omega$, $M(w)$ vanishes for $w > \Omega$, and the finite energy E_m of the signal is, by Parseval's theorem

$$\int_{-\infty}^{\infty} |m(t)|^2 dt = \frac{1}{2\pi} \int_0^{\Omega} |M(w)|^2 dw \quad (3.0-12)$$

Let $z = \tau + j\sigma$ define a complete variable. By inverse Fourier transformation

$$m(z) = \frac{1}{2\pi} \int_0^{\infty} M(w) \exp jw\tau \, dw \quad (3.0-13a)$$

$$= \frac{1}{2\pi} \int_0^{\infty} M(w) \exp -w\sigma \exp jw\tau \, dw. \quad (3.0-13b)$$

It becomes evident that given the integrability and convergence properties for the existence of the Fourier transform that (3.0-13) must converge for any $\sigma \geq 0$. Therefore, $m(z)$ must be free of zeros in the upper half of the z -plane.

If we let $m(z)$ be bandlimited to Ω , from (3.0-13) we have,

$$|m(z)|^2 = \left[\frac{1}{2\pi} \int_0^{\Omega} M(w) \exp -w\sigma \, dw \right]^2. \quad (3.0-14)$$

From the Schwartz inequality (3.0-14) becomes

$$\begin{aligned} |m(z)|^2 &= \frac{1}{2\pi} \int_0^{\Omega} M(w) \, dw \frac{1}{2\pi} \int_0^{\Omega} \exp -2w\sigma \, dw \\ &= E_M \frac{1 - \exp(-2\Omega\sigma)}{4\pi\sigma} \end{aligned} \quad (3.0-15)$$

where E_m is the finite energy given by (3.0-12).

This shows that $m(z)$ is bounded everywhere in the finite lower half and whole upper half of the z -plane. When $M(z)$ is bandlimited, then $m(z)$ must be an entire function. This relationship does not depend on bandwidth limitations. With $\Omega = \infty$, (3.0-15) is finite for any $\sigma > 0$ provided that $m(t)$ is square integrable. A finite bandwidth insures that the lower half plane singularities are at infinity. The Hilbert transform can also be used to describe the relationships between the modulus $|m(t)|$ and the phase $\phi(t)$ of an analytic signal. It is assumed that $M(w)$ is bandlimited. Equation (3.0-2) can be written in phasor notation as

$$m(t) = |m(t)| \exp \phi(t) \quad (3.0-16)$$

where

$$|m(t)| = \sqrt{f^2(t) + \tilde{f}^2(t)} \quad (4.0-17a)$$

$$\phi(t) = \arctan \tilde{f}(t)/f(t) \quad (3.0-17b)$$

By taking the complex logarithm of (3.0-16) we have

$$\ln m(t) = \ln |m(t)| + j \phi(t) \quad (3.0-18)$$

in which the logarithmic modulus and the phase are the real and imaginary parts of a time function. Certain conditions have to be imposed in order for the Hilbert relation to hold between the modulus and phase. We first note that $\ln m(t)$ is not square integrable, and in general, $m(t) \rightarrow 0$ as $t \rightarrow \infty$ and thus $\ln m(t) \rightarrow -\infty$ as $t \rightarrow \infty$. However, in certain instances, we can modify $m(t)$ by the addition of a constant unit amplitude so that the modified function $\ln(1+m(t))$ is square integrable if $|m(t)|$ is chosen to be less than one [41].

Another way to avoid the problem is to study

$$\ln' m(z) = \frac{d}{dz} \ln m(z) \quad (3.0-19a)$$

$$= \ln' m(z) + j \phi'(t) \quad (3.0-19b)$$

$$= m'(z)/m(z) \quad (3.0-19c)$$

From the Paley-Wiener theorem [42], if $m(z)$ is entire and square integrable along the real axis, and if $M(w)$ is band-limited to Ω , then

$$m(z) = O(\exp(\Omega |z|)) \quad (3.0-20)$$

where O means "order of" defined as the maximum absolute value. This means that the maximum absolute value of $m(z)$

is increasing exponentially with radius $r=|z|$. From this we have that $\ln m(z)$ at worst will vary linearly with $|z|$, and $\ln'm(t)$ must therefore vanish or tend to a finite constant in the extremities of the z -plane.

Because $m(z)$ is analytic, $\ln'm(z)$ will have upper half plane singularities only if $m(z)$ has zeros in the upper half plane. If $\ln'm(z)$ is square integrable, we then have the relationships

$$\phi'(t) = H[\ln' m(t)] \quad (3.0-21a)$$

$$\ln'|m(t)| = -H[\phi'(t)] \quad (3.0-21b)$$

where $m(z)$ must be zero free in the upper half of the z -plane. The relationship where the phase and magnitude are related through the Hilbert transform is known as the minimum phase condition where the phase displacement is the smallest possible for its gain.

From (3.0-21) we can always calculate $\phi(t)$ and $\ln m(t)$ by integration. The results obtained will generally not be unique. In certain applications the fact that the solution is not unique does not play a role in the solution [35].

The theory just described has been for analytic time signals whose spectrum has zero negative frequency

components. A dual of this is a time signal that has no negative time components. It can be shown that the real and imaginary parts of the spectrum are related by the Hilbert transform. Signals that have no negative time components are termed causal. In cybernetics, a causal signal that is also square integrable is called a wavelet [37].

The solution of the phase retrieval problem can either be solved for by relying on the analyticity of the signal where the Hilbert transform can be used, or a computational procedure. In the case of what in optics is called a weak object [43,44] one has a signal $F(w)$ given by

$$F(w) = 1 + M(w) \quad (3.0-22)$$

where

$$|M(w)| \ll 1.$$

With this condition we can approximate the real part of the signal $M(w)$ as

$$\text{Re}[M(w)] \approx 0.5(F(w) - 1) \quad (3.0-23)$$

and the imaginary part of the signal $M(w)$ as

$$\text{Im } [M(w)] \approx H [\text{Re } M(w)] \quad (3.0-24)$$

As we can see we have to have the special condition that the signal $M(w)$ has a constant dc offset and the signal magnitude is much smaller than the offset.

Another procedure is the apodizing technique. In this technique, the function $m(t)$ is modified so that the zeros of the modified function are displaced so that their contribution to the phase is diminished. The logarithmic Hilbert transform can then be used to calculate the phase. The apodization concept follows from considerations of the bandlimited Fourier transform [33]:

$$F(z) = \int_a^b f(t) \exp(-yt) \cos(xt + \arg f(t)) dt \\ + j \int_a^b f(t) \exp(-yt) \sin(xt + \arg f(t)) dt \quad (3.0-25)$$

where $z = x + jy$. If $f(t)$ is made to decrease more rapidly, near the lower limit of the integrals then larger x, y must be required. This means that a larger zero-free area about the origin is created, by reducing the phase contributions of the zeros in the lattice by having $f(t)$ decrease more rapidly near the edges of the window. This can be accomplished by multiplying $f(t)$ by a suitable filter. Nakajima and Asakura [45] have used the Gaussian, sinc and

triangular filters to perform the apodization which is a multiplication of the autocorrelation of the signal with the desired filter function. The autocorrelation is the inverse Fourier transform of the magnitude in the frequency domain.

As was already mentioned, it becomes difficult to obtain the phase from magnitude measurements if the function has zeros in the upper half of the z -plane. Procedures have been developed to determine where in the upper half plane the zeros occur so that they could be flipped into the lower half plane. By accomplishing this flip, the magnitude in the frequency domain remains the same. Nakajima and Asakura [46] have devised a method to determine the position of the zeros from the magnitude of the signal and the magnitude of the Fourier transform of the signal. From this along with the logarithmic Hilbert transform and a nonlinear least-squares parameter estimation technique, they have been able to determine the phase.

Gerchberg and Saxton [47,48] were first to suggest the use of both the magnitude of the signal and the magnitude of the spectrum to obtain the phase. Misell [49] proposed the use of the intensity distributions of two slightly defocused images. In the Gerchberg-Saxton algorithm, at each step the computed values of the intensity are cor-

rected by combining with the measured values. Other suggestions [50] for use of the magnitudes of the signal and the spectrum have involved the solution of algebraic equations which connect the sampled magnitudes in time and frequency with coefficients of the discrete Fourier transforms of the function.

Bates et al., [51,52,53] have obtained a simple algebraic derivation to the phase problem, and have devised an easily implementable algorithm. The algorithm works for images that are weakly localized. What this means is that the energy of each sample is slightly spread about the sample.

An alternative approach to phase retrieval problem is to employ one of the gradient search methods. It has been shown, [54], that one such method, the steepest-descent method, is closely related to the error reduction algorithm. Its one drawback is that it converges slower than other gradient search methods that are available.

Much work has recently been done in reconstructing the signal from its phase [60,61,62,63]. This is because it is possible to relate the phase of a signal to the signal under certain conditions, which makes it easier to perform than to obtain the signal from its magnitude.

In this chapter we describe a new form of the Hilbert transform which is based on finite time observations of a signal. It will be shown that the kernel does not have the inherent singularity that the regular Hilbert transform exhibits. We will show that the modified Hilbert transform has similar properties of the regular Hilbert transform. The modified Hilbert transform will be used with a method that we call the method of partitioning to determine the phase of a function given its magnitude. Numerical results will be used to show how this new method works.

3.1 Modified Hilbert Transform

In section 3.0 we have shown the Hilbert relationship between the real and imaginary part of a signal given that the Fourier transform of the signal has no components on the negative side of the axis. For this case the Hilbert transform can be written in the form given by Papoulis [55]:

$$R(w) = -\frac{2}{\pi} \int_0^{\infty} \int_0^{\infty} X(y) \sin yt \cos wt \, dy \, dt \quad (3.1-1)$$

$$X(w) = -\frac{2}{\pi} \int_0^{\infty} \int_0^{\infty} R(y) \sin wt \cos yt \, dy \, dt \quad (3.1-2)$$

AD-A143 984

OPTICAL ACQUISITION IMAGE AND DATA COMPRESSION(U) CITY

2/2

COLL NEW YORK DEPT OF ELECTRICAL ENGINEERING

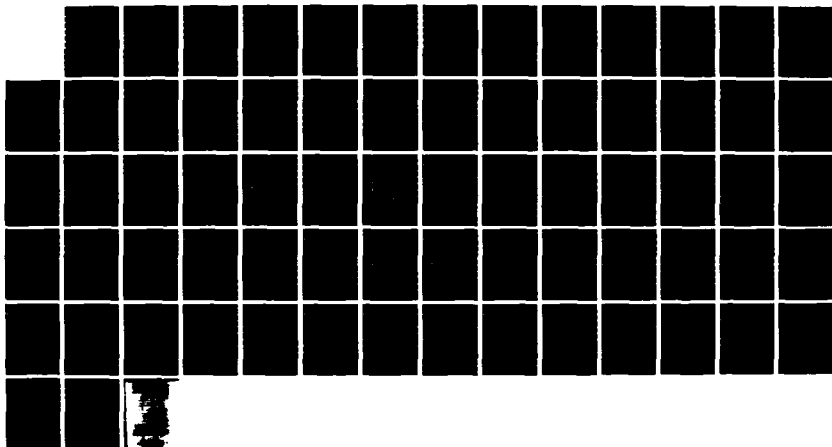
G EICHMANN JUN 84 447104-1 AFOSR-TR-84-0611

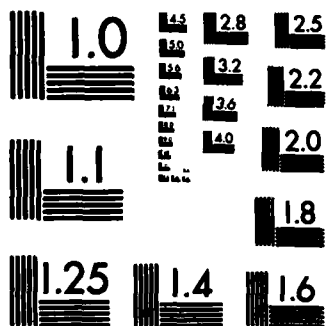
UNCLASSIFIED

AFOSR-83-0081

F/G 17/8

NL





MICROCOPY RESOLUTION TEST CHART
NATIONAL BUREAU OF STANDARDS-1963-A

where $R(w)$ is the real part and $X(w)$ is the imaginary part of the complex signal. By looking at (3.1-1) and (3.1-2) we see that the integrals are evaluated in both the time and frequency domains, and because of the even symmetry the integrals are also evaluated for only positive values.

If we were to assume that the signal is observed in the time domain for a finite time T , then in (3.1-1) and (3.1-2), the upper limit of integration for t is T . For simplicity we will obtain the modified Hilbert transform from (3.1-2) with the understanding that the procedure is applicable to (3.1-1). With T as the upper limit, (3.1-2) can be written as

$$X(w) = -2 \int_0^{\infty} R(y) \int_0^T \sin wt \cos yt \, dt \, dy \quad (3.1-3)$$

We see from (3.1-3) that the integral evaluated over t can be evaluated to give the equation only in terms of w and y . The integration gives us the following

$$2 \int_0^T \sin wt \cos yt \, dt = \frac{1 - \cos(w+y)T}{(w+y)} - \frac{1 - \cos(w-y)T}{(w-y)} \quad (3.1-4)$$

which can be placed back into (3.1-3). Therefore, we have from (3.1-3) and (3.1-4)

$$X(W) = -\frac{1}{\pi} \int_0^{\infty} R(y) \left[\frac{1 - \cos(w+y)T}{(w+y)} + \frac{1 - \cos(w-y)T}{(w-y)} \right] dy. \quad (3.1-5)$$

If the complex signal is assumed to be bandlimited to $w = \Omega$ we can rewrite (3.1-5) as

$$\begin{aligned} X(w) = & -\frac{1}{\pi} \int_0^{\Omega} R(y) \frac{1 - \cos(w+y)T}{(w+y)} dy \\ & -\frac{1}{\pi} \int_0^{\Omega} R(y) \frac{1 - \cos(w-y)T}{(w-y)} dy \end{aligned} \quad (3.1-6)$$

where we have broken the integral into the sum of two integrals. The two integrals can be combined into one by changing the variable in the first integral to give the final result

$$X(w) = -\frac{1}{\pi} \int_{-\Omega}^{\Omega} R(y) \frac{1 - \cos(w-y)T}{(w-y)} dy \quad (3.1-7)$$

The above equation can also be written with different limits of integration. It is seen that both the variables w and y take on the values

$$-\Omega = w = \Omega$$

$$-\Omega = y = \Omega.$$

If new variables are defined given by

$$w' = w/\Omega$$

$$y' = y/\Omega$$

we can rewrite the inequalities as

$$-1 = w' = 1$$

$$-1 = y' = 1$$

With these new variables (3.1-7) can be written in the form

$$X(\Omega w') = -\frac{1}{\pi} \int_{-1}^1 R(\Omega y') \frac{1 - \cos \Omega T(w' - y')}{(w' - y')} dy' \quad (3.1-8)$$

A reason why one may be interested in this form of the equation is that the time-bandwidth product is directly incorporated into the equation. This is the form of the transform we have termed the modified Hilbert transform. From (3.1-1) we can go through the same analysis to obtain

$$R(w) = -\frac{1}{\pi} \int_{-\Omega}^{\Omega} X(y) \frac{1 - \cos(w - y)T}{(w - y)} dy \quad (3.1-9)$$

$$R(\Omega w') = -\frac{1}{\pi} \int_{-1}^1 X(\Omega y') \frac{1 - \cos \Omega T(w' - y')}{(w' - y')} dy' \quad (3.1-9b)$$

Equations (3.1-7) and (3.1-9a) can be rewritten using trigonometric identities as

$$x(w) = -\frac{1}{\pi} \int_{-\Omega}^{\Omega} R(y) \frac{\sin^2 0.5T(w-y)}{0.5(w-y)} dy \quad (3.1-10a)$$

$$R(w) = -\frac{1}{\pi} \int_{-\Omega}^{\Omega} X(y) \frac{\sin^2 0.5T(w-y)}{0.5(w-y)} dy \quad (3.1-10b)$$

which if we take a closer look at the kernel, contains the sampling function given by

$$\text{sinc} 0.5Tw = \sin 0.5Tw / (0.5Tw) \quad (3.1-11)$$

This sampling function is a consequence of the finite time observation of the signal. We see that the modified Hilbert transform is a convolution of a signal with a kernel evaluated over a finite bandwidth. The difference between the regular and modified Hilbert transform is the kernel given by

$$K(w) = \frac{1 - \cos Tw}{w} = T \sin 0.5wT \text{sinc} 0.5wT \quad (3.1-12)$$

which differs with the kernel of the Hilbert transform given by

$$K'(w) = 1/w. \quad (3.1-13)$$

In (3.1-13) we see that the kernel has a singularity at $w=0$ where the function approaches infinity. For the modified Hilbert transform kernel we see that in the limit as w approaches to zero, the sampling function approaches one and the sine approaches zero giving the overall limit as zero. The kernel of the modified Hilbert transform has an envelope which is identical to the kernel $K'(w)$ with sinusoidal variations which makes it go to zero as w goes to zero. In Fig. 3.1.1 we see the kernel $K(w)$ for $T=1$ and $f=12$ where we have that $w=2\pi f$. We see that for positive frequencies the kernel has only positive values and for negative frequencies only negative values as in the case of $K'(w)$. In Fig. 3.1.2 we have expanded a portion of the spectrum and evaluated the kernel for frequencies up to $f=3$ with $T=1$. From this and the previous figure we note that the majority of the energy is located in the lower frequencies.

By a change in variables we can get the equivalent forms of (3.1-10a) as

$$X(w) = -\frac{1}{\pi} \int_{-\Omega}^{\Omega} \text{sinc} 0.5(w+y)T \sin 0.5(w+y)T R(y) dy \quad (3.1-14a)$$

$$X(w) = -\frac{1}{\pi} \int_{-\Omega}^{\Omega} \text{sinc} 0.5yT \sin 0.5yT R(w-y) dy \quad (3.1-14b)$$

which can be extended to (3.1-10b).

To evaluate the integral we replace the integral by a summation to give us (3.1-10a) in the form

$$X(\Delta_j) = -\frac{1}{\pi} \sum_{i=1}^{M+1} \frac{(1 - \cos((\Delta_j - \Delta_i)T)) R(\Delta_i) \Delta}{\Delta_j - \Delta_i} \quad (3.1-15)$$

where M is the number of intervals the integral is broken into, and

$$\begin{aligned} \Delta &= 2\Omega/M \\ \Delta_j &= (j-1)\Delta - \Omega \\ \Delta_i &= (i-1)\Delta - \Omega \quad i, j = 1, 2, \dots, M \end{aligned} \quad (3.1-16)$$

Using (4.1-16) we can rewrite (3.1-14) as

$$X(\Delta_j) = -\frac{1}{\pi} \sum_{i=1}^{M+1} \frac{(1 - \cos((j-i)\Delta T)) R(\Delta_i)}{(j-i)} \quad (3.1-17)$$

To rewrite (3.1-10b) the X and R need only be interchanged.

As an example to show how this modified Hilbert transform evaluates the imaginary part from the real part of the Fourier transform of a causal signal we have chosen our

signal $f(t)$ to be a unit amplitude step for a duration T . Therefore, we have $f(t)$ given as

$$f(t) = \begin{cases} 1, & 0 \leq t \leq T \\ 0, & \text{otherwise} \end{cases} \quad (3.1-18)$$

The Fourier transform of $f(t)$ is given by

$$\begin{aligned} F(w) &= 0.5T \text{sinc} 0.5wT \exp(-j0.5wT) \\ &= 0.5T \text{sinc} 0.5wT (\cos 0.5wT - j \sin 0.5wT) \end{aligned} \quad (3.1-19)$$

Therefore, if $R(w)$ is the real part of the signal given by

$$R(w) = 0.5T \cos 0.5wT \text{sinc} 0.5wT \quad (3.1-20)$$

then the modified Hilbert transform should yield the imaginary part $X(w)$ given by

$$X(w) = -0.5T \sin 0.5wT \text{sinc} 0.5wT \quad (3.1.21)$$

In Fig. 3.1.3, the real part of the signal $R(w)$ is given by the solid line. It is seen to be an even function. To obtain the imaginary part $X(w)$, (3.1-17) was used with $M=256$, $T=1$ and $f=\Omega/2\pi=12$. The imaginary part is drawn using a dashed line. To see how closely the result corresponds to the actual values, (3.1-21) was also drawn

using a dotted line. We see that the actual and the calculated imaginary part are overlapping, indicating that the calculated function is identical to the actual one. As a convenience for graphing, all of the functions will be normalizing. The normalized constant is obtained by finding the maximum absolute value of the function and dividing the function by this value. This assures us that the magnitude of the function will always be less than or equal to one. In Fig. 3.1.3, as will always be the case, the normalizing constant K_R for the real part of the signal is given by 0.5. The normalizing constant for the actual imaginary part K_I is given by 0.362, and the normalizing constant of the calculated or estimated function, K_E is given by 0.360. From the normalizing constants K_I and K_E we see again that the results obtained using the modified Hilbert transform are very close.

In (3.1-16) we have that the spacing between samples is

$$\Delta = 2\Omega/M = 4\pi f/M \quad (3.1-22a)$$

or

$$\Delta' = \Delta/2\pi = 2f/M \quad (3.1-22b)$$

From the sampling theorem for the Hilbert transform [57],

we have that

$$\Delta' = 1/T \quad (3.1-23))$$

from which we can obtain an expression for the time-bandwidth product TBP associated with the sampling interval Δ' . From (3.1-22) we can deduce that the bandwidth B is given by

$$B = M \Delta' / 2 = f \quad (3.1-24)$$

From (3.1-23) and (3.1-24) we have

$$f = M/2T \quad (3.1-25a)$$

or

$$fT = M/2 \quad (3.1-25b)$$

Equation (3.1-25b) states that if one is to sample according to (3.1-23) then the time-bandwidth product is equal to $M/2$. In the case where the time-bandwidth product is less than $M/2$, the signal is being oversampled, and if the product is greater than $M/2$, the signal is undersampled. In speech analysis [58,59], for certain processing techniques, one finds it necessary to oversample the signal.

In the example of Fig. 3.1.3, the $TBP=12$ which tells us that we are oversampling by 10.67 times. To test the modified Hilbert transform in how well it works for calculating the real part of the signal from the imaginary part with identical constants as before, we use the negative of (3.1-21) to see how closely our results match (3.1-20). Fig. 3.1.4 shows the results where we see that the graph of the actual real part of the signal given by the dotted line and the graph of the calculated real part are overlapping. The imaginary part of the signal is given by the solid line, where for quick identification we note that the imaginary part is odd. The normalizing constants for Fig. 3.1.4 are $KI=0.326$, $KR=0.5$ and KE the normalizing constant of the estimate to the real part of the signal is 0.494. With the shape of the estimate being identical to the shape of the actual signal, and having the normalizing constants in close agreement, we can say that the estimate is exact.

In the above examples the bandwidth of the signal was taken to be 12. This bandwidth gave us the limits of integration, and we observed that the calculated estimates of the real and imaginary parts of the signal were almost identical to the actual values. To see what effect reducing the bandwidth would have on our solution, we next chose to have the bandwidth $f=3$. Again we have $M=256$ and $T=1$. The TBP here is given by 3 so that we are oversampling

by 42.67 times. Equation (3.1-20) was used as the input and we wanted to see how closely our results using the modified Hilbert transform would be to (3.2-21). In Fig. 3.1.5 the solid line is the function given in (3.1-20) with $KR=0.5$. The dotted line is the actual solution which is given by (3.1-21), and its normalizing constant is $KI=0.362$. The solution obtained by the modified Hilbert transform is shown by the dashed line with the normalizing constant given by 0.356. We notice that at the edges of our window, the estimate does not correspond to the actual values. This phenomenon is caused by the windowing. The real part of the signal does not have all of the energy or most of the energy concentrated in the region up to $f=3$. The same can be said for the kernel of the transform which we have shown in Fig. 3.1.2. By taking the convolution of this signal with the kernel over such a small region, the effect is to produce smearing at the limits of integration. The estimate about the origin is seen to be very close to the actual values because in this region the convolution involves the main lobes of the functions which have enough energy to produce good estimates. In this situation, we notice that the sampling interval or consequently the TBP did not have an effect on our results. It was our choice of bandwidth that caused the smearing at the edges.

The next example that we wanted to choose was a causal signal that would have all of its energy in the short time that it would be observed. For this we chose

$$f(t) = 12\exp(-6t)u_T(t) \quad (3.1-26)$$

where

$$u_T(t) = \begin{cases} 1, & 0 \leq t \leq T \\ 0, & \text{elsewhere} \end{cases}$$

The Fourier transform of (3.1-26) is calculated to be

$$F(w) = \frac{12(1 - \exp(-(6+jw)T))}{6+jw} \quad (3.1-27)$$

By choosing $T=1$, the magnitude of the exponential is 2.48×10^{-3} so that (3.1-27) can be approximated by

$$\begin{aligned} F(w) &= \frac{12}{6+jw} \\ &= \frac{72}{36+w^2} - j \frac{12w}{36+w^2} \end{aligned} \quad (3.1-28)$$

With this choice of T , we find that 99.9% of the energy is in the signal. This satisfies the condition that we wanted

for our signal, in that most of the energy is contained in the signal for the short time that it is observed. Next we wanted to calculate the bandwidth so that 95% of the energy be contained up to that frequency. The energy in the frequency domain is given by

$$E = (2/\pi) \arctan(2\pi f/6) \quad (3.1-29)$$

The signal in (3.1-26) has been normalized so that its total energy equals one. Therefore, from (3.1-29) we find that for $f=12$, 94.9% of the energy is contained in that part of the spectrum. Using the real part of (3.1-28) we wanted to see how well the calculated imaginary part is to the actual values. With $M=256$, $f=12$ and $T=1$, Fig. 3.1.6 shows the results obtained. The solid line is the real part of (3.1-28) with a normalizing constant $KR=2.0$. The actual imaginary part shown by a dashed line, overlaps to look as if the graph is one solid line. The normalizing constants are $KI=1.0$ for the actual plot and $KE=1.0$ for the estimate plot. We see that the modified Hilbert transform gives exact results if the limits of integration are chosen such that most of the energy of the signal is located between the limits. From this example we can assume that the bandwidth can be chosen so that 95% of the energy is located in that region. This way the integration does not have to be done over the entire frequency spectrum.

In the next section we will use the logarithmic form of the modified Hilbert transform to evaluate the phase of a signal from its magnitude. We will also show a new method of partitioning the spectrum to obtain better estimates of the phase.

3.2 Phase Retrieval Problem

In section 3.0, we discussed how for a signal $m(t)$ there exists a relationship between the real and imaginary parts of the complex logarithm of $m(t)$. If $m(t)$ is bandlimited, and it can be written in phasor notation as

$$m(t) = |m(t)| \exp j\phi(t) \quad (3.2-1)$$

then by taking the complex logarithm of (3.2-1) we have

$$\ln m(t) = \ln|m(t)| + j\phi(t) \quad (3.2-2)$$

The $\ln|m(t)|$ is the real part of the signal and $\phi(t)$ is the imaginary part. From this we then have that the phase $\phi(t)$ is related to the log of the magnitude by the Hilbert transform. In the notation of the modified Hilbert transform we have

$$\phi(w) = -\frac{1}{\pi} \int_{-\Omega}^{\Omega} \ln|A(y)| \frac{1 - \cos(w-y)T}{w-y} dy \quad (3.2-3)$$

The above equation relates the phase of the spectrum with the magnitude of the spectrum when the time signal is causal and real. If we are dealing with an analytic signal, where the spectrum is real and contains only positive frequency components, then the logarithmic modified Hilbert transform is given by

$$\phi(t) = -\frac{1}{\pi} \int_{-\tau}^{\tau} \ln|m(\tau)| \frac{1 - \cos(t-\tau)}{t-\tau} d\tau \quad (3.2-4)$$

As an example we will use the one-sided exponential pulse given by (3.1-22). As a matter of convenience, we rewrite the Fourier transform of this signal when $T=1$ as

$$F(w) = \frac{12}{6+jw} \quad (3.2-5)$$

The magnitude and the phase of (3.2-5) can be calculated to give

$$|A(w)| = 12/(36+w^2)^{0.5} \quad (3.2-6a)$$

$$\phi(w) = \arctan(-w/6) \quad (3.2-6b)$$

From (3.2-6a) we notice that the magnitude approaches zero when w approaches infinity. This tells us that the log of the amplitude is not square integrable as is the necessary condition for using the logarithmic form of the Hilbert transform in determining the phase. In the limit as w goes to infinity we have that the log of the magnitude also goes to infinity, and we get

$$\int_{-\infty}^{\infty} |\ln|A(w)||^2 dw \rightarrow \infty \quad (3.2-7)$$

In the previous section we found that if f is chosen to be 12, that 94.9% of the energy is included in the spectrum. It is with these limits that we would like to determine the phase when using the logarithmic modified Hilbert transform. If we take the bandwidth of the signal to be 12 we have that with $\Omega = 2\pi f$

$$\int_{-\Omega}^{\Omega} |\ln|A(w)||^2 dw < \infty \quad (3.2-8)$$

because within these limits the log of the magnitude never goes to infinity. By this we have bandlimited the signal. In Fig. 3.2.1, the solid line represents the log magnitude, with a normalizing constant given by $KR=1.841$. The dotted line is the phase given by (3.2-6b) with a nor-

malizing constant $KI=1.491$. The estimate of the phase using the logarithmic modified Hilbert transform is shown with the dashed line. Its normalizing constant is given by $KE=2.561$. From this figure we see that the estimated phase is incorrect. There are two reasons why the estimate is incorrect. The first, which is hardly noticeable is that we have bandlimited the function so that there may be some smearing of the estimate. The second reason which is the major one is that the magnitude has a pole in the upper half of the z -plane. This can be seen if the log of the magnitude is written as

$$\begin{aligned}\ln A(w) &= 0.5 \ln (144/(36+w^2)) \\ &= 0.5 \ln (144/(6+jw)(6-jw))\end{aligned}\quad (3.2-9)$$

From this we see that a pole occurs at $w=j6$ which is in the upper half of the z -plane. It is because of this pole that the function is not square integrable and leads to such poor results.

In Fig. 3.2.2 we have decided to evaluate the phase of the same function as before for a bandwidth of $f=0.1$. The horizontal line is the log of the magnitude in that region with $KR=0.693$, and the actual phase and estimated phase are superimposed over each other. The normalizing constant for the actual phase is $KI=0.104$ and for the estimate

$KE=0.082$. The estimated phase is close to the actual values. Fig.3.2.3 shows the results when the bandwidth is increased to $f=0.5$. The solid line is the log of the magnitude with $KR=0.693$, the dotted line is the actual phase with $KI=0.482$, and the estimate of the phase is given by the dashed line with $KE=0.520$. By increasing the bandwidth of the signal we see that the estimate is less accurate because the pole is having a larger effect on the results. In Fig. 3.2.4 we have further increased the bandwidth to $f=2.0$ with the solid line representing the log magnitude with $KR=0.693$, the dotted line representing the actual phase with $KI=1.125$, and the estimate given by the dashed line with a normalizing constant $KE=0.473$. We see that here there is a very large error between the estimate and the actual value because of the pole. In order to improve the results, methods must be introduced that will reduce the effect of this pole.

MATHEMATICAL FILTERING METHOD

With the method described by Nikajama and Asakura [46] we will attempt to obtain a better phase estimate by first preprocessing the magnitude, using the method where the magnitude squared is smoothed by convolving it with a filter. The filter we have chosen is the Gaussian filter, with the understanding that there are other filters which

could have been used such as the triangular or low-pass filter. The Gaussian filter used has zero mean and variance σ^2 . Its form is given by

$$G(t) = \exp(-t^2 / 2 \sigma^2) \quad (3.2-10)$$

In Fig. 3.2.4 we saw that the estimate of the phase is very much in error, and it is in this region that we wish to improve the estimate. The magnitude was first smoothed by the Gaussian filter with variance $\sigma^2=4.0$. The resultant log magnitude is shown in Fig. 3.2.5 by a solid line with a normalizing constant $KR=2.461$. We note that the smoothing has raised the log magnitude above zero and has made the function constant over a larger portion before it began to roll off at the edges. The actual phase is given by the dotted line with a normalizing constant $KI=1.125$, and the estimated phase given by the dashed line has $KE=2.390$. We see that the estimated phase is beginning to approach the actual phase in its shape. In our next attempt the variance of the filter is lowered to $\sigma^2=0.5$. The log magnitude after the smoothing is given by the solid line in Fig. 3.2.6 with $KR=2.133$. The actual phase is given by the dotted line having the same KI as before. The dashed line which is the estimate of the phase has a normalizing constant of $KE=1.981$. The shape of the estimate has not changed from the previous case, but the constant has de-

creased towards the desired value. After changing the variance to $\sigma^2=0.01$ the estimated phase is very close to the actual phase. Fig. 3.2.7 shows the log magnitude given by the solid line with $KR=1.161$. The estimated phase given by the dashed curve is seen to follow closely the shape of the actual phase curve given by the dotted line. The normalizing constant for the estimate is $KE=0.821$ as compared to the constant of the actual phase given by $KI=1.125$. The constants are close enough that we wanted to see how the real and imaginary parts of the spectrum using the estimated phase, compare to the spectrum when the actual phase is used. Fig. 3.2.8 show the real part of the spectrum. The dotted line is the actual signal and the dashed line is the one obtained when the estimated phase is used. In both cases the normalizing constant is given by 7.389. The imaginary part of the spectrum is shown in Fig. 3.2.9. The dotted line is the actual curve with a normalizing constant $KI=2.97$ and the dashed curve is the estimate with $KE=2.46$. In Fig. 3.2.10 we show the Fourier transform of the estimated spectrum to see how closely it relates to the actual exponential signal. As can be seen, the dashed line which represents the estimate is in close agreement to the actual exponential signal. The method just described is used before the estimate is obtained. Next we would like to discuss a method to use after the phase has been estimated.

CORRECTION FACTOR METHOD

In a paper by Ford [56] a correction factor can be found if the assumption is made that

$$|\phi(w) - B| < \epsilon \quad w > \Omega \quad (3.2-11)$$

What this assumes is that for $|w| > \Omega$, the phase can be represented by a constant with only a small error in the assumption. In the case of the exponential signal, we have seen that the phase of the spectrum becomes constant as it approaches $f=12$. Therefore, we will use the same method as Ford to obtain a similar correction factor.

Using the modified Hilbert transform we can write the phase $\phi(w)$ as the sum of three integrals given by

$$\begin{aligned} \phi(w) = & -\frac{1}{\pi} \int_{-\infty}^{-\Omega} K(w,y) \phi(y) dy - \frac{1}{\pi} \int_{-\Omega}^{\Omega} K(w,y) \ln|A(y)| dy \\ & - \frac{1}{\pi} \int_{\Omega}^{\infty} K(w,y) \phi(y) dy = I_1 + I_2 + I_3 \end{aligned} \quad (3.2-12)$$

where $K(w,y)$ is the kernel given by

$$K(w,y) = \frac{1-\cos(w-y)T}{w-y} \quad (3.2-13)$$

If we make use of (3.2.11) we can rewrite the integrals I_1 and I_3 as

$$I_1(w) = -\frac{B}{\pi} \int_{(w+\Omega)T}^{\infty} \frac{1-\cos z}{z} dz \quad (3.2-14a)$$

$$I_3(w) = -\frac{B}{\pi} \int_{-\infty}^{(w-\Omega)T} \frac{1-\cos z}{z} dz \quad (3.2-14b)$$

It can be shown that because of the odd symmetry of $I_1(w)$ and $I_3(w)$, that (3.2-14) can be written in the form

$$I_1(w) + I_3(w) = -\frac{B}{\pi} \int_{(w-\Omega)T}^{-(w-\Omega)T} \frac{1-\cos z}{z} dz \quad (3.2-15)$$

which is the correction factor to be added to (3.2-3). Equation (3.2-15) has no closed form solution so that the integral has to be evaluated using numerical methods. In Fig. 3.2-11 we have evaluated the integral with $B=1$ and $T=1$ up to $f=12.0$. In Fig. 3.2.12 we have added the correction factor to the phase estimate where the normalizing constant of the estimate is $KE=1.355$ as compared with the actual $KI=1.491$. We see that up to $f=3.75$, we have been

able to almost have an exact estimate. This tells us that the correction factor is good only in the region where there is a constant slope. Once the slope tends to zero, the factor is of no use. This is what is observed in Fig. 3.2.12, that in the region where the slope was getting smaller, the correction factor was unable to improve the estimate.

METHOD OF PARTITIONING

The method to be described here is based on partitioning the spectrum into small intervals and estimating the phase for that small interval. Once all the estimates have been obtained for each interval, they are combined to form the total estimate. If we were to take a look again at Fig. 3.2.2 we would see that in the region up to $f=0.1$ we were able to obtain a close approximation of the phase. Based on this we want to break the spectrum into intervals whose spacing is $f=0.1$. What we intend to do is to shift the log magnitude of that interval down to the dc, and evaluate the modified Hilbert transform to obtain an estimate of the phase, and afterwards shift the estimate back into the proper interval. In Fig. 3.2.13, we have shifted the log magnitude of the Fourier transform of the exponential signal between $f=.1$ and $f=.2$ to the dc and because of the overlap at $f=0$, we have made it equal to zero. (We found

that had we added the overlap at $f=0$, we would have obtained the same results.) By using the modified Hilbert transform we obtained an estimate whose slope of the line is close to the actual value. The slope of the estimate is 0.081 as compared to 0.102 of the phase in the interval $f=.1$ to $f=.2$. In Fig. 3.2.14 we have taken the interval $f=2.0$ to $f=2.1$ and shifted it to obtain the phase. The slope of the estimated phase is 0.073 and the actual slope is 0.019. We see that the estimate is increasing more rapidly. Fig. 3.2.15 shows the results when the interval taken was between $f=6.5$ and $f=6.6$. The slope of the estimate is 0.032 as compared to the slope of the actual phase of 0.002. We see that the slope of the estimate follows the phase of the actual phase for the lower frequency intervals. In Fig. 3.2.16 we have taken the region to $f=1.0$ and divided it into 10 intervals, each of which had its log magnitude shifted so that the phase could be determined. Once the phase was determined, it was shifted back to its original interval and added to the previous results. We have the slope of the estimate given by 0.804 which is very close to the actual slope of the phase of 0.808. Therefore, we have that in the case of a spectrum that contains a pole in the upper half of the z -plane, this method has given good results in estimating the phase when using the modified Hilbert transform.

PERIODIC ANALYTIC SIGNALS

In this section we would like to take a look at a special class of signals known as periodic analytic signals. These signals are periodic and have the property that the spectrum contains components for positive frequencies only. This is the dual of causal time signals. We are given a time signal $f(t)$ that can be written in the form

$$f(t) = \prod_{i=1}^n (1 - a_i \exp j(\Omega t - \theta_i)) \quad (3.2-16a)$$

$$= \sum_{k=0}^n c_k \exp jk\Omega t \quad (3.2-16b)$$

In (3.2-16b) we recognize this to be the Fourier series representation of the signal $f(t)$. The fundamental frequency is given by Ω and we see that the signal $f(t)$ has a bandwidth given by $n\Omega$, and that the signal is represented in terms of only positive frequencies. Equation (3.2-16a) is a factored form of (3.2-16b) from which the location of the zeros can be obtained. The reason why the zeros of $f(t)$ are of interest is because in order to obtain the phase of $f(t)$ from its magnitude, all of the zeros must lie in the lower half of the complex z -plane. Once the signal has been factored, all one has to do is to check the magnitude of a_i . If the magnitude of a_i is less than one, then the zero of that term, z_i , is in the lower half

plane. To see just where the zeros are located, we first consider when a is positive with a magnitude less than one. Then the zeros are located at

$$z = \frac{2\pi n + \theta_1}{\Omega} + j \frac{\ln |a_1|}{\Omega} \quad (3.2-17)$$

where we see that since the magnitude is less than one, the log will be negative and the zeros are in the lower half plane. We notice that the location of the zeros are periodic. If the value of a is negative and the magnitude is less than one, the zeros are located at

$$z_1 = \frac{2\pi(n+1) + \theta_1}{\Omega} + j \frac{\ln |a_1|}{\Omega} \quad (3.2-18)$$

again showing that the zeros are periodic and located in the lower half of the z -plane.

Let us examine the case when $n=1$. We have that the signal $f(t)$ is given by

$$f(t) = 1 - a \exp j(\Omega t - \theta) \quad (3.2-19)$$

from which we obtain the magnitude and phase as

$$|f(t)|^2 = (1+a^2) - 2a \cos(\Omega t - \theta) \quad (3.2-20a)$$

$$\phi(t) = \arctan \frac{-a \sin(\Omega t - \theta)}{1 - a \cos(\Omega t - \theta)} \quad (3.2-20b)$$

Using the magnitude of (3.2-20) and the Hilbert relationship of (3.2-4) we want to obtain an estimate of the phase given by (3.2-20). The constants that were used are $a=0.2$, $T=0.5$ and $f=1.0$ with $M=256$. The results are shown in Fig. 3.2.17. the solid line is the log magnitude with a normalizing constant given by 0.233. The actual phase is shown by the dotted line with a normalizing constant of $KI=0.201$. The estimated phase is shown by the dashed line with $KE=0.201$. We can see that the estimate is a good one with the graph almost identical to the actual graph.

In the next example we wanted to investigate the case when $n=2$ and the coefficients a_i are both equal to 0.2. Therefore, we have

$$f(t) = (1 - 0.2 \exp(j\Omega t))^2 \quad (3.2-21)$$

The bandwidth of this signal is 2Ω . For the choice of $f=1$ and $T=12$, the resulting phase is obtained in Fig. 3.2.18 which was obtained by taking the magnitude of (3.2-21) and using (3.2-4). The actual phase is given by the dotted line with $KI=0.403$ and the dashed line is the

estimated phase with $KE=0.416$. We again see that the estimated phase is close, and all because the zeros of the function are in the lower half plane, which makes it possible to use the logarithmic Hilbert transform for the determination of the phase.

In the previous cases we were investigating the signal given in (3.2-16). We next would like to take a look at the following type of signal

$$f(t) = \exp(-j\Omega t) - a \exp(-j\theta) \quad (3.2-22)$$

One difference in this form of the signal is that rather than $f(t)$ having a periodic set of zeros, there is only one given by

$$z = \frac{\theta}{\Omega} + j \frac{\ln|a|}{\Omega} \quad (3.2-23)$$

if the constant a is positive, and

$$z = \frac{\theta - \pi}{\Omega} + j \frac{\ln|a|}{\Omega} \quad (3.2-24)$$

if the constant a is negative. If we look at the magnitude and phase we have

$$f(t) = (1+a^2)^{-1/2} \cos(\Omega t - \theta) \quad (3.2-25a)$$

$$\phi(t) = - \arctan \frac{\sin \Omega t - a \sin \theta}{\cos \Omega t - a \cos \theta} \quad (3.2-25b)$$

The first thing that we notice is that the magnitude of (3.2-25) is identical to (3.2-20a) but that the phases are not the same. By choosing $|a| < 1$ we should be able to obtain the phase from the magnitude by using the Hilbert transform. But we have already seen that by using (3.2-25a) the phase that we obtain is given by (3.2-20b) and by (3.2-25b). To see what is happening we have to look at the Fourier transform of (3.2-19) and (3.2-22). The Fourier transform of (3.2-19) has two impulses that are on the positive side of the spectrum and (3.2-22) has two impulses that are on the negative side of the spectrum. Therefore, we see that we are unable to use the phase-magnitude relationship for (3.2-25) because of the position of the spectrum it occupies. Equation (3.2-22) can be rewritten in the form

$$f(t) = \exp -j \Omega t (1 - a \exp j(\Omega t - \theta)) \quad (3.2-26)$$

where the bracketed term is the same as (3.2-19). Therefore, to obtain the phase of (3.2-25b) we must first modulate the signal of (3.2-22) so that it is in the positive side of the spectrum. After this the phase of the signal can be obtained using the logarithmic Hilbert transform. Once

the phase is found, the linear phase $-\Omega t$ is added so that we obtain the phase of (3.2-25).

3.3 Conclusion

We have shown a new form of the Hilbert transform, which has the property that it possesses no singularity. It has been applied to determining the phase from the magnitude of the special class of signals that have no zeros in the upper half of the z -plane. To improve the estimates because of poles, we have used smoothing, a correction factor, and a new method of partitioning. One advantage of the new transform is that in evaluating the convolution we do not use the fast Fourier transform. The reason for the advantage is that in evaluating the convolution using the fast Fourier transform, the frequency spread of the function may exceed the frequency domain defined by the inverse of the sampling distance, and as a consequence the desired Fourier transform of the function is distorted. Thus the evaluation of the convolution yields a large error.

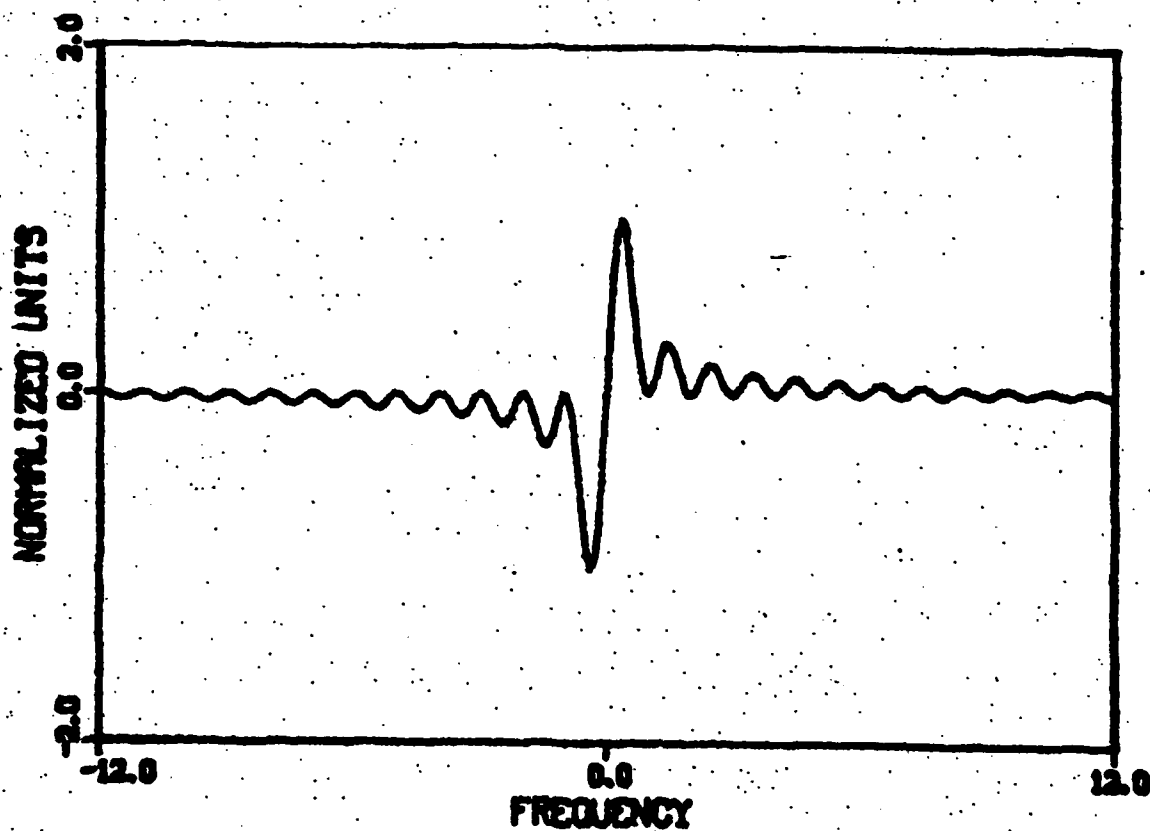


Fig. 3.1.1 Modified Hilbert transform kernel with TBP=12.

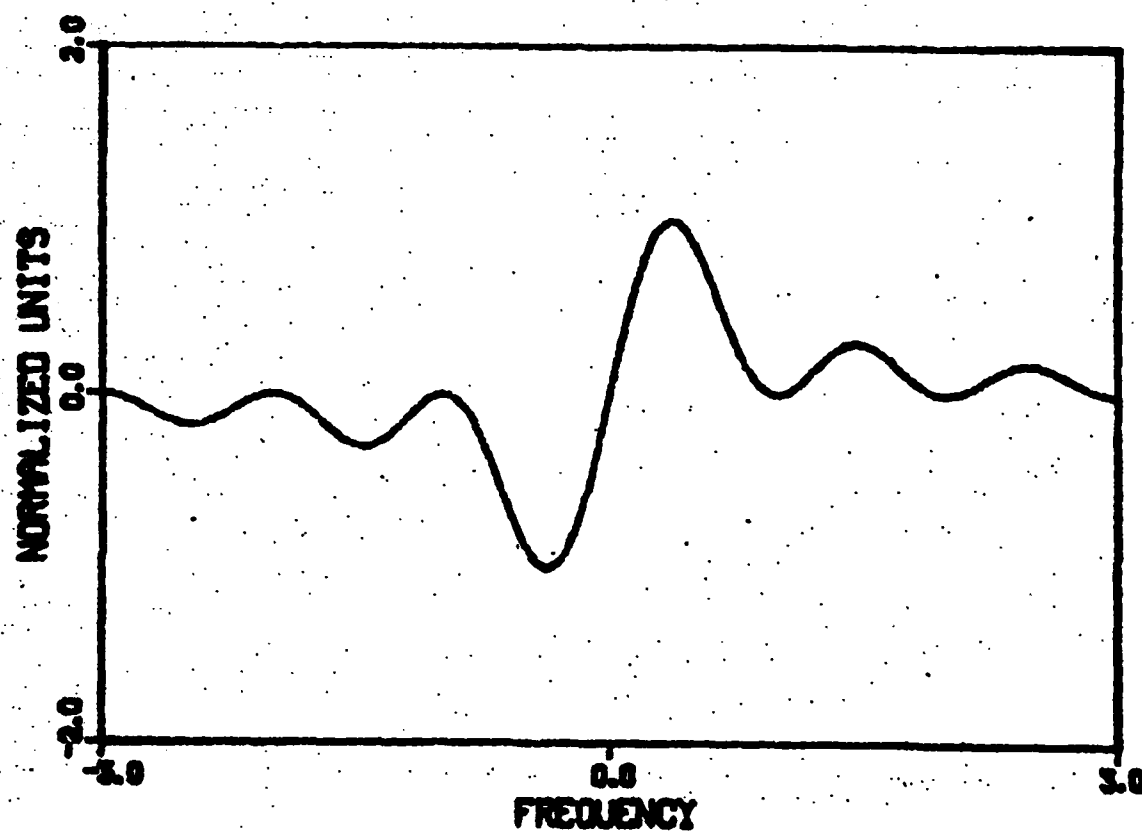


Fig. 3.1.2 Modified Hilbert transform kernel with TBP=3.

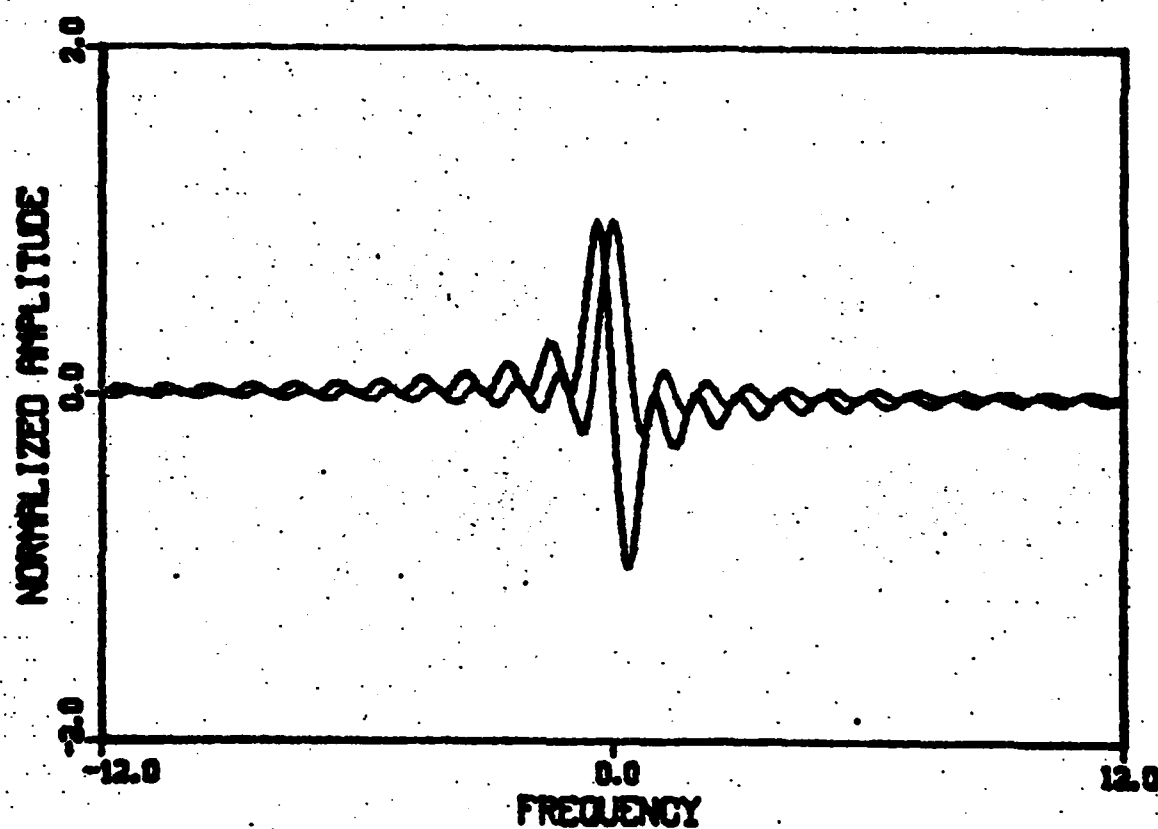


Fig. 3.1.3 Estimated imaginary part using the modified Hilbert transform with normalizing constants $KR=0.5$, $KI=0.362$ and $KE=0.360$.

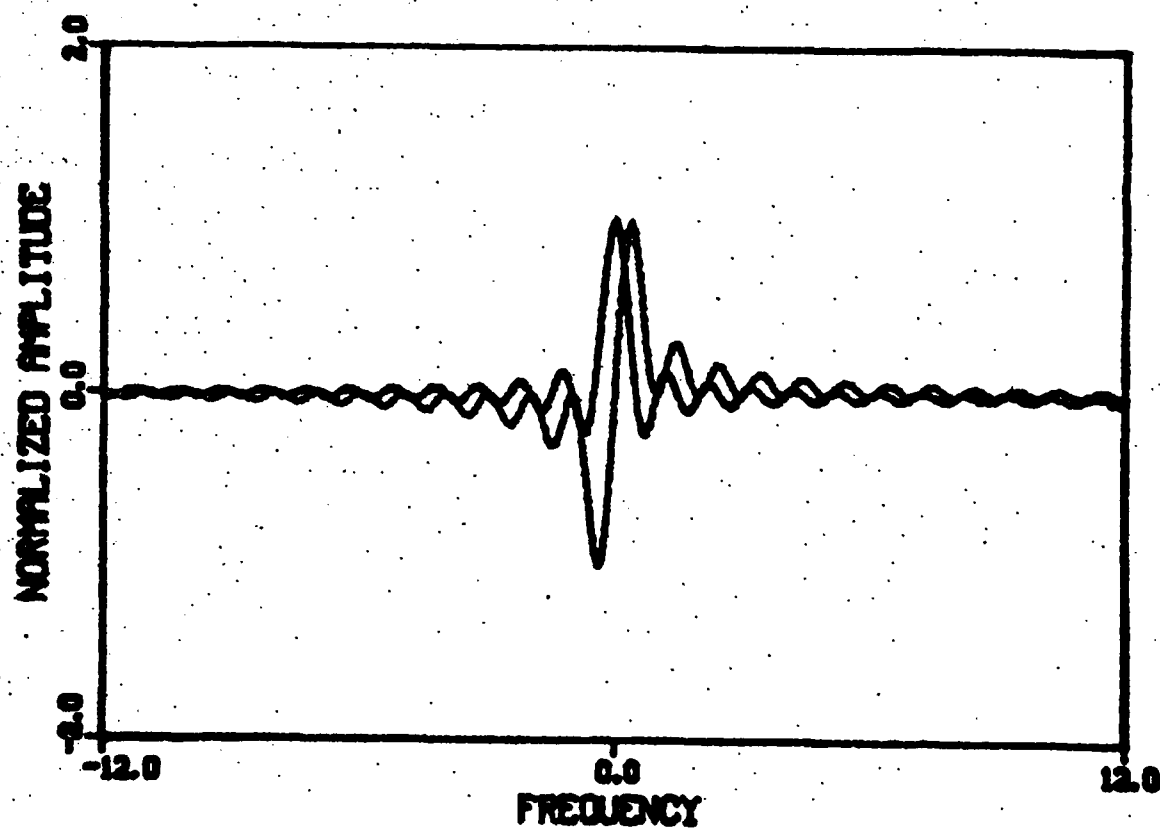


Fig. 3.1.4 Estimated real part using the modified Hilbert transform with normalizing constants $KR=0.5$, $KI=0.362$ and $KE=0.494$.

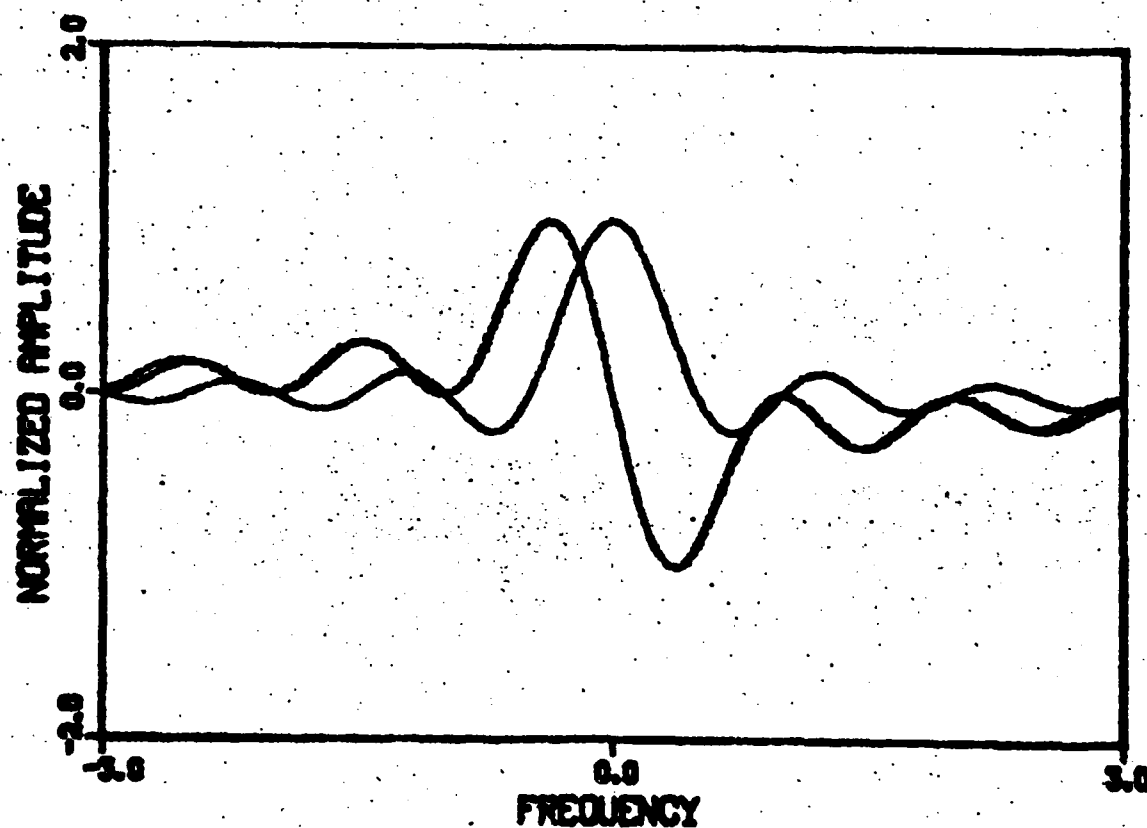


Fig. 3.1.5 Estimated imaginary part using the modified Hilbert transform where TBP is reduced to 3 with normalizing constants $KR=0.5$, $KI=0.362$ and $KE=0.356$.

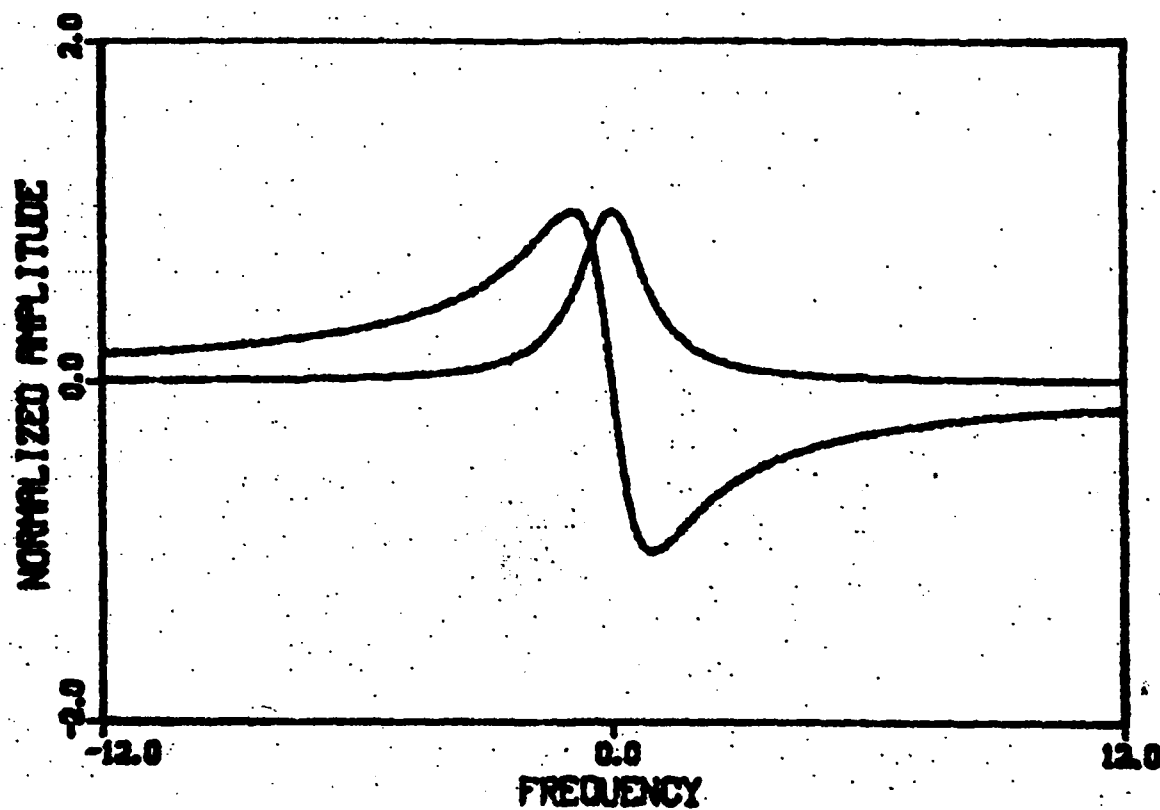


Fig. 3.1.6 Estimate of the imaginary part of the spectrum of an exponential function using the modified Hilbert transform, with normalizing constants $KR=2.0$, $KI=1.0$ and $KE=1.0$.

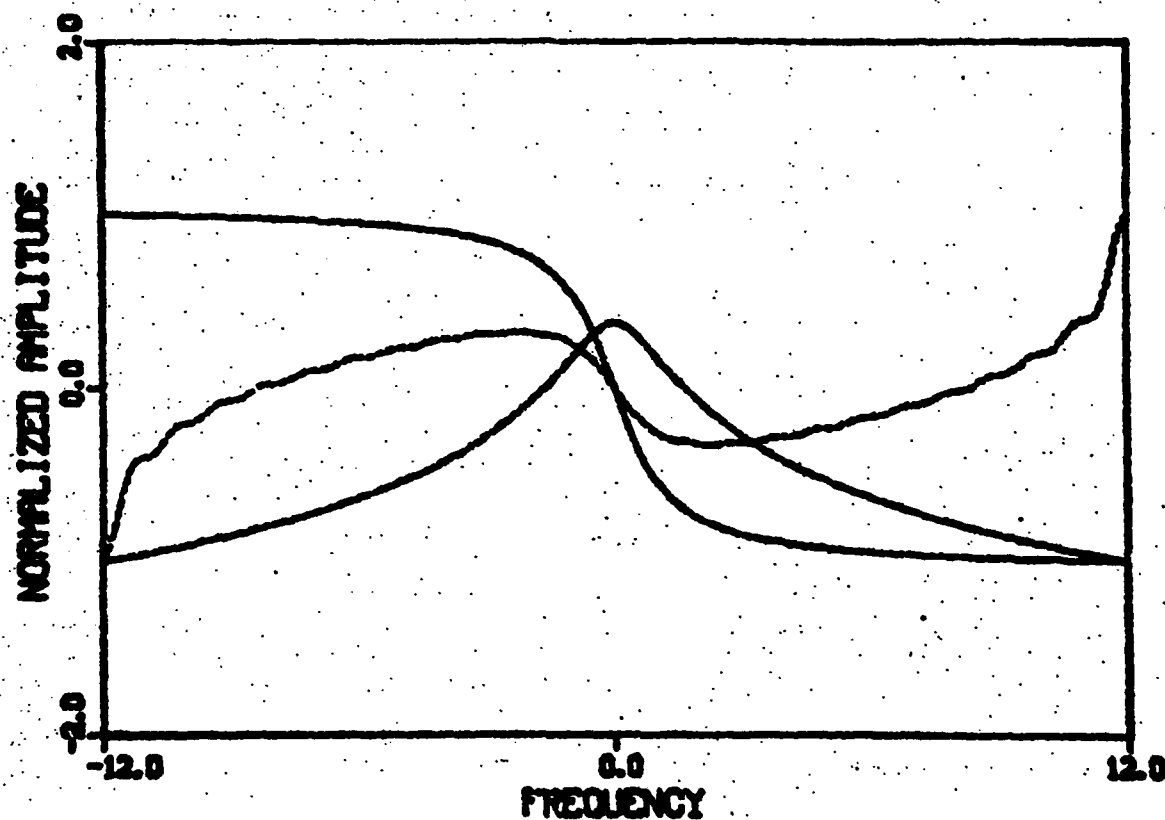


Fig. 3.2.1 Estimate of phase from magnitude measurement of the Fourier transform of the exponential signal with normalizing constants $K_R=1.841$, $K_I=1.491$ and $K_E=2.561$.

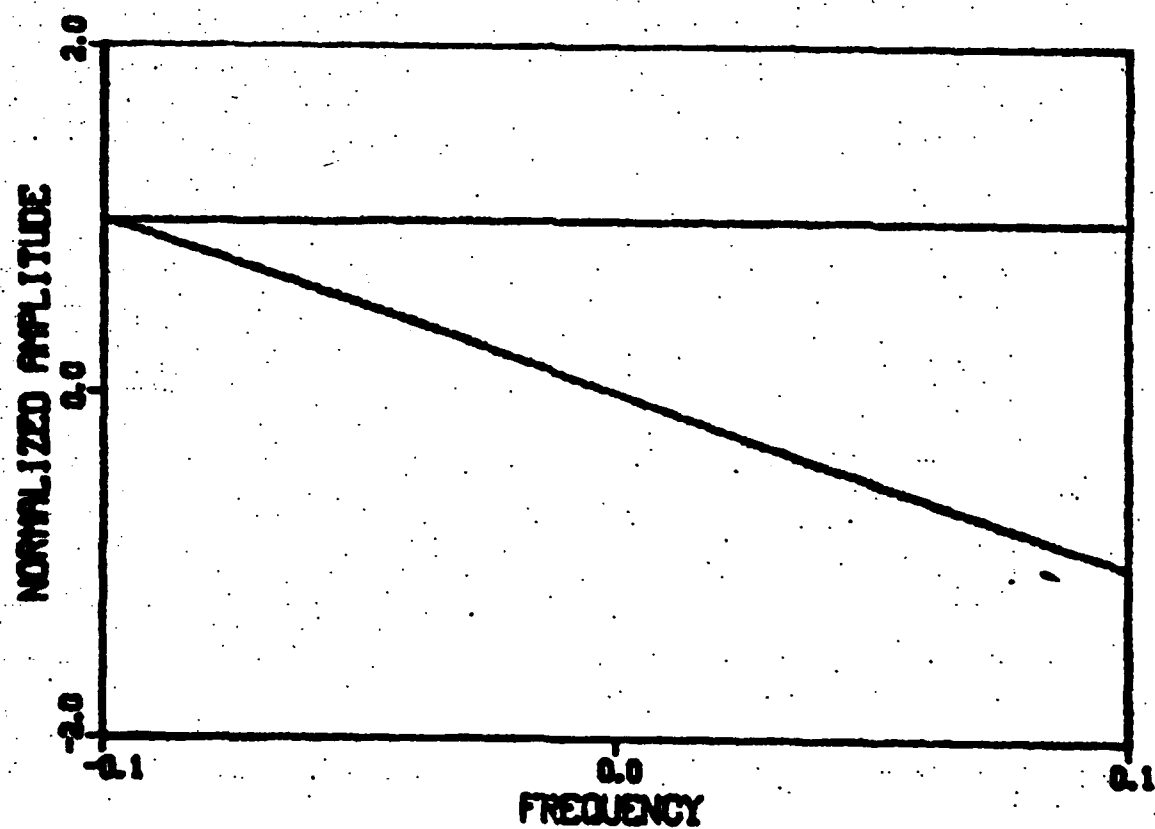


Fig. 3.2.2 Estimated phase of spectrum of an exponential signal for $TBP=0.1$ with $KR=0.693$, $KI=0.104$ and $KE=0.082$.

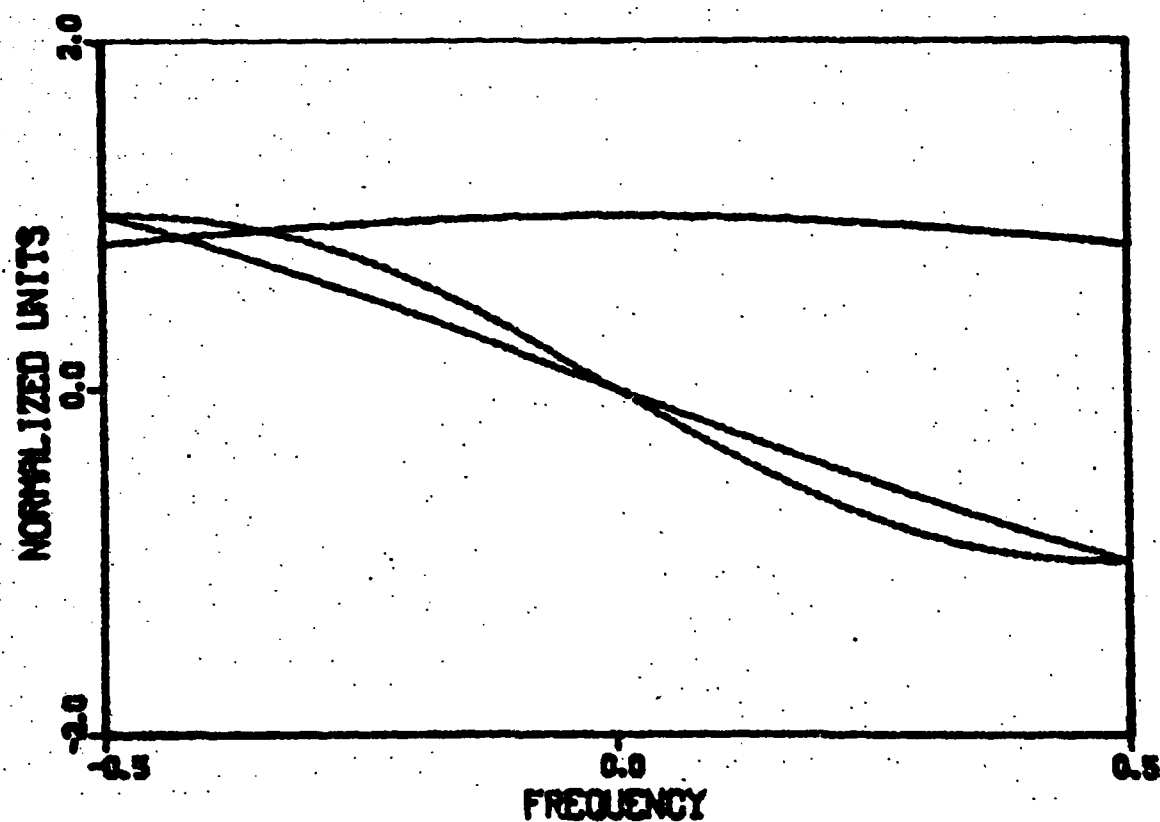


Fig. 3.2.3 Estimated phase of the spectrum of an exponential signal for $TBP=0.5$ with $KR=0.693$, $KI=0.482$ and $KE=0.520$.

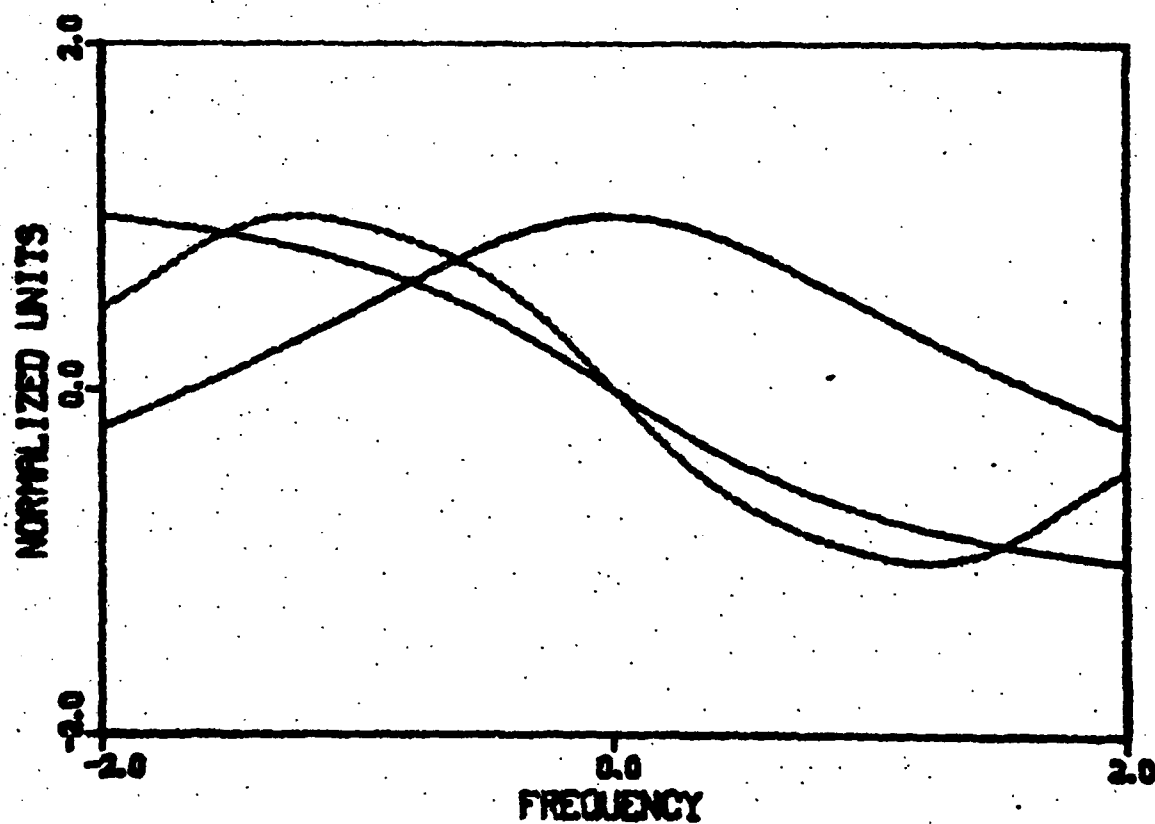


Fig. 3.2.4 Estimated phase of the spectrum of an exponential signal for $TBP=2.0$ with $KR=0.693$, $KI=1.125$ and $KE=0.473$.

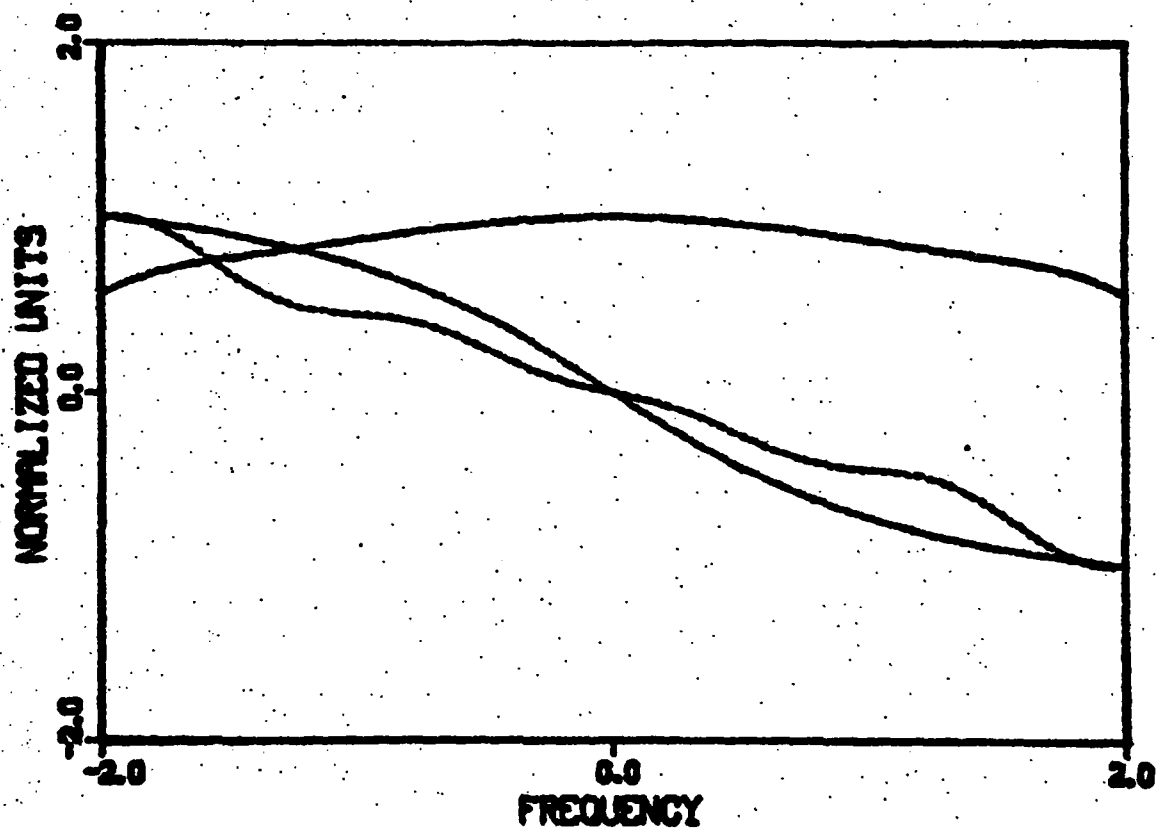


Fig. 3.2.5 Estimated phase of the spectrum of an exponential signal after Gaussian filtering with $\sigma^2=4.0$ where $KR=2.461$, $KI=1.125$ and $KE=2.390$.

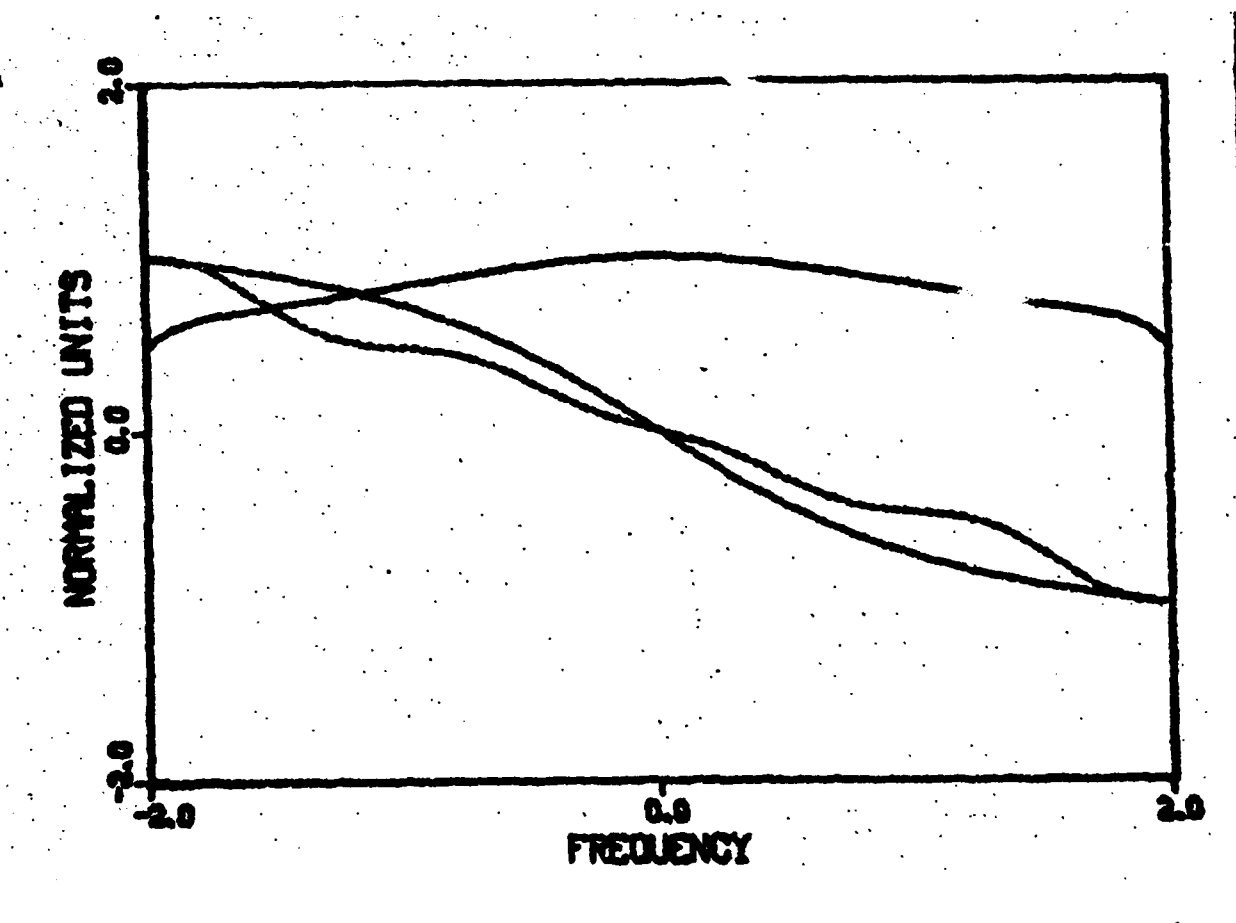


Fig. 3.2.6 Estimated phase of the spectrum of an exponential signal after Gaussian filtering with $\sigma^2=0.5$ where $KR=2.133$, $KI=1.125$ and $KE=1.981$.

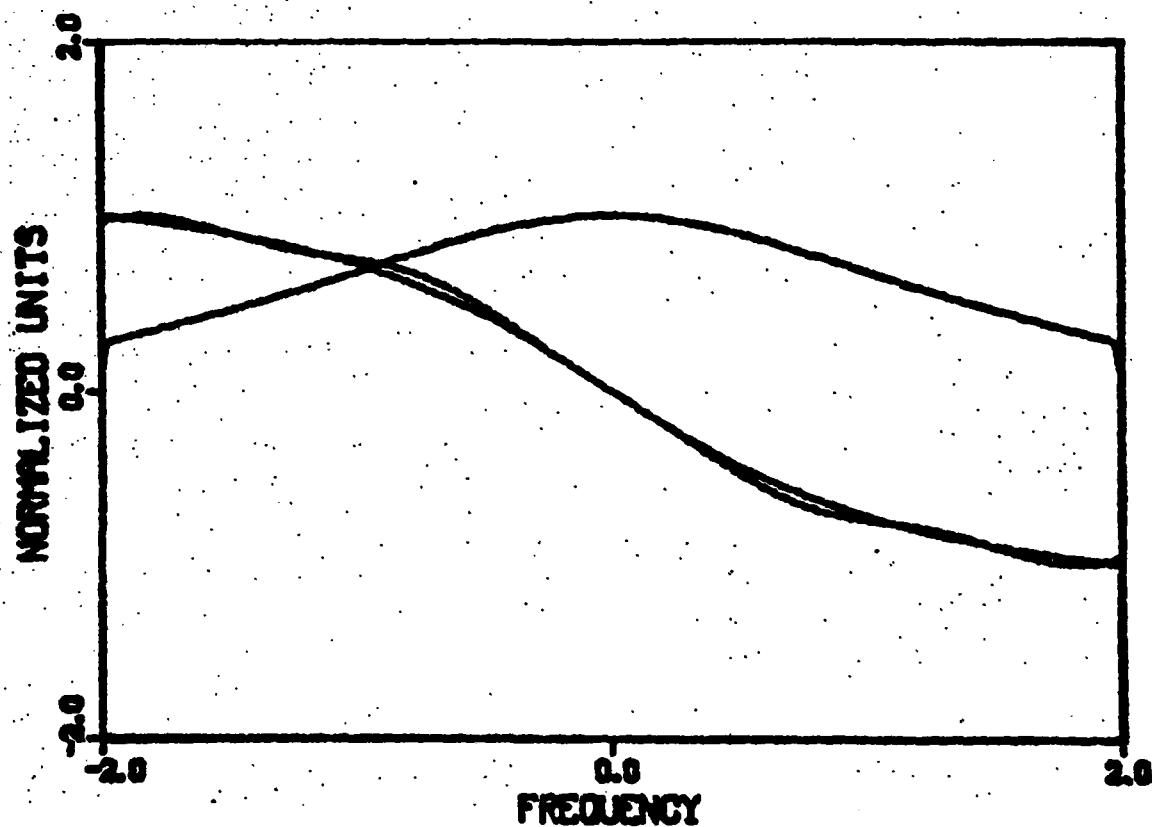


Fig. 3.2.7 Estimated phase of the spectrum of an exponential signal after Gaussian filtering with $\sigma^2=0.01$ where $KR=1.161$, $KI=1.125$ and $KE=0.821$.

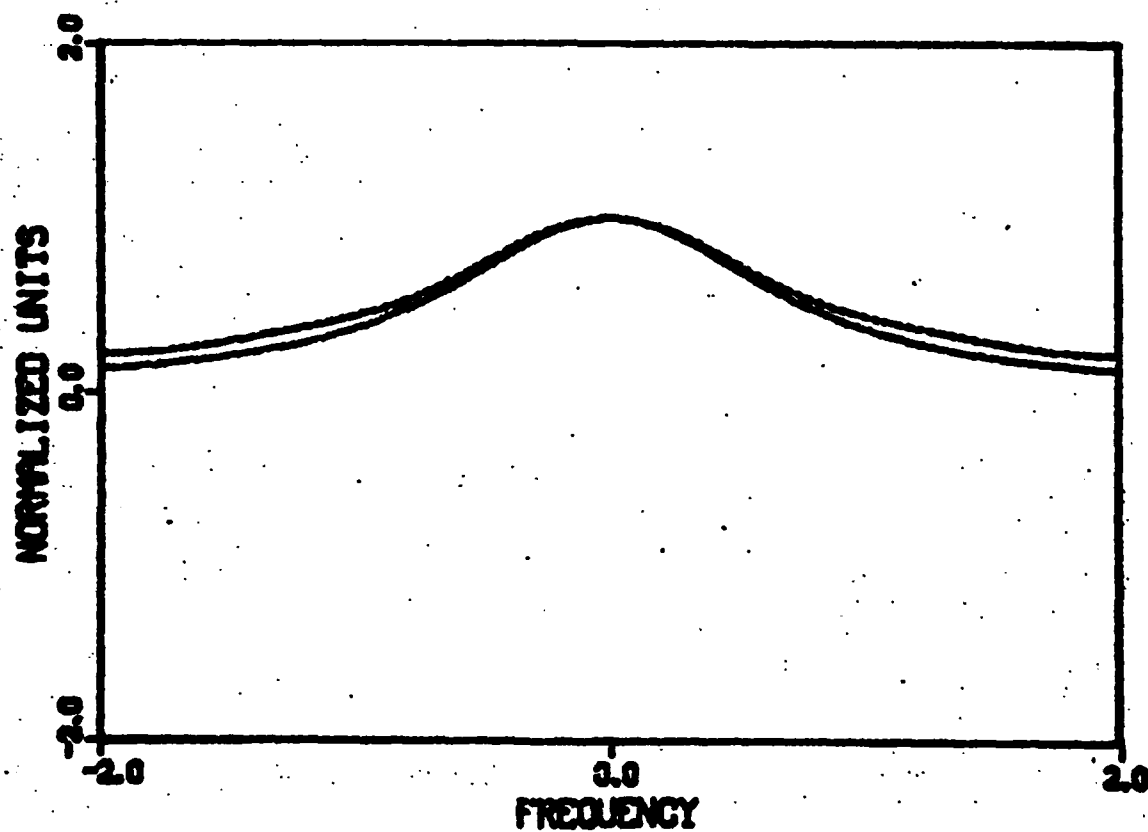


Fig. 3.2.8 Estimated real part of spectrum of exponential signal with $KR=7.389$ and $KE=7.389$.

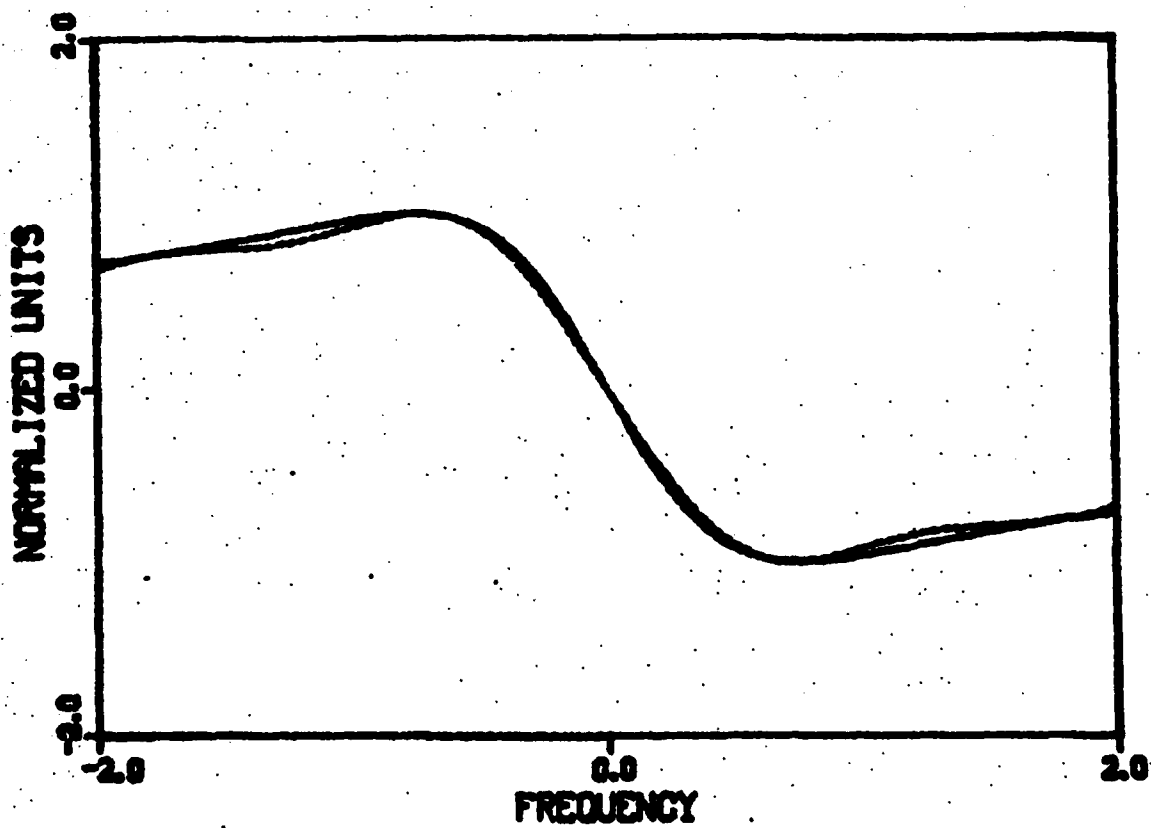


Fig. 3.2.9 Estimated imaginary part of spectrum of exponential signal with $KI=2.97$ and $KE=2.46$.

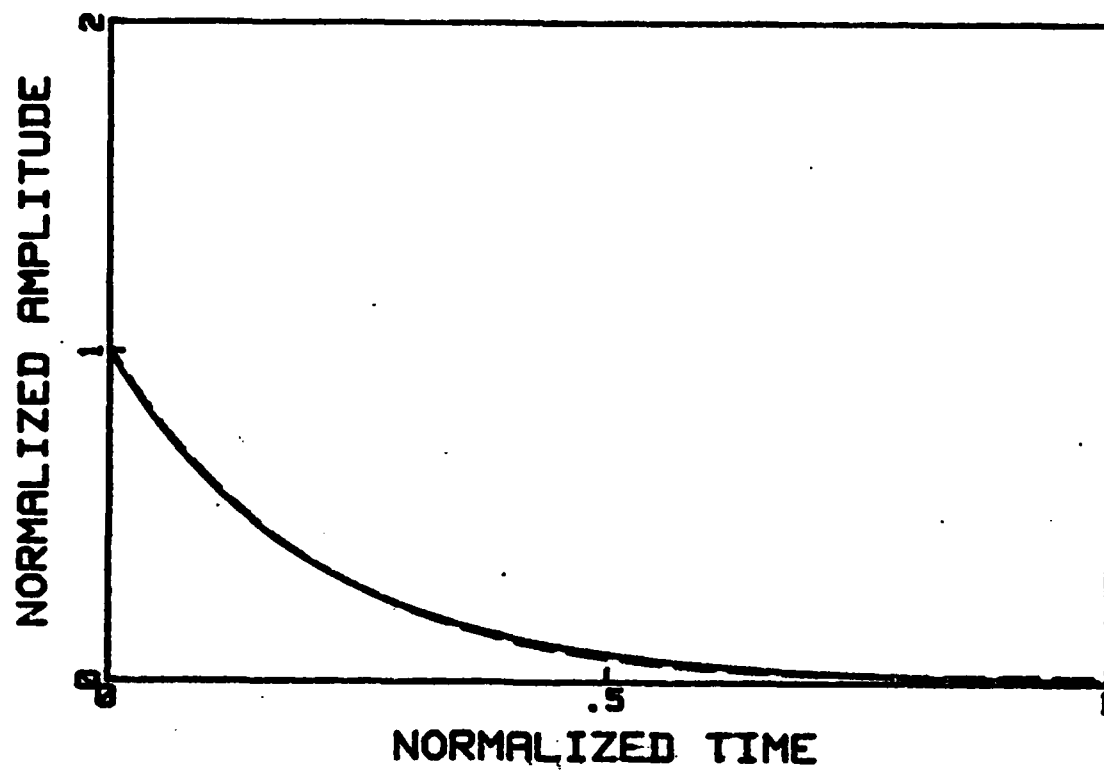


Fig. 3.2.10 Fourier transform of signal obtained from estimated real and imaginary parts.

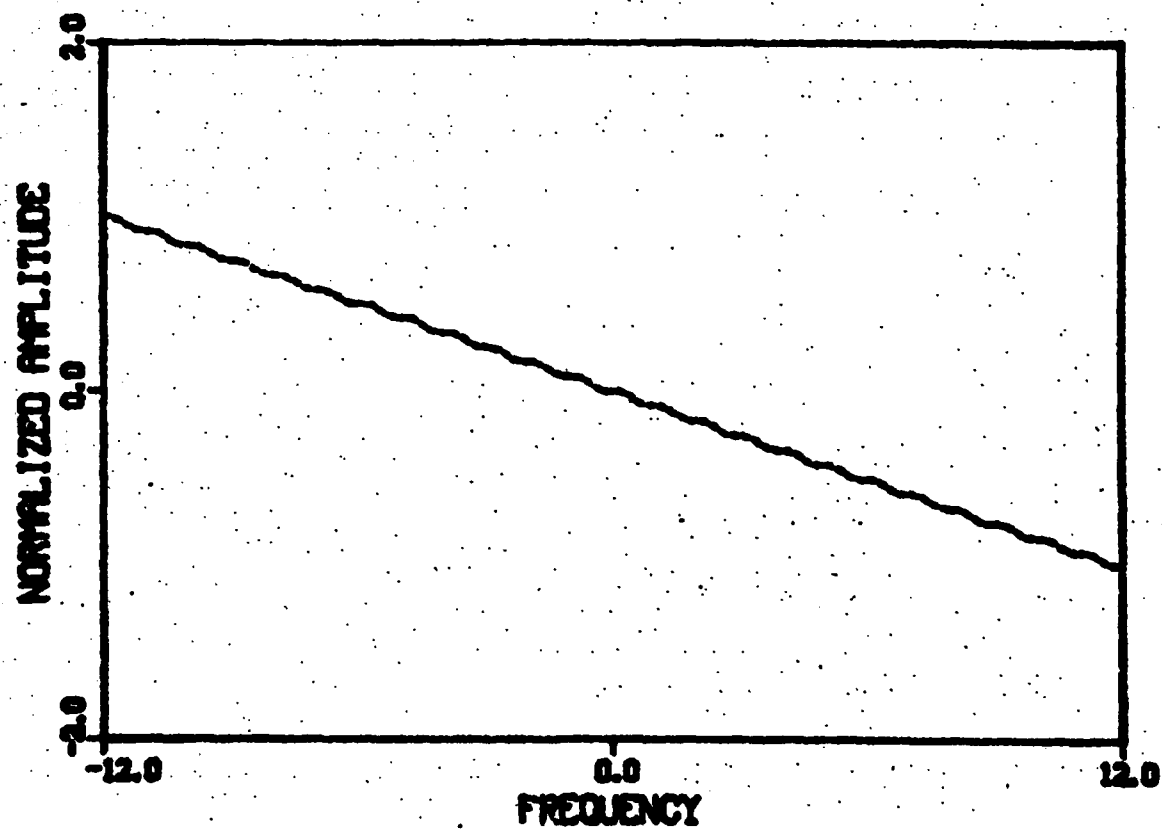


Fig. 3.2.11 Correction factor for phase estimation.

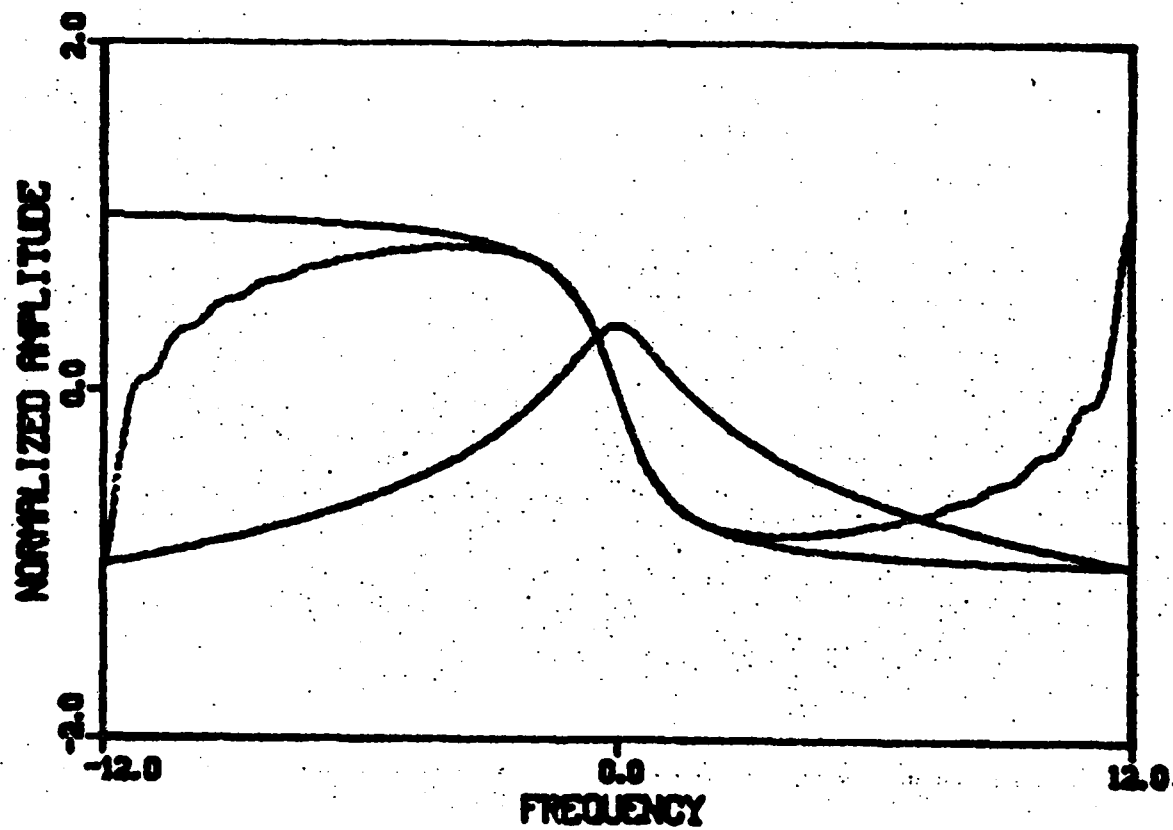


Fig. 3.2.12 Corrected phase estimate using the correction factor for the phase of the spectrum of an exponential signal.

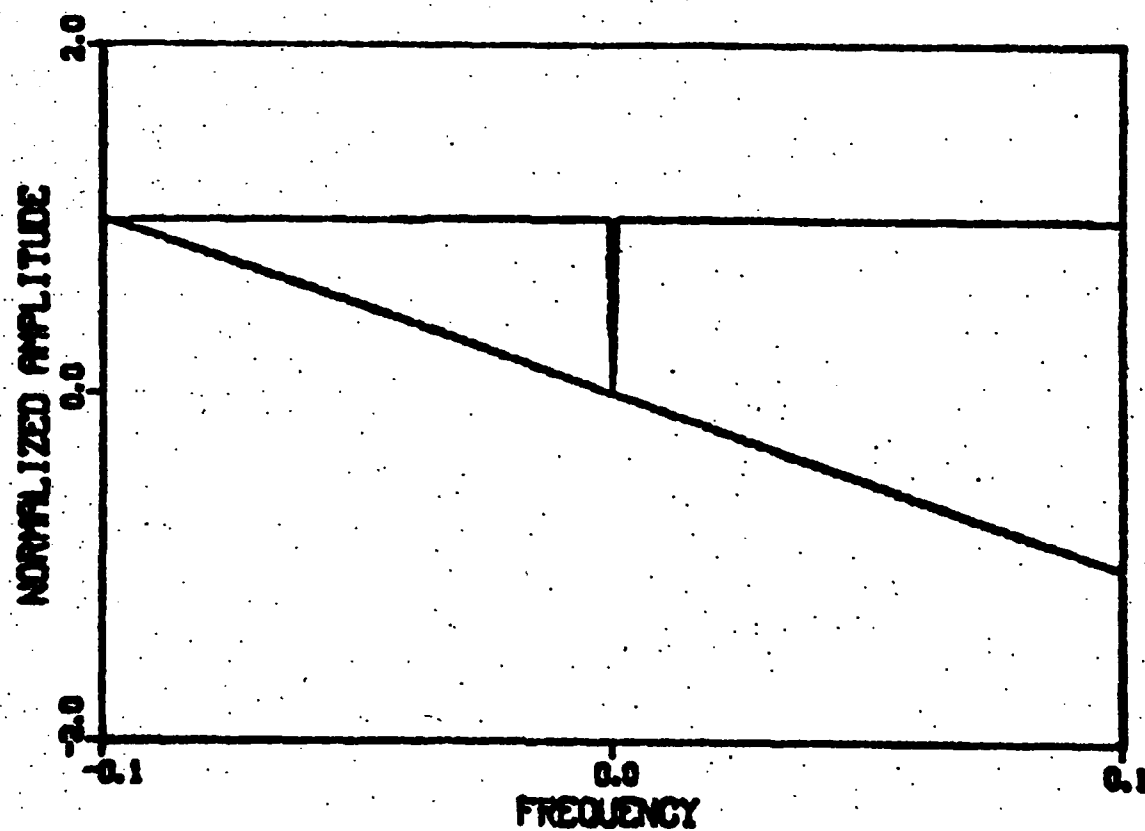


Fig. 3.2.13 Phase estimate of the shifted interval from $f=0.1$ to 0.2 of the spectrum of an exponential signal where $KI=0.102$ and $KE=0.081$.

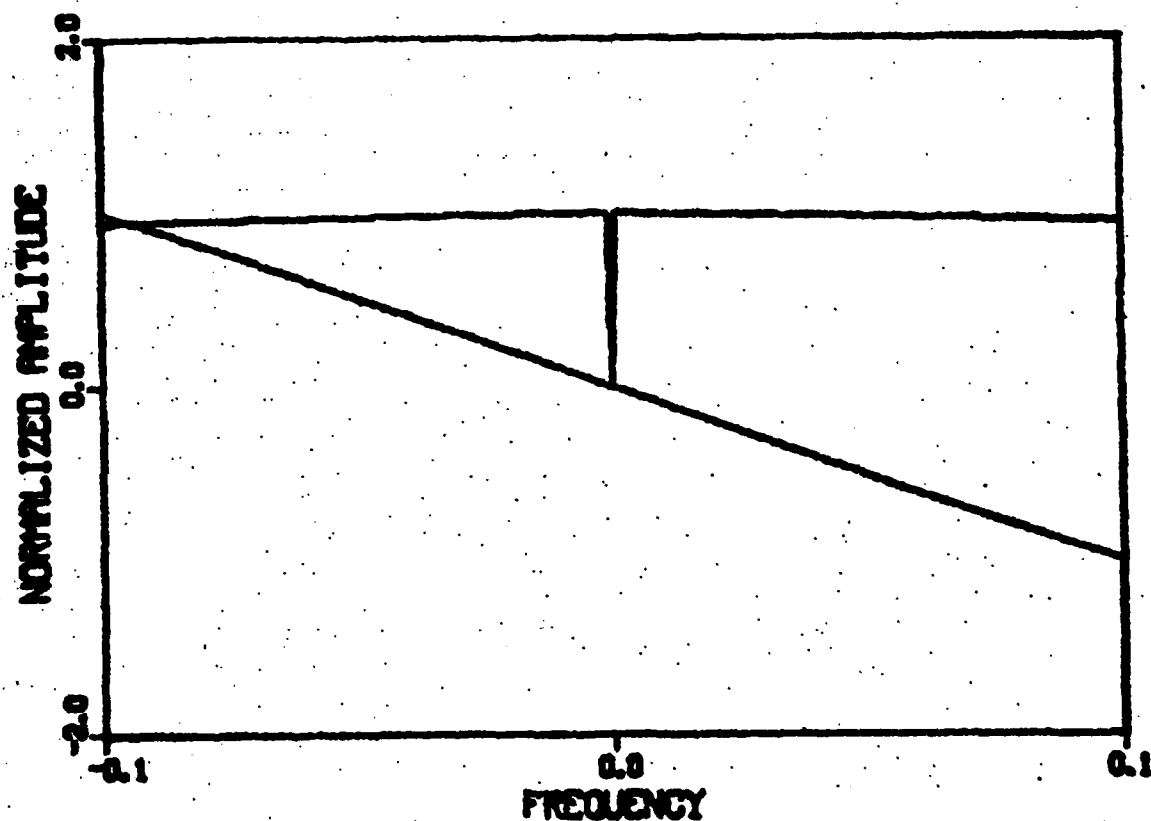


Fig. 3.2.14 Phase estimate of the shifted interval from $f=2.0$ to 2.1 of the spectrum of an exponential signal where $KI=0.019$ and $KE=0.073$.

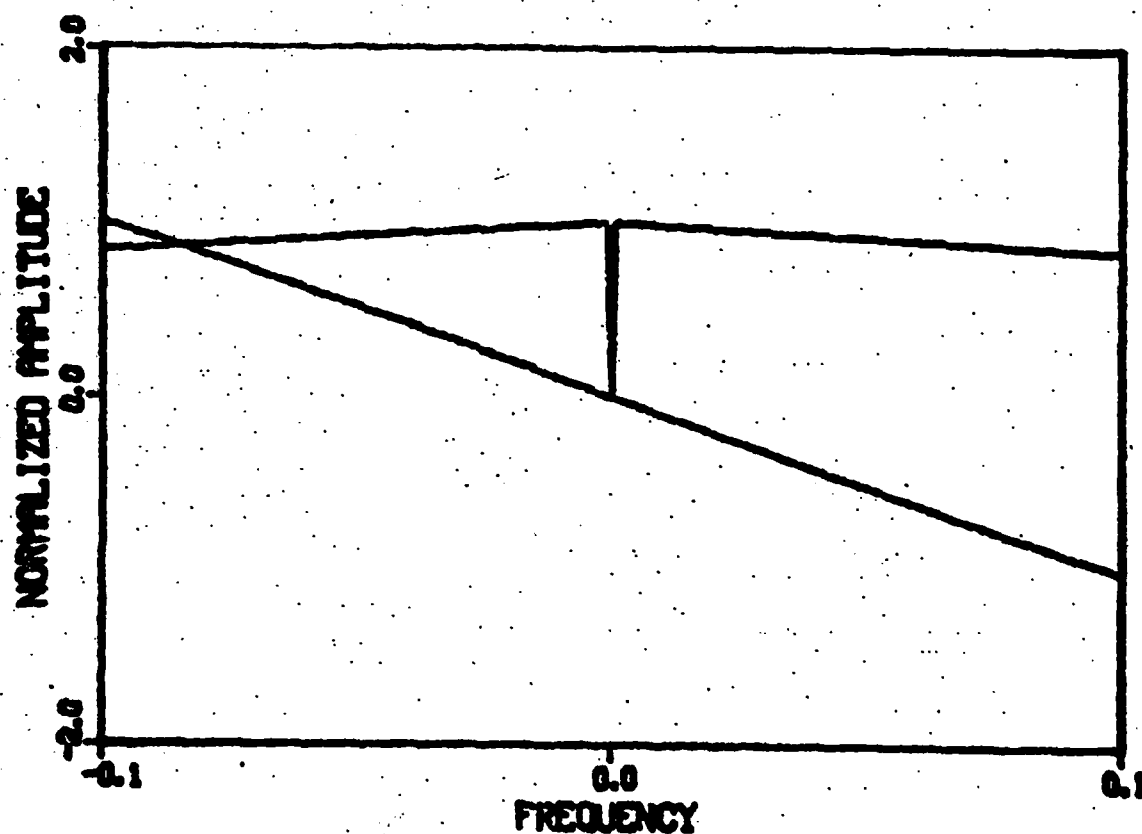


Fig. 3.1.15 Phase estimate of the shifted interval from $f=6.5$ to 6.6 of the spectrum of an exponential signal where $KI=0.002$ and $KE=0.032$.

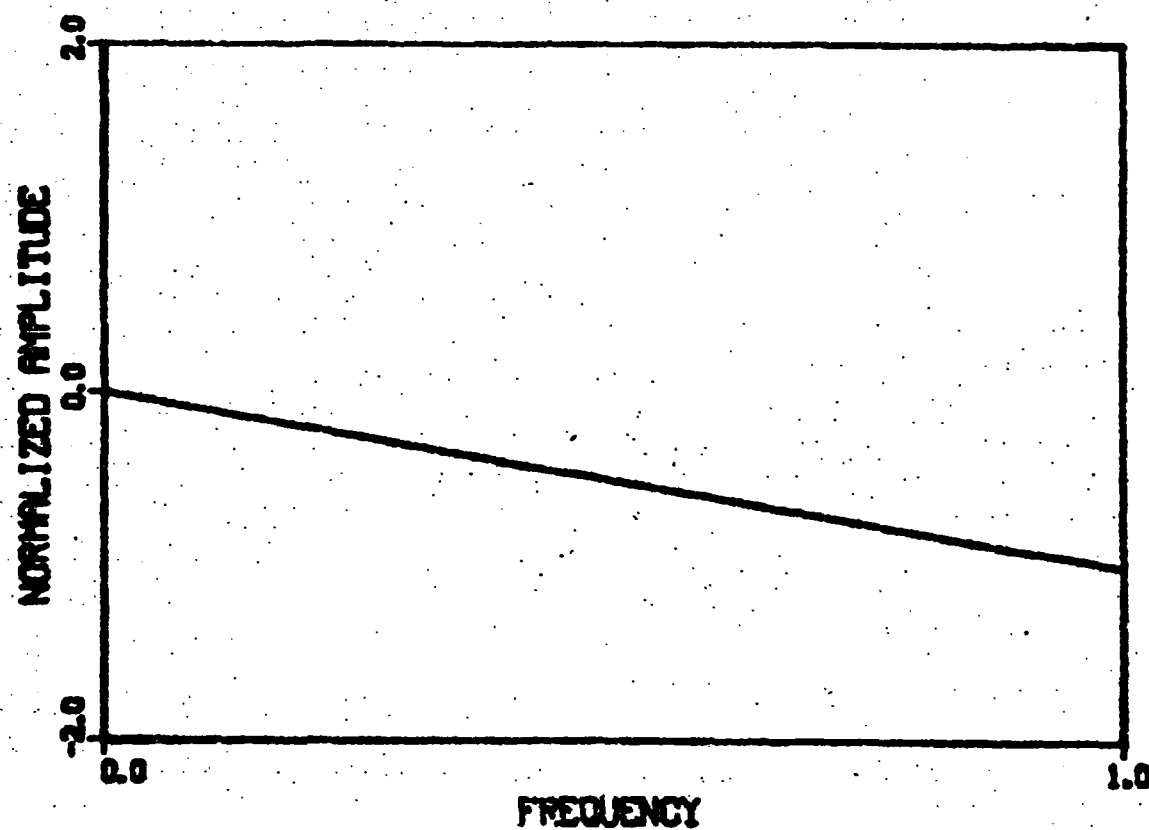


Fig. 3.2.16 Estimate of the phase of the spectrum of the exponential signal after having partitioned the interval into ten segments with $KI=0.808$ and $KE=0.804$.

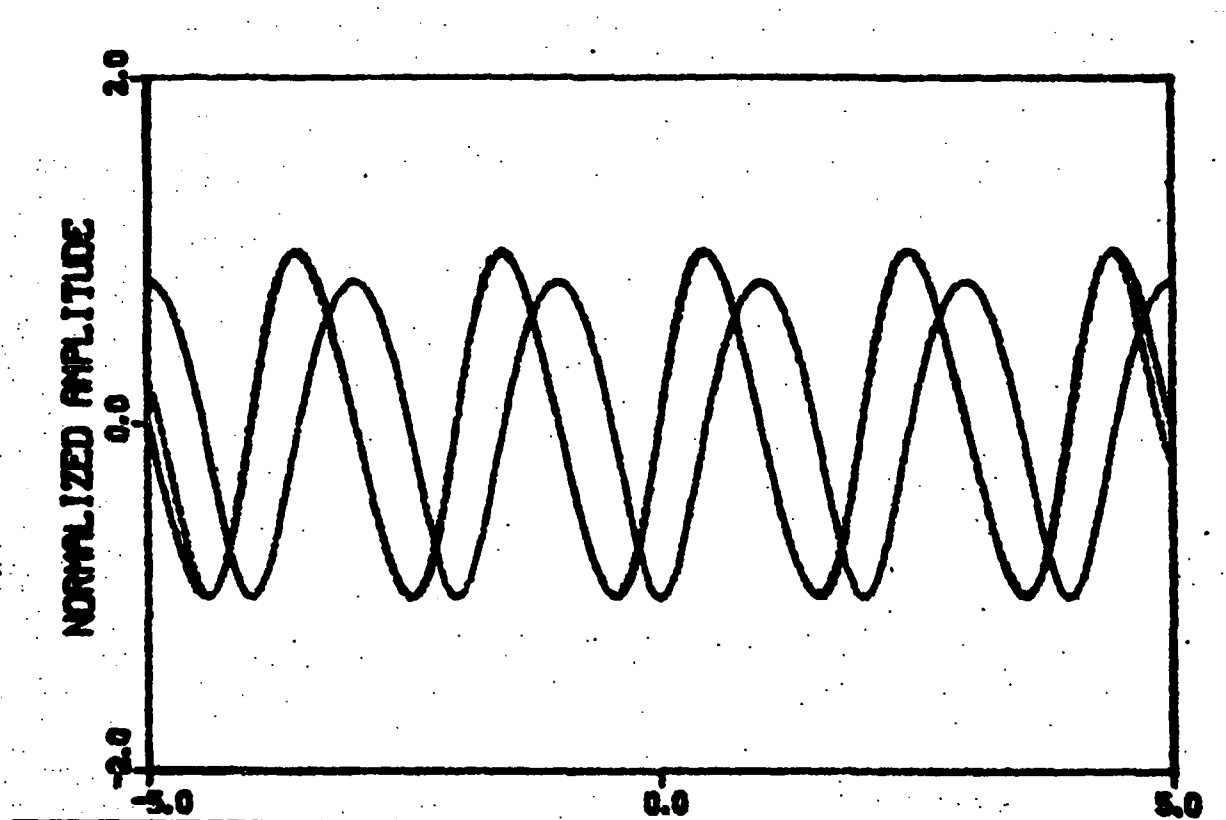


Fig. 3.2.17 Phase estimate of an analytic signal with $K_R=0.233$, $K_I=0.201$ and $K_E=0.201$.

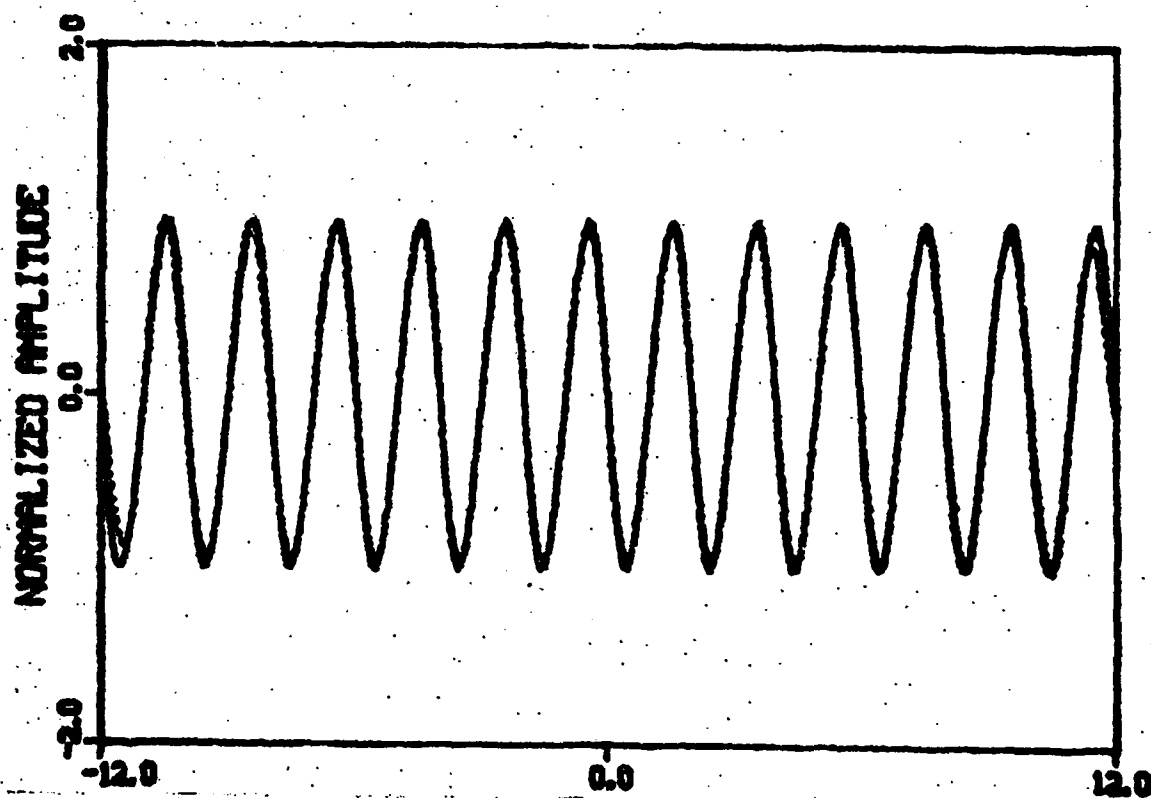


Fig. 3.2.18 Phase estimate of a periodic analytic signal whose bandwidth is larger with $KI=0.403$ and $KE=0.416$.

Chapter 4

SUMMARY AND EXTENSIONS

4.0 Introduction

A new method of resolving two frequencies spaced closely together buried in noise has been presented. The method involves knowing certain information about the signal a priori. This information was used to give a set of equations where there are less unknowns than there are equations. Since the system of equations is overdetermined, there are many possible solutions. We have selected the solution vector which yields the minimal norm of the residual error. By so doing, we were able to resolve the two frequencies of the signal beyond the limit imposed by the uncertainty principle of signal processing.

A second topic that was discussed is a new form of the Hilbert transform. An advantage of this new form is that it takes into account for signals that have been observed for short time durations. One use of the Hilbert transform is in phase estimation from magnitude measurements. This can be accomplished if the signal is causal and has zeros that occur only in the lower half of the complex z -plane.

If zeros occur in the upper half of the z -plane, methods have to be introduced to reduce the effects of the zeros on the phase estimation. A new method for estimating the phase was shown where the spectrum is partitioned. All methods were demonstrated via computer simulations.

The first chapter of this thesis contains material of an introductory nature. In Chapter 2, a new method of resolving two frequencies spaced closely together when the time-bandwidth product is very low was presented. The method was shown to give favorable results under low signal-to-noise ratios. In the process of resolving the frequencies, we obtained an estimate of the time signal. In Chapter 3, we introduced a new form of the Hilbert transform. With the new form of this transform we showed how the phase can be estimated from the magnitude of a signal, given that certain conditions are met. When these conditions cannot be met, modifications have to be performed before or after the estimate is obtained.

4.1 Extensions of Methods

There are many extensions that can be applied to the methods discussed in this thesis. In the case of spectral estimation, if it is known that there are three or more frequencies involved, then it is possible to obtain a set

of equations, and constraints on the solution vector in an identical manner as was described in Chapter 2. In two-dimensional signal processing such as is found in optics, When the two-dimensional signal is seperable, it is posible to use this method on each dimension to obtain better resolution for impulsive type spectra. This can be further investigated to be used for image enhancement of electron-microscope images, bandwidth compressed video images, and image enhancement of medical diagnostic images.

For the modified Hilbert transform, the formulation can be extended to n -dimensions if the signals are separable in each dimension. If involved with superresolution, methods can be developed that will utilize some superresolving methods to obtain a superresolving Hilbert transform. This could be used as a constraint for the estimation of causal signals that have reduced time-bandwidth products.

APPENDIX

Suppose we are given a set of data points

$$c(i), i=1,2,3,\dots,m \quad (1)$$

and a model depending upon certain parameters x

$$d(i,x), i=1,2,3,\dots,m \quad (2)$$

where x is a column vector containing n elements and we have $m > n$. A way of measuring how far the model is from the data for any choice of x is defined as the residual $f(x)$, and is a function of x , $d(i,x)$, and $c(i)$. Each of the $c(i)$ is a real number, the $d(i,x)$ are real-valued functions of x and f is a real-valued nonnegative function. The data-fitting problem consists of selecting the parameters x so as to minimize f . These problems have more structure than do general minimization problems because f is often of a form such as

$$\begin{aligned} f(x) &= \sum_i r(c(i)-d(i,x)) \\ f(x) &= \max_i r(c(i)-d(i,x)) \end{aligned} \quad (3)$$

for some, simple, nonnegative function $r(\cdot)$.

This data-fitting problem is linear if $d(i,x)$ has the form

$$d(i,x)=Dx \quad (4)$$

where D is an $m \times n$ matrix. If all x are feasible for consideration in finding the minimum of f , the problem is unconstrained. If the x are restricted to lie in some set S , then the problem is constrained. A common way to specify such feasible sets S is through the use of equalities and inequalities

$$S = \left\{ x \mid \begin{array}{l} p(j,x)=q(j) \ , \ j=1,2,\dots,i \\ g(k,x)=h(k) \ , \ k=1,2,\dots,l \end{array} \right\} \quad (5)$$

As an example of such problems one may have (4) where f involves summation with $r(.)=(\)^2$. This leads to the familiar linear least-squares problem

$$\min f(x) = \|c-Dx\| = \sum_i (c(i)-Dx)^2. \quad (6)$$

This problem becomes a linearly constrained problem if, for example, the elements of x must all be nonnegative.

If one was to restrict oneself to completely linear problems in which $r=|.|$, then this would involve l_1 and l_∞ data-fitting. The least-squares (l_2) criterion for meas-

uring the fit of a model to data is the most reasonable one to use if it is known that the data $c(i)$ are approximations to certain quantities $c'(i)$

$$c(i) = c'(i) + e(i) \quad (7)$$

where the errors $e(i)$ are all normally distributed with zero mean and common variance. This is the case when the $c(i)$ result from careful, bias-free observations of well behaved systems. However, if this is not the case then two other situations are very important:

(1) the observations are not always careful or bias-free, or the system is not always well-behaved (1,),.

(2) the measurements are exact, and all errors are zero (1∞).

In (1) there may be occasional errors $e(i)$ which are quite wild. It is desirable to ignore the corresponding observations and fit the model only to the good data. In (2), it is desired to get the model evenly close to every one of the observations $c(i)$. The l_1 norm can be expressed as

$$f(x) = \sum_i |c(i) - Dx| = \|c - Dx\|_1, \quad (8)$$

and the l_∞ norm can be expressed as

$$f(x) = \max_i |c(i) - Dx| = \|c - Dx\|_\infty. \quad (9)$$

The former case is of interest to statisticians (as robust regression) and the latter case to mathematicians (function approximation).

To see the difference between the three norms, Fig. (A.1) shows observations made of a 45° line over a unit square. If these observations are subject to minor random fluctuations, and if an attempt is made to fit the observations with a straight line, the l_∞ , l_2 , l_1 norms result in approximately the same solution as seen in Fig. (A.1). On the other hand, if one of the observations is widely at odds with the others, then the l_1 line will not be disturbed, the l_2 line will be displaced somewhat towards the wild point, and the l_∞ line will be centered between the wild point and the remaining ones as shown in Fig. (A.2).

It is for these reasons that the solution to the problem of section 3.1 will be solved for using the l_1 norm. The data $c(i)$ is very noisy causing wild fluctuations in the data, and it is the l_1 norm that will fit the model to the good data only.

The linear problem of section 3.1 can be written in the form

$$\begin{aligned}
 &\text{minimize } \sum_i (c(i) - Dx) \\
 &\text{subject to } Px = q \\
 &\quad Gx = h
 \end{aligned} \tag{10}$$

whose solution can be arrived at using linear programming. Since the solution x and the residual need both be negative as well as positive, and because linear programming gives only positive solutions, $3m$ additive variables must be introduced. This gives us

$$\begin{aligned}
 c - Dx + dy &= v - u \\
 x &\geq 0 \\
 y &\geq 0 \\
 v &\geq 0 \\
 u &\geq 0
 \end{aligned} \tag{11}$$

so that (10) can be written as

$$\begin{aligned}
 &\text{minimize } \sum u + v \\
 &\text{subject to } Px - Py = q \\
 &\quad Gx - Gy = h \\
 &\quad Dx - Dy - u + v = c
 \end{aligned} \tag{12}$$

which can be solved by a method such as the simplex method.

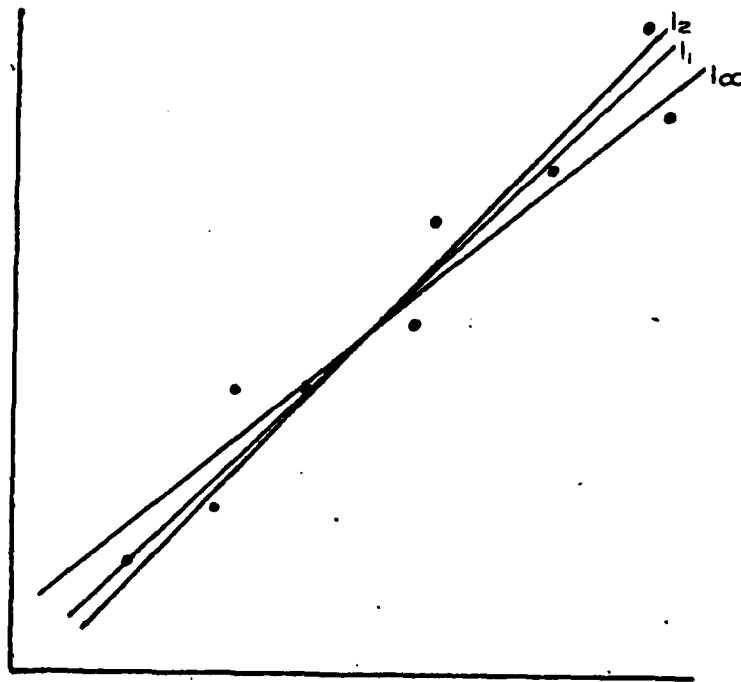


Fig. A.1 Observations of a 45° line over a unit square showing the l_1 , l_2 and l_∞ curve fits of the line.

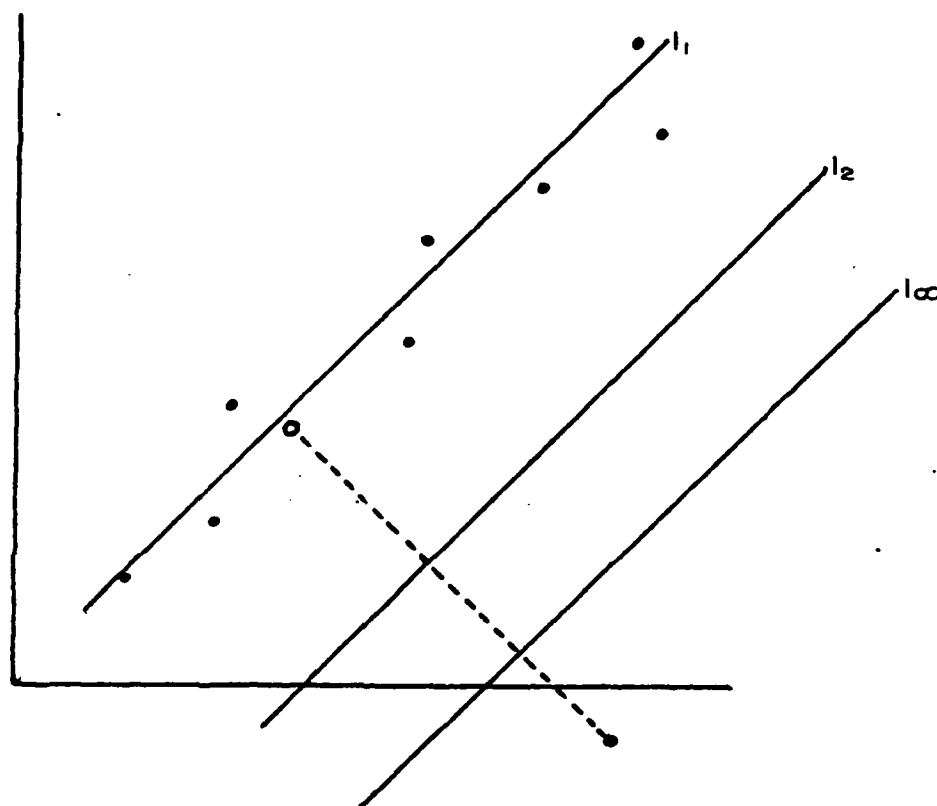


Fig. A.2 The l_1 , l_2 and l_∞ fits when one of the observations is wild.

REFERENCES

- 1 D.S. Slepian and H.O. Pollack, "Prolate spheroidal wave functions, Fourier analysis and uncertainty principle," "Bell Syst. Tech. J.", vol. 40, no. 1, pp. 43-84, 1961.
- 2 A. Papoulis, "A new algorithm in spectral analysis and bandlimited extrapolation," "IEEE Trans. Circuits Systems", vol. CAS-22, pp. 735-742, Sept. 1975.
- 3 R.W. Gerchberg, "Super-resolution through error energy reduction," "Optica Acta", vol. 9, no. 9, pp. 709-720, 1974.
- 4 M.S. Sabri and W. Steenaart, "An approach to band-limited signal extrapolation: the extrapolation matrix," "IEEE Trans. Circuits Syst.", vol. CAS-25, pp. 76-78, Feb. 1979.
- 5 J.A. Cadzow, "Improved spectral estimation from incomplete sampled data observations," presented at the RADC Spectral Estimation Workshop, Rome, NY May 24-26, 1978.
- 6 A.V. Oppenheim and R.W. Schaffer, Digital Signal Processing Englewood Cliffs: Prentice-Hall 1975.
- 7 F.J. Harris, "On use of windows for harmonic analysis with the discrete Fourier transform," "Proceedings IEEE", vol. 66, no. 1, pp. 51-83, Jan. 1978.
- 8 W. Gersch, "Spectral analysis of EEG's by autoregressive decomposition of time series," "Math. Biosci.", vol. 7, pp. 205-222, 1970.
- 9 T. Bohlin, "Comparison of two methods of modeling stationary EEG signals," "IBM J. Res. Dev.", pp. 194-205, May 1972.
- 10 L.C. Wood and S. Treitel, "Seismic signal processing," "Proceedings IEEE", vol. 64, no. 4, pp. 649-661, April 1975.
- 11 B.S. Atal and S.L. Hanauer, "Speech analysis and synthesis by linear prediction of the speech wave," "J.

- Acoust. Soc. Amer.", vol. 50, no. 2, pp. 637-655, 1971.
- 12 J. Makhoul, "Speech analysis of speech by linear prediction," "IEEE Trans. Audio Electroacoust.", vol. AU-21, pp. 140-148, June 1972.
 - 13 F.M. Hsu and A.A. Giordano, "Line tracking using autoregressive spectral estimates," "IEEE Trans. Acoustics, Speech Processing", vol. ASSP-25, pp. 510-519, Dec. 1975.
 - 14 G. Prado and P. Moroney, "Linear predictive spectral analysis for Doppler sonar applications," Charles Stark Draper Laboratory, Tech. Rep. R-1109, Sept. 1977.
 - 15 W.F. Gabriel, "Spectral analysis and adaptive array superresolution techniques," "Proc. IEEE", vol. 68, pp. 654-666, June 1980.
 - 16 R.B. Blackman and J.W. Tukey The Measurement of Power Spectra From the Point of View of Communications Engineering. New York: Dover 1959.
 - 17 N. Wiener, "Generalized harmonic analysis," "Acta Mathematica", vol. 55, pp. 117-258, 1930.
 - 18 J.W. Cooley and J.W. Tukey, "An algorithm for machine calculation of complex Fourier series," "Math. Comput.", vol. 19, pp. 297-301, April 1965.
 - 19 J.P. Burg, "Maximum entropy spectral analysis," Ph.D. dissertation, Dept. Geophysics, Stanford Univ., Stanford, CA, May 1975.
 - 20 J. Makhoul, "Linear prediction: a tutorial review," "Proc. IEEE", vol. 63, pp. 561-580, April 1975.
 - 21 N. Levinson, "The Wiener (root mean square) error criterion in filter design and prediction," "J. Math. Phys.", vol. 25, pp. 261-278, 1947.
 - 22 J. Durbin, "The fitting of time series methods," "Rev. Inst. Int. de Stat", vol. 28, pp. 233-244, 1960.
 - 23 A.K. Jain and S. Ranganath, "Extrapolation algorithms for discrete signals with applications to spectral estimation," "IEEE Trans. Acoustics, Speech, Signal Processing", vol. 29, no. 4, pp. 830-845, Aug. 1981.

- 24 S.M. Kay and S.L. Marple, "Spectrum analysis- a modern perspective," "Proc. IEEE", vol. 69, no. 11, pp. 1380-1419, Nov. 1981.
- 25 M. Kaveh, "High resolution spectral estimation for noisy signals," "IEEE Trans. Acoustics, Speech, Signal Processing", vol. ASSP-27, no. 3, pp. 286-287, June 1979.
- 26 J.A. Cadzow, "High performance spectral estimation- a new ARMA method," "IEEE Trans. Acoustics, Speech, Signal processing", vol. ASSP-28, no. 5, pp. 524-529, Oct. 1980.
- 27 R. Mammone and G. Eichmann, "Superresolving image restoration using linear programming," "Applied Optics", vol. 21, no. 3, pp. 496-501, Feb. 1982.
- 28 R. Mammone and G. Eichmann, "Restoration of discrete Fourier spectra using linear programming," "J. Opt. Soc. Am.", vol. 72, no. 8, pp. 987-992, Aug. 1982.
- 29 S. Levy, C. Walker, T.J. Ulrych and P.K. Fullagar, "A linear programming approach to the estimation of the power spectra of harmonic processes," "IEEE Trans. Acoustics, Speech, Signal Processing", vol. ASSP-30, no. 4, pp. 675-679, Aug. 1982.
- 30 G.B. Dantzig, "Inductive proof of the Simplex method," "IEM J. of Res. and Dev.", vol. 14, no. 5, 1960.
- 31 S.I. Gass Linear Programming, Fourth Edition, New York: McGraw-Hill, 1975
- 32 R.V. Churchill, Complex Variables and Applications, New York: McGraw-Hill, 1953
- 33 L.S. Taylor, "The phase retrieval problem," "IEEE Trans. Antenna Propagat.", vol. AP-29, no. 2, pp. 386-391, March 1981.
- 34 H.M. Nussenzweig, "Phase problem in coherence theory," "J. Math. Phys.", vol. 8, pp. 561-572, 1967.
- 35 H.B. Voelcker, "Toward a unified theory of modulation, Part I: Phase-envelope relations," "Proc. IEEE", vol. 54, pp. 340-353, 1966.
- 36 A.D. Whalen, Detection of Signals in Noise, New York: Academic press, 1971.

- 37 E.A. Robinson, Random Wavelets and Cybernetic Systems, New York: Hofner Publishing Co., 1962.
- 38 T.T. Taylor, "Design of line-source antennas for narrow beamwidth and low side lobes," "IRE Trans. Antennas Propagat.", vol. AP-3, pp. 16-28, 1955.
- 39 A. Walther, "The question of phase in image formulation," "Opt. Acta", vol. 10, pp. 33-40, 1963.
- 40 D.A. Huffman, "The generation of impulse-equivalent pulse trains," "IRE Trans. Info. Theory", vol. IT-8, pp. 510-516, 1962.
- 41 D.L. Missel, "A reply to Saxton's letter on phase determination in bright field electron microscopy using complementary half plane apertures," "J. Phys. D: Appl. Phys.", vol. 7, pp. L69-L71, 1974.
- 42 R.E.A.C. Paley and N. Wiener, Fourier Transforms in the Complex Domain, New York: American Mathematical Society, 1934.
- 43 D.L. Misell, R.E. Burge and A.H. Greenway, "Phase determination from image intensity measurements in bright-field optics," "J. Phys. D: Appl. Phys.", vol. 7, pp. L27-L30, 1974.
- 44 W.O. Saxton, "Phase determination in bright field electron microscopy using complementary half-phase apertures," "J. Phys. D: Appl. Phys.", vol. 7, pp. 163-164, 1974.
- 45 N. Nakajima and T. Asakura, "Phase retrieval of the scattered complex wave function from the far-field intensity distribution by using the mathematical filter," "Optik", vol. 60, pp. 181-198, 1982.
- 46 N. Nakajima and T. Akasura, "Extraction of the influence of zeros from the image intensity in the phase retrieval using logarithmic Hilbert transform," "Optik", vol. 63, no. 2, pp. 99-108, 1983.
- 47 R.W. Gerchberg and W.O. Saxton, "Phase determination from image and diffraction plane pictures in electron microscopy," "Optik", vol. 33, pp. 275-284, 1971.
- 48 R.W. Gerchberg and W.O. Saxton, "A practical algorithm for the determination of phase from image and diffraction plane images," "Optik", vol. 35, pp. 237-246,

1972.

- 49 D.L. Missel, "An examination of an alternate method for the solution of the phase problem in optics and electron optics: I Test calculations," "J. Phys. D:Appl. Phys.", vol. 6, pp. 2200-2216, 1973.
- 50 W.J. Dallas, "Digital computation of image complex amplitude from image and diffraction intensity: an alternative to holography," "Optik", vol. 44, pp. 45-59, 1975.
- 51 R.H.T. Bates, "Fourier phase problems are uniquely solvable in more than one dimension. I: Underlying theory," "Optik", vol. 61, pp. 247, 262, 1982.
- 52 K.L. Garden and R.H.T. Bates, "Fourier phase problems are uniquely solvable in more than one dimension. II: One-dimensional considerations," "Optik", vol. 62, pp. 131-142, 1982.
- 53 W.R. Fright and R.H.T. Bates, "Fourier phase problems are uniquely solvable in more than one dimension. III: Computational examples for two dimensions," "Optik", vol. 62, pp. 219-230, 1982.
- 54 J.R. Fienup, "Phase retrieval algorithms: a comparison," "Appl. Optics", vol. 21, no. 15, pp. 2758-2769, 1982.
- 55 A. Papoulis, The Fourier Integral and its Applications, New York: McGraw-Hill, 1962.
- 56 W.T. Ford, "Estimation of a minimum-phase operator from a portion of its amplitude spectrum," "IEEE Trans. Geoscience Electron.", vol. 47, pp. 1-2, 1967.
- 57 D.A. Linden, "A discussion of sampling theorems," "Proc. IRE", vol. 47, pp. 1219-1226, 1959.
- 58 E.A. Rosenberg, R.W. Schafer and L.R. Rabiner, "Effects of smoothing and quantizing the parameters of formant-coded voice speech," "J. Acoust. Soc. Amer.", vol. 50, pp. 1532-1538, 1971.
- 59 R.W. Schafer and L.R. Rabiner, "Design and simulation of speech analysis-synthesis system based on short-time Fourier analysis," "IEEE Trans. Audio Electroacoust.", vol. AU-21, pp. 165-174, 1973.

- 60 M.H. Hayes, J.S. Lim and A.V. Oppenheim, "Signal reconstruction from phase or magnitude," "M.I.T. Lincoln Lab., Lexington, Ma, 1979-64, Sept. 1979.
- 61 A.V. Oppenheim, J.S. Lim, G. Kopec and G. Pohlig, "Phase in speech and pictures," in Conf. Rec. ICASSP'79, Apr. 1979, pp. 634-637.
- 62 M.H. Hayes, J.S. Lim and A.V. Oppenheim, "Phase only signal reconstruction," in Proc. 1980 Int. Conf. Acoustic., Speech, Signal Processing, Apr. 1980, pp. 437-440.
- 63 G.A. Merchant and T.W. Parks, "Reconstruction of signals from phase: Efficient algorithms, segmentations, and generalizations," "IEEE Trans. Acoust., Speech, Signal Processing," vol. ASSP-28, pp. 1135-1147, Oct. 1983.

FILMED

9-31